IOWA STATE UNIVERSITY
Digital Repository

1996

Preparation of biomimetic species from iodophenylalanine

Andrei Dan Stefanescu
Iowa State University

www.manaraa.com

INFORMATION TO USERS

This manuscript has been reproduced from the microfilm master. UMI films the text directly from the original or copy submitted. Thus, some thesis and dissertation copies are in typewriter face, while others may be from any type of computer printer.

The quality of this reproduction is dependent upon the quality of the copy submitted. Broken or indistinct print, colored or poor quality illustrations and photographs, print bleedthrough, substandard margins, and improper alignment can adversely affect reproduction.

In the unlikely event that the author did not send UMI a complete manuscript and there are missing pages, these will be noted. Also, if unauthorized copyright material had to be removed, a note will indicate the deletion.

Oversize materials (e.g., maps, drawings, charts) are reproduced by sectioning the original, beginning at the upper left-hand corner and continuing from left to right in equal sections with small overlaps. Each original is also photographed in one exposure and is included in reduced form at the back of the book.

Photographs included in the original manuscript have been reproduced xerographically in this copy. Higher quality 6" x 9" black and white photographic prints are available for any photographs or illustrations appearing in this copy for an additional charge. Contact UMI directly to order.

Preparation of biomimetic species from iodophenylalanine

by

Andrei Dan Stefanescu   .

A dissertation submitted to the graduate faculty

in partial fulfillment of the requirements for the degree of

DOCTOR OF PHILOSOPHY

Major: Chemistry

Major Professor: Alan W. Schwabacher

Iowa State University

Ames, Iowa

1996

UMI Number: 9712608

UMI
300 North Zeeb Road
Ann Arbor, MI 48103

Graduate College

Iowa State University

This is to certify that the doctoral dissertation of

Andrei Dan Stefanescu

has met the dissertation requirements of Iowa State University

Signature was redacted for privacy.

Major Professor

Signature was redacted for privacy.

For the Major Program

Signature was redacted for privacy.

For the Graduate College

To Iulia, Matei, and Anca

TABLE OF CONTENTS

NOMENCLATURE

AMP	- adenosin-monophosphate
BDAP	- bis-[4-(2(S) 3-diaminopropyl) phenyl] phosphinate
BOC	- *tert*-butoxycarbonyl group
BOC$_2$O	- di-*tert*-butoxycarbonyl dicarbonate
CAC	- critical aggregation concentration (in M)
Cd	- cyclodextrin
CD	- circular dichroism
COD	- 1,5-cis cyclooctanediol
d	- doublet (NMR)
δ	- chemical shift (NMR, in ppm)
EM	- effective molarity (in M)
en	- ethylenediamine
ESI-MS	- electrospray mass spectrometry
Et$_2$O	- diethyl ether
EtOAc	- ethyl acetate
EtOH	- ethanol
HPLC	- high performance liquid chromatography
HSA	- hexanesulfonic acid, sodium salt
IR	- infrared absorption spectrometry
K	- association (affinity, stability) constant (in M^{-1})
K$_D$	- dissociation constant (in M)
λ	- wavelength (UV, in nm)
MALDI-MS	- matrix assisted laser desorption ionization mass spectrometry
MeOH	- methanol

mp	- melting point
NMR	- nuclear magnetic resonance
PBP	- phosphinyl bis phenylalanine
q	- quartet (NMR)
R_f	- retention factor (TLC)
R_T	- retention time (HPLC)
sDHB	- 2,5 dihydroxybenzoic acid + 10% w/w 2-hydroxy-5-methoxybenzoic acid
t	- triplet (NMR)
TFA	- trifluoroacetic acid
THF	- tetrahydrofuran
TLC	- thin layer chromatography
TNBS	- 2, 4, 6-trinitrobenzenesulfonic acid
UV	- ultraviolet absorption spectrometry

ACKNOWLEDGMENTS

Working with my major professor, Alan Schwabacher has been a special formative experience: I became professionally richer as a result of his guidance, support and creative thinking. I thank him for teaching me correct and innovative experimental procedures and how to try to explain and utilize experimental observations, results and even failures.

I thank Dr. Valerie Sheares for her moral and financial support, and for encouraging and allowing me to use the synthetic experience I have accumulated in this study, in polymer synthesis projects.

I am grateful to my committee members, Drs. Nenad Kostic, Glen Russel, Robert Thornburg and Walter Trahanovsky for their expert advice and valuable suggestions related to my research.

In addition, I would like to thank my family for their constant love, encouragement and support.

I. INTRODUCTION

I.1 Molecular Recognition

Molecular recognition is the study of the noncovalent, spontaneous and specific associations between molecular species. The strength of these associations is reflected by the value of the binding constant, sometimes referred to as stability, association or affinity constant K_a.

Binding is based on the stereoelectronic and steric complementarity between the interacting entities. The stereoelectronic determinants of the binding are what usually is defined as intermolecular attraction forces: Van der Waals, coulombian, hydrogen bonding etc. If, in the absence of steric repulsions, the enthalpic resultant of these forces is comparable or larger than the entropic cost of bringing the molecular species together, a significant binding constant can be evaluated for the macroscopic system.

In aqueous solvents, a good steric complementarity may bring a significant entropic contribution to the binding, through the hydrophobic interaction. In water a hydrophobic molecule decreases locally the entropy by restricting the variability of the intermolecular bonds of the solvent. Two approaching hydrophobic surfaces increase the entropy of the system by "liberating" the constrained solvent molecules. Binding based on the hydrophobic effect is always achieved on the expense of the entropy increase in the surrounding system. Therefore, in water, it is critical to amend any elemental combination of stereoelectronic and steric interactions with a systemic contribution of the hydrophobic interaction.

The preorganization of the host molecule in a relatively rigid structure, complementary to the guest has been a main focus in many molecular recognition studies. This preorganization avoids the entropic losses during the binding process.[1, 2, 3] The preorganization is essential for binding, especially in systems where the enthalpic

components of binding are weaker. The preorganization-based binding is frequently

encountered in biological systems. In a recent example, alcaligin,[4] a highly preorganized,

naturally occurring chelator was shown to bind iron 100 times stronger than any other more

flexible, natural siderophore.

Opposite to the trend of designing more and more preorganized host systems, added

flexibility is a design goal of transport and carrier systems.[5, 6] In these hosts the energy loss

due to the conformational changes upon binding is fully compensated by favorable

intermolecular forces. Their carrier and transport action is also based on high association

and dissociation rates, which in this case are prevalent over a strong binding constant

requirement. Drug carrier systems[5] or synthetic ionic channels[6] are direct applications of the

flexible hosts, able to wrap and unwrap around a guest which templates the formation of its

own binding site. Catalysis, also, take place easier in flexible hosts.

In addition to the enhancing effect on binding, the high rigidity of the hosts is a

requirement when the stereoselective binding is targeted. Size, shape and even diastereo-

and enantio-selectivity are strongly influenced by the rigidity of the host. Rigid hosts were

used in stereoselective resolution of compounds in solid or liquid biphasic systems.[7] Other

applications of synthetic systems derived from molecular recognition studies are the

construction of molecular sensors based on fluorescence or UV-VIS absorption and

nanoscale molecular devices.[7, 8, 9]

I.2 Representative Macrocyclic Hosts

Cyclodextrins were among the first naturally occurring series of hosts studied by

molecular recognition. The interest for the pioneering work of Cramer[10] is evidenced by

today's abundant applications of these host molecules. For example, synthetic catalysts were

obtained by functionalization of the parent compounds to imidazole-Cd's with ribonuclease

activity by Anslyn,[11] to amino-Cd's able to bind nucleosides and nucleotides by Schneider[12] or to synthetic transaminases by Breslow[13] (see section I.5). Cd's have found applications as sensors[14] or as threads[15, 16] and as potential ionic wires.[17]

The crown ethers discovered by Pedersen,[18] are the first designed and synthesized hosts able to bind metallic cations. The enhancement of cation solvation and binding by increasing the preorganization of the "p"-electron shells held together by the crown frame was continued by Cram[19, 20] and many other followers. Evolved forms characterized by high binding affinities are used today in catalysis and biological system simulations. Some examples are the binucleating aza-crowns,[21] the flexible lariat ethers[22] (crowns with linear side-chains), and the rigid, highly organized, bridged cryptand, spherand or carcerand structures.[23] For the rigid polycyclic structures, it was found that the selectivity for different cations follows the size matching model.[23] On the other hand, simple and more flexible crowns behave differently. The smaller aza-12-crown-4 binds better large cations than the larger aza-14-crown-4 due to the relief in conformational strain.

Following the highly organized models of the natural ionophores, other interesting preorganization-related studies make use of the non-macrocyclic synthetic hosts podands[7] or of the cyclic oligolides.[24] Their ionophoric action is based upon the effect of the additional hydropyranic rings, fused to the main linear or cyclic polyether chain and capable to induce strains leading to preorganization. These conformationally more homogenous host populations present stronger cation solvation and higher shape, diastereoselective and enantioselective recognition. Recently, aquaphoric activity was detected in certain aza-cryptands.[25] The water uptake is determined by the highly organized structure able to tetrahedrally bind the water molecule through H-bonds.

I.2.1 Hydrophobic, Van der Waals and π–π Interactions

Calixarenes are cyclophanic hosts resulting from phenolic condensations, which are used for cation or small molecule binding.[26] Water soluble versions $\mathbf{1}$[27] allow the qualitative evaluation of the electrostatic and hydrophobic contributions to binding. The binding constants determined by ^{1}H-NMR titrations for the guests $\underline{2a}$, $\underline{2b}$, and $\underline{2c}$ were $K_a =$ $(1.1\pm0.1)\times10^5$M^{-1}, $(7.6\pm0.7)\times10^4$M^{-1}, $(3.7\pm0.4)\times10^4$M^{-1}, respectively. These results suggested a convergence of a weaker ion pairing and a stronger hydrophobic inclusion interaction in the first two cases. Analyzing the ^{1}H-NMR shifts of the guest, the largest shifts were found for the ferrocenyl residue, while the proton shifts of the C$_7$-alkyl chain of $\underline{2b}$ were insignificant. This supports an inclusion topology of the ferrocenyl residue in the calixarenic cavity. The lower affinity of the positively charged $\underline{2b}$ may be the result of the steric interference due to the aliphatic chain with the ion-pairing interaction.

|	X
$\underline{2a}$:	$^+$NMe$_3$
$\underline{2b}$:	$^+$NMe$_2$C$_7$H$_{15}$
$\underline{2c}$:	OH
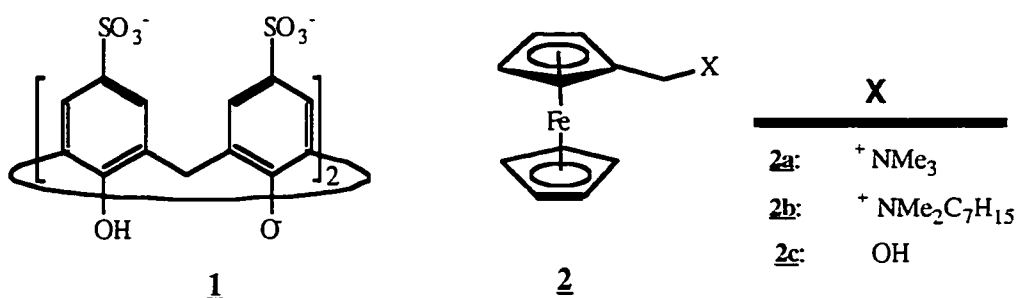
The conformational isomerism of the calixarenes is well known.[26] Larger conformational freedom degrees are found in urea calixarene analogs[28] or calixarenes with side-chains. Therefore, the binding to one of the calixarenic conformations - usually in the cavity of the full cone - has a significant energetic cost. However, the flexible (2-hydroxyethyl)-piperidinomethyl substituted calix[4]arene synthesized by Atwood and

coworkers[29] is able to bind tightly guests with different structures, precisely due to its conformational freedom. X-ray structures have shown that such a calixarene buries ethyl acetate in a deep cavity while the more voluminous N-hydroxyethylpiperidine guest is bound in a shallow cavity. In this "Venus flytrap", the cost of the reorganization between the different binding conformations is probably paid by the energetic gain resulted after the maximization of the hydrophobic host-guest contact surface.

In other cyclophane hosts, the connectivity of the benzene ring might vary from the o,o'-phenolic position of calixarenes. Therefore, there is much more freedom for the design of hosts for specific purposes. This is important, especially for binding studies with water soluble receptors. In order to obtain high binding constants, comparable to those found in the mimicked biological systems, it is important to rely upon the convergence of several intermolecular forces. An array of functional groups chosen to be complementary to those of the inclusion guest, is able to cooperatively enhance the binding by several orders of magnitude. Due to the strong solvent competition, the hydrogen bond formation between the host and guest is attenuated. Only weaker Van der Waals, electrostatic and inter-aromatic $\pi-\pi$ interactions are available to enhance the binding, which is mainly based on the hydrophobic interaction. Therefore, the design of these hosts focuses on the maximization of the host-guest contact surface and of the number of other parallel interactions. The directionality aspects of the electrostatic and Van der Waals interactions are less stringent than in the case of the H-bonds. Probes and models show that in the case of the less understood inter-aromatic[30, 31, 32, 33, 34, 35, 36, 37] $\pi-\pi$ stacking and edge-to-face ("T shaped", "π-aromatic H-bond") interactions, the directionality plays a significant role.

Nevertheless, there are other principles and restrictions which need to be considered in the design of efficient cyclophane hosts. The simple steric fit model of the guest "key" in the cyclophanic" hole" (E. Fischer) must be carefully considered, since in many cases has been misleading. The complexes of the Stetter's[38] cyclophane 3 with benzene and dioxane

are not able to form real inclusion complexes, due to the intramolecular, hydrophobic collapse of the flexible cavity. Therefore, rigid elements are needed for the preorganization of the shape of the cyclophanic cavity closer to the binding conformation. The diphenylmethane bridges incorporated in the host-cyclophanes **4** by Koga, are not allowing the intermolecular interaction (collapse) of the benzenic rings. The X-ray spectra[39] of the crystalline complexes support an inclusion topology. Several other cyclic "collapse-proof" hosts, based on the diphenylmetane motif, will be presented in the next sections. Other designs of anticollapse spacers, have been successfully used. For example, linear, enynic spacers were incorporated into acridinic hosts, designed to be used as DNA intercalands.[40]


3, n=2-4

4, n=2, 3
R=H or CH₃
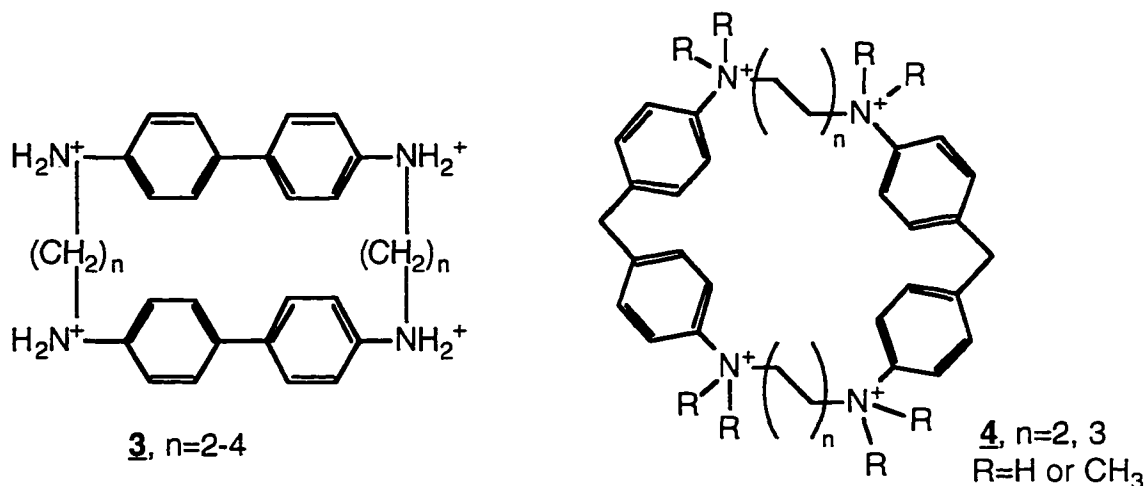
Koga's cyclophanes are soluble in aqueous or HCl solutions (**4** R = CH₃ or H respectively). By determining the stability constants of a large variety of guests,[41] it has been found that the selectivity of these para-cyclophanes is significantly higher for anionic naphthalene derivatives. These outstanding selectivities suggested a convergent binding mechanism: the hydrophobic inclusion is enhanced by parallel electrostatic and π–π inter-aromatic attractions. Also, a pronounced complementarity in shape selectivity was detected for the two hosts. Higher affinities of **4**, n = 2 for 2,7- substitution and of **4**, n = 3 for 1,8-

and 1,5-substitution pattern of the naphthalenic guests are due to the preferential binding in axial and equatorial conformations, respectively.

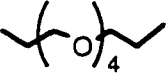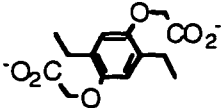## I.2.2 Interactions in Aqueous Systems: Hydrogen Bonding and Related Aspects
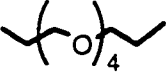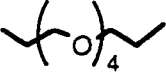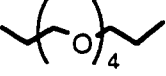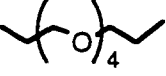
The isolation in space, of the charged (solvated) groups form the internal binding surfaces of the cyclophanic cavity is a further improvement in the design of these hosts. Thus, the interference of the solvation spheres of the solubilizing and other hydrophilic groups with the inclusion of guests within the host cavity is avoided.[42, 43]
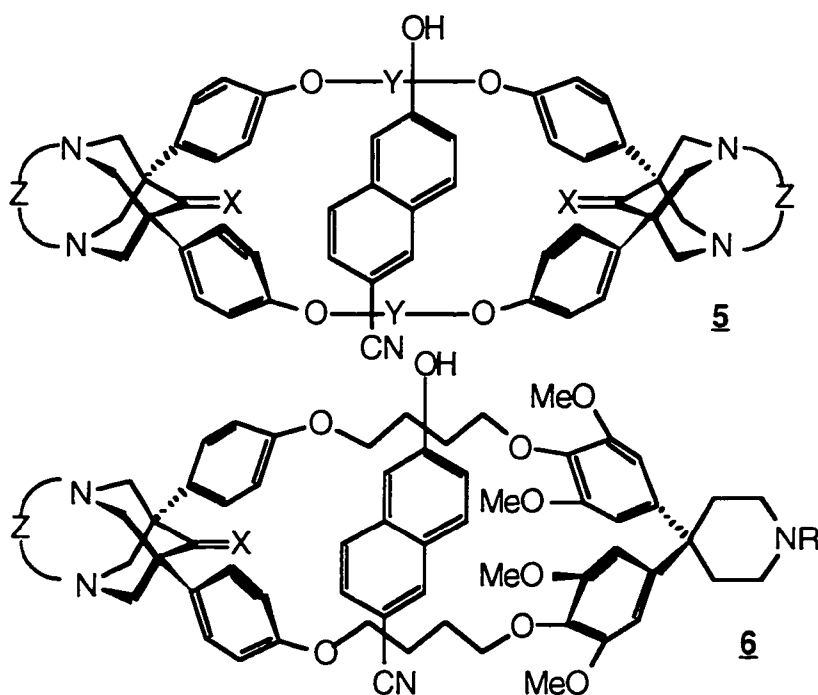
Diederich and coworkers[44] attempted to obtain several large cavity cyclophanes able to cooperatively bind steroids. The design was based on the intra-cavity location of the convergent functional groups capable to form H-bonds with guests in aqueous systems. The failure to produce high affinity hosts was disappointing, but a series of interesting

conclusions were drawn during this study, regarding the effect of intracavity hydration on the binding. Recently, a less elaborated steroid binding receptor was designed by Breslow[45] by linking 2 molecules of β–Cd *via* a sulfide bridge. The resulting ditopic receptor binds cholesterol with 2 orders of magnitude better than any other comercially available Cd derivatives.

Table 1   Structural elements and effects for paracyclophanes synthesized by Diederich[44]

| Cmpd	X	Y / R	Z	EFFECT
5a	O	(aryl structure)	-(CH$_2$)$_2$-	insoluble in acidic aq. soln.
5b	O	(aryl structure)	(–O–)$_4$ chain	CAC = 1x10^{-4}M soluble in 1.5M HCl[1]
5c	O	(aryl structure with $^-$O$_2$C, O, CO$_2^-$)	(–O–)$_4$ chain	CAC = 2x10^{-4}M soluble in 0.01M Na$_2$CO$_3$[1]
5d	O	(alkyl chain)	(–O–)$_4$ chain	CAC = 5x10^{-4}M soluble in 1.5 M HCl[1]
5e	H, OH	(alkyl chain)	(–O–)$_4$ chain	CAC = 3x10^{-3}M soluble in 1.5 M HCl[1]
6a	O	R = CH$_3$	(–O–)$_4$ chain	K$_D$ = 9x10^{-3}M [2]
6b	O	R = H	-CH$_2$-	K$_D$ = 3x10^{-2}M [2]
6c	H, OH	R = H	-CH$_2$-	K$_D$ >> 10^{-1}M [2]
6d	H$_2$	R = H	-CH$_2$-	K$_D$ = 5x10^{-3}M [2]

[1] No binding detected
[2] CAC ≥ 7x10^{-3}M, in MeOH-H$_2$O = 4:6

Symmetrical cyclophanes **5a-e** were unable to bind any guests with significant

strength due to various reasons. Host **5a** was insoluble even at high HCl concentrations due

to its high structural rigidity/crystallinity. The low binding ability, together with the low

critical aggregation concentration (CAC), prevented the evaluation of the more soluble **5b**.

The CAC value increased by enhancing the solubility of **5c**, but did not produce a better

host. The failure was attributed to the solvation of the carboxylate groups which interferes

with the inclusion in the host's cavity. As expected, the solubility and the CAC values

increased by reducing **5d** to **5e** but no significant binding was detected in this case either.

Disappointingly, the intra-cavity solvation of the C=O and C-OH groups designed to

cooperatively enhance the binding was precisely the effect which energetically defavored

the inclusion process. Removal of one of the convergent X = O or H, OH functionalities by

replacing one half of the cyclophanic ring with a shorter diphenylmethanic unit, finally

conferred to the resulting **6a-d** structures affinities for 2,6-naphthalenic derivatives as well

as for a bulky [4,2]-paracyclophane diol.

Analyzing the magnitude of ^{1}H-NMR shifts of the guest and those of the

diphenylmethanic and 1,3-diphenylpropanic residues from the host led to the following

conclusions: (i) naphthalenic guests bind axially; (ii) binding takes place closer to the

diphenylmethanic residue, where the most favorable interactions are taking place; (iii) no

gain results through intracavity H-bond formation between the host and the guest; on the

contrary, the observed binding free energies are smaller due to the desolvation of the

intracavity O atoms. Recently,[46] Diederich reported the successful use of 4 intra-cavity

convergent phosphate groups capable of forming ion-hydrogen bonds with disaccharides in

less associated MeCN-MeOH solvent systems. Association constants of $\sim 10^4 M^{-1}$ order of

magnitude were found for disaccharides while the corresponding monosaccharides have low

affinity for this receptor. This size-fit behavior in the absence of a hydrophobic effect, may

indicate that at least two of the interaction points are situated on different residues of the disaccharide.

However, the use of hydrogen bonds in complexations taking place in aqueous systems is experimentally precedented and even predicted as possible by Monte Carlo simulations.[47] The anomalously exothermic ΔH and negative T ΔS found in the binding of 7 host to p-cresol indicate the intermolecular formation of a H-bond. Two alternatives were considered: without and with the participation of water in the host-guest H-bond. The statistical mechanics simulations demonstrated that the second alternative is correct, i.e. the phenolic group interacts through its hydration water molecule with the acceptor groups on the host as part of an extended hydrogen bonded network on the host's surface.
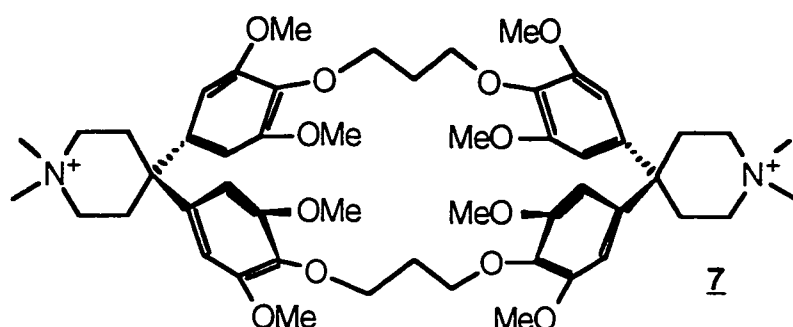
This type of binding behavior of the host 7 could be, to some extent, considered as mimicking the modulation by the bound water molecules of the substrate affinity detected[48] in biological systems. Compared to the model p-xylene complexation by the same host 7, the overall energetic balance of the H-bond association with the p-cresol remains slightly unfavorable. This is due to the entropic cost of ordering the hydration network of the entire complex. Similar conclusions were drawn in the case of the biological systems. The notable difference is that the overall energetic balance of the H-bond association in biological systems turns out to be favorable, due to their refined design.

For certain deoxygenated polysaccharide probes,[49] the binding to lectin epitopes was found to be weaker than for the corresponding hydroxylated analogs. The formation of an extra H-bond enhances the overall binding ($\Delta\Delta G = \Delta G_{deoxy} - \Delta G_{hydroxy} < 0$) but has the same partially compensating effects on the ΔH ($\Delta\Delta H < 0$) and on the entropic term ($\Delta\Delta S > 0$) as those found in the complex with p-cresol of the synthetic host $\underline{7}$. Similar in principle, a recent aminoacid mutagenesis study made by Schultz and coworkers,[50] has shown a gain of 1 to 2 Kcal/mol for each H-bond in folded proteins, relative to the corresponding H-bonds with the solvent of the denatured protein.
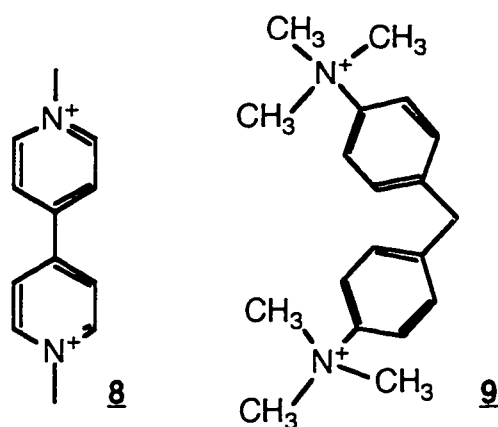
Schneider[51] extracted valuable information by comparing the inclusion complexation of naphthalene, diiodomethane, dichlorometane and other guests in the cyclophanic cavity of $\underline{4}$, n = 3 with the "open" receptors $\underline{8}$ and $\underline{9}$. It was determined experimentally that all the guests prefer the macrocyclic host $\underline{4}$ relative to the half macrocycle $\underline{8}$ by ~1.7kcal/mol. The authors explain this almost constant difference based on entropic effects or, enthalpically, considering that fewer molecules of water must be removed (desolvated) from a closed cavity than from outside the cavity. Molecular mechanics simulations show that the macrocycle's cavity contains only 4 water molecules participating to 5 H-bonds, while outside the cavity the average of H-bonds/water molecule

is 4. The difference between the experimental binding ΔG for the macrocyclic **4** and the double of the ΔG of the half-open receptor **8** is ~0.2-0.6 kcal/mol. The magnitude of this difference represents the extent of the cooperativity in binding of the two halves which form the macrocycle **4**. Using the more descriptive term introduced by Jenks,[52] the effective molarity value describing the cooperation of the 2 halves is EM = ~2M. In a similar study Lehn and coworkers[53] found that the 3-D macrobicyclic receptors are more efficient hosts than the monocyclic or half-open analogs.

I.2.3 Electrostatic and Polar Interactions

Electrostatic pole-quadrupole (cation-π) and induced pole-dipole interactions, as well as guest polarizability together with hydrophobic effects are important factors which influence the binding to the receptors **4**, **8** and **9** in aqueous systems. This combination of effects was used by Dougherty and coworkers for the complexation of organic ammonium salts. In the chiral host **10**, the Diels-Alder bicyclic adduct plays the role of a rigid, exo-cavity solvation element. Hosts **10a-c** having rigid X bridges bind with ~2kcal/mol stronger then **10d** as a result of the preorganization.

X	
[phenyl structure]	**10a**
[phenyl structure]	**10b**
[cyclohexyl structure]	**10c**
-CH₂-	**10d**, n=3-5

10   **11**
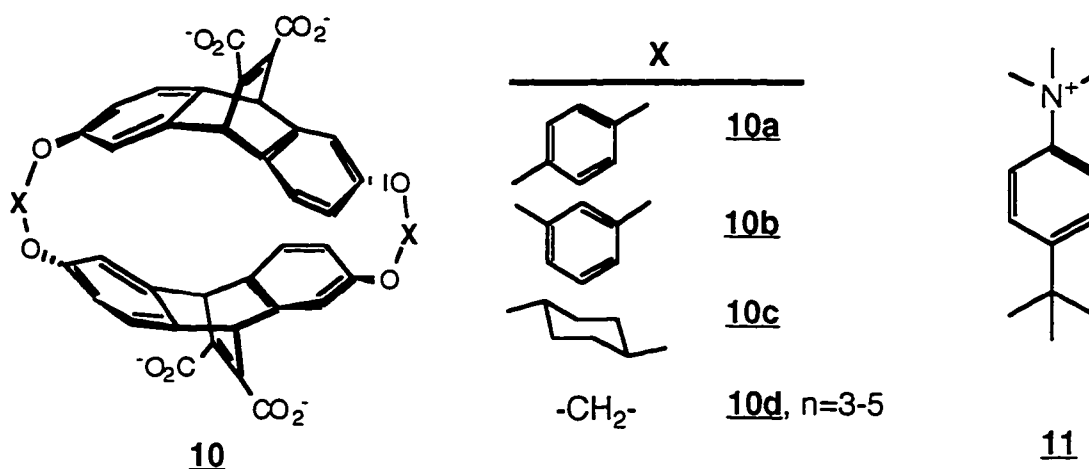
For uncharged aromatic guests, the main forces participating to binding are:

hydrophobic and π-stacking donor-acceptor interactions. The fact that the less hydrophobic

quinolinium salts, bind with ~1kcal/mol more tightly to hosts **10a**, **b** is a direct effect of the

cation-π interaction. Comparing the variation of chemical shifts of the methyl group protons

when the guest **11** saturates the host **10a** or **10d** revealed that the more hydrophilic Me_3N^+

group is included in the cavity instead of the more hydrophobic *tert*-butyl substitutent.

Studies revealed moderate enantioselectivities between the isomers of N-1-(1-

naphthyl)-ethane-N,N,N-trimethylammonium salts[54] and affinity for the acetylcholine

neurotransmitter.[55] Subsequent studies[56] extended the range of neutral, positively charged,

aliphatic or aromatic guests. The use of a newly developed CD and data work-up technique

provided important structural insights into the geometries of the complexes. In the same

time, CD allowed the determination of exceptionally high binding constants of azulenes and

other guests presenting cationic mesomers to receptors **10** ($K_a = \sim10^8 M^{-1}$). Several other

derivatives of **10**[56, 57] were used to probe the magnitude of the π-cation effect, shown to be

strong enough to determine directional preferences and internal conformational twists inside

the host-guest complexes.

X, n=0-1

12a, meta
12b, para

12c

12d

12

13
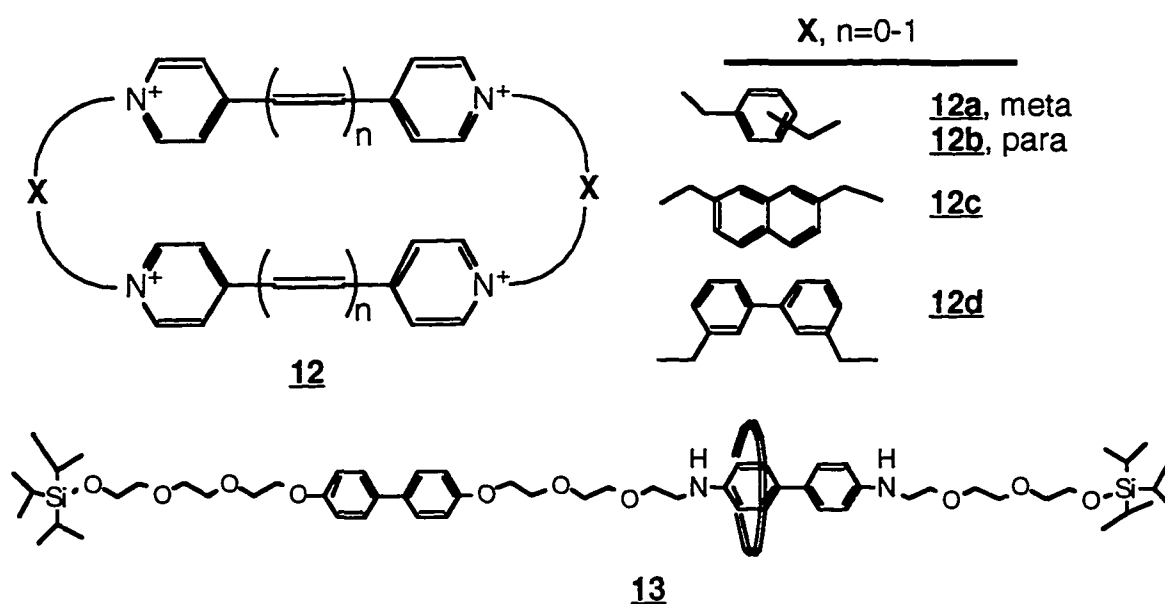
In the case of pyridinium cyclophanes **12**, a charge transfer character of the interactions with electron-rich guests was predominant. The hosts **12a**, **12c** and **12d** are able to form inclusion complexes[58] with naphthols or naphthylamines without notable conformational rearrangements from their free "sandwich"-like conformations. With strong enthalpic charge transfer interactions and low entropic preorganization cost, the high binding affinities of hosts **12** seem not to be influenced by the charge which is adjacent to the cavity.

Host **12b**, n = 0, is a frequently used constituent element in the rotaxanes and catenanes studied by Stoddart and coworkers.[59, 60, 61] The charge transfer interaction between the macrocycle **12b**, n = 0, locked onto the polyethyleneglycolic thread containing two competitive electron-rich guest motifs is used as a templating driving force[59] in the synthesis of the rotaxane **13**. In the free rotaxane the macrocyclic ring prefers the interaction with the benzidinic ring. Protonation or eletrochemical oxidation of the rotaxane are determining the formation of cationic centers on the benzidinic unit of the thread and the decrease of the affinity of **12b** for this motif. Therefore, the macrocycle "shuttels" to the other guest "station" in a process which allows the comparison of the rotaxane **13** with a "nanoscale molecular switch". Such a device, as well as other similar rotaxanes which are light activated[60] may be useful in future information storage systems.

Organic anion complexation is also possible by ion pairing interactions. In organic solvents, H-bonds or ion-dipole interactions may represent enough driving force for high affinity complexations. Ammonium, guanidinium, phorphirin complexes, and cobaltocenium groups are efficient[62] counterions which have been incorporated in various water soluble phosphate hosts. Several examples of the complexation of the physiologically important organic phosphate anion are given next.

I.2.4 Effects of multipoint binding

By converging the ion pairing with several other interactions, such as H-bonds, Van der Waals and hydrophobic interactions, a higher specificity for certain organic anions is obtained. High specificities for the organic or the inorganic residue of the phosphorylated species are reached by multipoint binding, where the binding site is more or less separated from the discrimination site. Significant selectivity differences between the binding of AMP, ADP and ATP nucleoside-phosphates were obtained by using the multicationic host 14.[63] pH-modulated selectivity and different binding sites (extra- or intra-concavity) for guests of different sizes and charges are the characteristics of this aza-crown-like host.
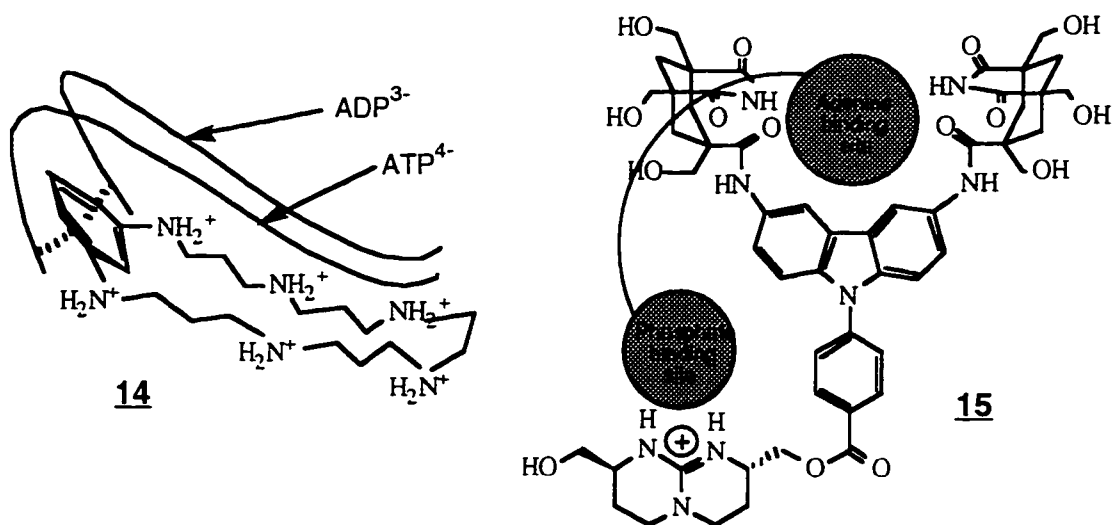
The discrimination of the nucleobase was reached by Rebek and coworkers.[35] The specificity of the discrimination site in the host 15 is given by Watson-Crick and Hoogsten H-bonding, π–π stacking and hydrophobic interactions. Receptor 15 shows selectivity for 2',3'- and 3',5'-cyclic AMP over the corresponding cyclic GMP species.

Phosphate ligation may constitute an important contribution in the multipoint binding by hosts containing metallic cations. The dinuclear chelate-host 16[64] shows ditopic

binding of the phosphates ($K_a = 10^4 M^{-1}$) but fails to hydrolyze them. The effective molarity [EM $= (K_D^{Zn\text{-phosphate}})x(K_D^{Zn_2\text{-phosphate}})xK_a)][52] characterizing the phosphate complexation is estimated to 0.4M when a value of pK $= 2.4$[65] is used as a reference for the phosphate ligation. This calculated value must be considered as a lower limit for the EM, because the binding of phosphate to a second Zn center is probably characterized by a lower pK (which is not available from literature data).

16
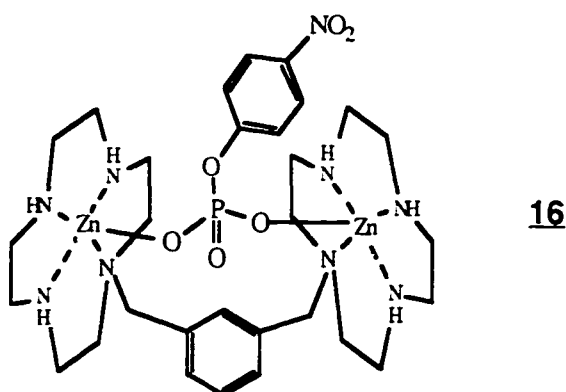
Similar multipoint binding with bis-metal chelate clefts, which includes aromatic stacking, has been used for the binding of other more complex bidentate ligands, such as bis-imidazoles.

I.3 Stereoselectivity

Stereoselective binding, one of the most desired and difficult to achieve goals in the design of a host, is also a result of a multipoint interaction. There is general agreement,[23,66,67] that no direct correlation exists between the binding affinity and selectivity in general. High enantioselectivies have been achieved when the chiral hosts were designed with separated binding and selectivity sites. The binding site is responsible for the attractive interaction, while in the selectivity site, both attractive and repulsive interactions (steric,

electrostatic, solvation based etc.) are possible. Thus, di- or poly-topic attractive interactions

determine higher affinities for certain substrates. On the other hand, repulsions at the

selectivity site will diminish the overall binding constant of the substrate due to the

energetical cost of the conformational rearrangements of the host. The latter, constrictive

way to achieve stereoselectivity is also common for receptors with no obvious separation of

the selectivity and the binding sites. Since the directionality of the H-bonds is less available

in aqueous systems, the design of the stereoselective host is more difficult and needs to

relay upon the cooperativity between π-stacking, electrostatic and hydrophobic interactions.

In many cases, the initial binding studies made on the achiral cyclophanic hosts are

continued on a chiral analog of it which has incorporated a chiral or prochiral synthon.

Enantioselective "Koga macrocycles" **17**[68] (R = H) towards aromatic amines, hydroxyacids

or aminoacids were obtained by incorporating tartaric acid derived bridges. The highest

stereoselectivity value found was of R/S = 0.60.

The frequently used major groove of the 1,1'-binaphthyl constituted a common

chiral recognition motif. The Diederich's cyclophanes **18**[69] showed enatioselectivity towards

naproxene derivatives and quinolinic alkaloids (R/S = 0.56).

Ethanolic solutions of calixarenes **19**[8] were used as molecular sensors to distinguish

between the enantiomers of benzylamine and phenylethylamine derivatives. The significant

color changes noticed when the host binds selectively a certain enantiomer, is probably the

result of the use of EtOH instead of water as a solvent, which allows more directional and

therefore more specific interactions to occur.

The minor groove of the 1,1'-bis-β-naphthol discrimination site was used in

Stoddart's macrocycle **20**, yielding hosts with R/S = 2.4 towards tyrosine in water.

Remarkably higher enantioselectivities and binding constants were obtained for the same

receptor and N-Ac-Tyr-OMe in nonprotic media: R/S = 0.13.

Analyzing some of the results obtained in this preliminary study (Figure 1) leads to

several interesting conclusions: (i) the weak binding of acetylated phenylalanine to **20** is due

to weaker charge-transfer interactions; (ii) the low affinities of the tyrosine methyl-esters

indicate that the carboxylic acid function contributes to the binding even in aqueous

solutions; (iii) the reversed selectivities and large affinity variations found in non-protic

solvents suggest a qualitative change in the attractive interactions at the discrimination site,

possibly a preponderance of the H-bonding in the complexation of (L)-N-Ac-Tyr-OMe.
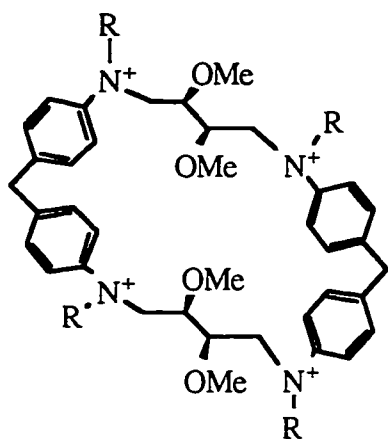
17
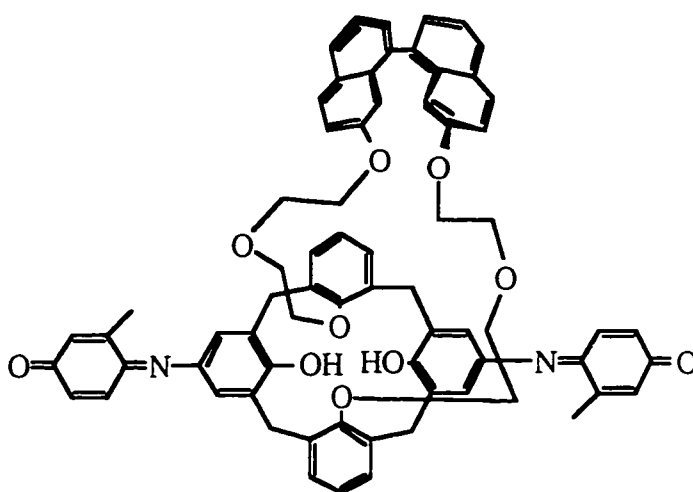
19
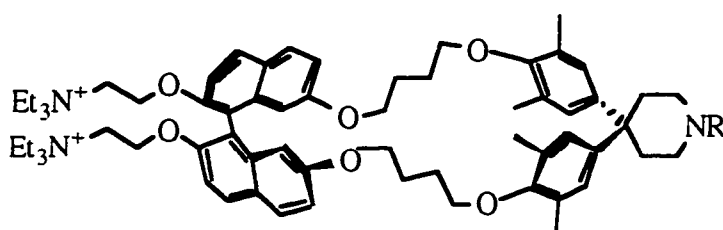
18

Other chiral and rigid discrimination sites incorporated in cyclophanic hosts are

Dougherty's dibenzo-bicyclooctane adduct (in cyclophane **10**) and the Troger's base used by

Wilcox and others. Dougherty's hosts show modest enantioselectivities for quaternary

aromatic ammonium salts[54, 70] and Wilcox's enantioselectively bind terpenes.[54, 70] A podand

ionophore[7] is an example of open (acyclic) but highly organized host, capable to resolve derivatives of racemic aminoacids.

One of the highest values of enantioselection in aqueous systems was found by Lee and Schwabacher[71, 72] for the self-assembled cyclophanic host **31**. The ratio of R/S = 0.11 determined for 2-(1-naphthoxy)-propionate is due to the constrictive binding conditions: the methyl group of the R isomer is hindering the adoption of a conformation suitable for a ditopic binding.
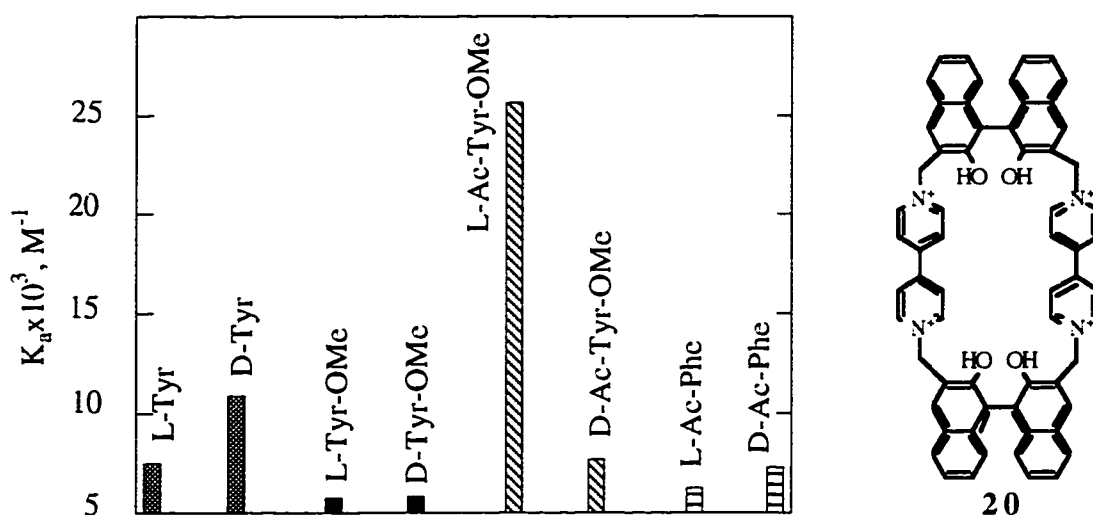
Figure 1   Association constants for tyrosine (Tyr) and its derivatives in aqueous media
- for free Tyr and its Me esters (-OMe)- or nonprotic media, in MeCN-DMF
= 9:1 - for acetyl derivatives, (Ac-)

A promising future source for stereoselective hosts is combinatorial organic synthesis. Still and coworkers have obtained encoded combinatorial libraries of receptors for steroids[73, 74] and unnatural peptides.[75, 76, 77] These libraries are usually biased, their characteristic variability starting from known motifs previously studied by "conventional" molecular recognition methods.

I.4 Self-Assembled Water-Soluble Receptors

Mimicking more and more complex self-assembly processes at control levels comparable with those found in the biological systems is another goal of molecular recognition. Usually, the self-assembly processes consist of single or multiple recognition steps between host and guest species capable to generate ordered and stable structures. Self-assembly is a convenient synthetic way to build complex receptor structures by a "one pot" formation of several covalent or noncovalent bonds. Self-assembled synthetic hosts may bring new insights into the corresponding formation processes of catalytic or receptor sites in biological systems. Self-assembled monolayers and nanoscale devices are potentially useful in electronic and information storage applications.

In the design of hosts soluble in organic solvents, H-bonds are the most frequently used driving force for self-assembling. Their directionality and significant enthalpic contribution yields highly ordered and stable complexes. Rebek's self-complementary ligands,[78, 79, 80] capable to reversibly form "tennis ball" shaped capsules around various templating guests, constitute a promising class of drug-carrier candidates. When a mixture[79] of different ligands is used, the ratio of the formation of homo- and hetero-capsules is dictated by the size of the encapsulated guest. The release of the guest from these capsules occurs in hours. However, their applications as retard-effect drug carriers is limited to nonprotic solvent media as it happens with the buckyballs related in shape. On the other hand, the template assisted cyclizations and the self-assembly of rotaxanes and catenanes by the method pioneered by Stoddart was able to pass the gap between organic[59, 61] and aqueous[60] media. These processes are based on the preponderent charge-transfer and $\pi-\pi$ interaromatic interactions which are less solvent dependent (see structures 12 and 13).

Chelation and complexation are the most frequently used directing mechanisms for self-assembling processes in aqueous solutions. In many cases, the hosts assembled through

metal complexation behave as allosteric ditopic binding sites, analogous to those found in biological systems. The metal has a structural role in preorganizing the host in a conformation suitable for binding. In addition to this structural role, the metal may influence the binding and catalytic properties of the host. In these cases, the metallic center also plays a major functional role.

Slow ligand exchanging metals such as Pd and Pt were used by Fujita and coworkers[81] in the self-assembling of polynuclear complexes **21**. In subsequent studies the similar affinity of **21** for dimethoxy or dicyanobenzene ($K_a = 2.0 \times 10^3 M^{-1}$) decreases with the polarity of the solvent, from water to 1:1 water-MeOH. This suggests that the hydrophobicity and not charge-transfer has the main role in these binding processes.

Hydrophobicity is also the main driving force[82] that directs the quantitative self-assembly of the remarkably ordered [2]-catenane, when the same reactants used in the synthesis of **21**, 1,4-bis[(4-pyridyl)methyl]benzene and $enPd(NO_3)_2$, are mixed at concentrations of $\sim 1mM$.

Selective assembly of macrotricyclic hosts was also achieved by using the ligands **22** (Py = 4-pyridyl) in the presence of suitable templates.[83] The similar self-assembly yields obtained in the presence of different templates, varying from p-xylene to 1-adamantane-carboxylate, suggested that the hydrophobic effect is again the preponderant driving mechanism. The sharp drop in yields from 72-94% to 0-36% when naphthalenic guests were used suggested to the authors an "induced fit" effect in this templated self-assembly process.

An even more complex adamantane-like host **24** ($Pd = Pden_2^{2+}$, Tr = **23**) was produced with 90% yield, when ligands **23** containing a triazine core (Ar = p-phenylene or 4,4'-biphenylene, Py = 4-pyridyl) were used.[84] A complex of the host **24** encapsulating 4 molecules of adamantyl-1-carboxylate has been isolated and studied. The obvious potential use of these "container molecules" is as drug carriers.

21

22

24

23
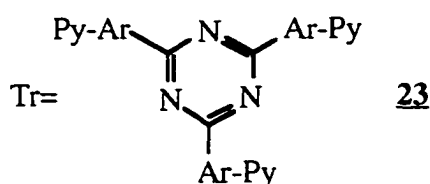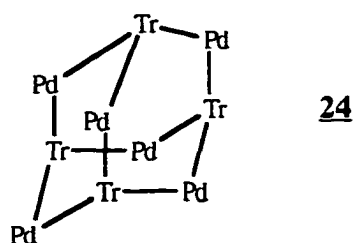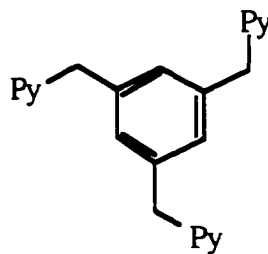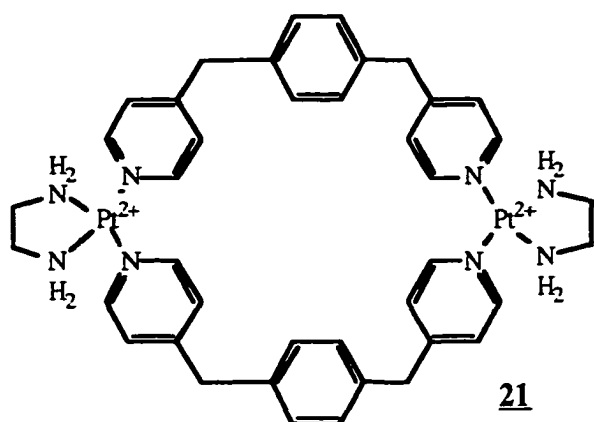
Different synthetic strategies were used in the self-assembly of hosts 25 and 26. The fluorescence intensity of mixtures of the free ligand corresponding to 25 and TNS (toluidino-naphthalenesulfonic acid) show large increases upon addition of aqueous $CaCl_2$ solution.

The amphiphilic mixture of 26 and the corresponding bis-cobaltocenium macrocyclic dimers[85] are obtained with low yields when the preformed cobaltocenium bis-acyl chloride was treated with (ethylenedioxy)bis(ethylamine) in conventional, low dilution, acylation conditions. A self-assembling preparation might constitute a better approach allowing selectivity control between the monomeric or dimeric macrocyclic species. The increased ligation of halide anions in DMSO by hosts 26 relative to an acyclic cobaltocenium control molecule was explained briefly as a "macrocyclic anion effect". This probably means that the Co atom plays both structural and functional roles in these macrocyclic hosts.

The cofacial binuclear complex 27 was isolated and characterized by Maverick.[86]

The copper plays an essential functional role in the polytopic binding of pyrazine substrates in organic solvents. The highest affinity was found for aminopyrazines ($K_a \sim 10^2 M^{-1}$) due to concomitant ligation to both metal centers and H-bonding to one of the pentanedionic chelating groups.

25, n=3,4

26

27

X

27a

27b
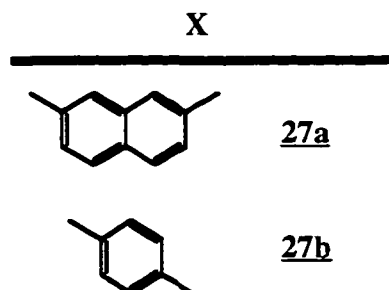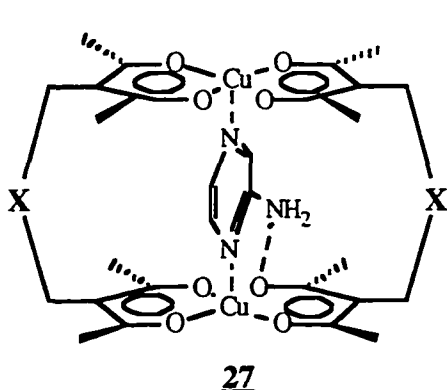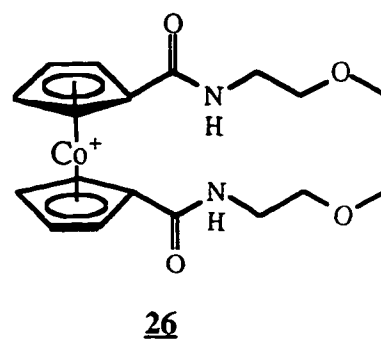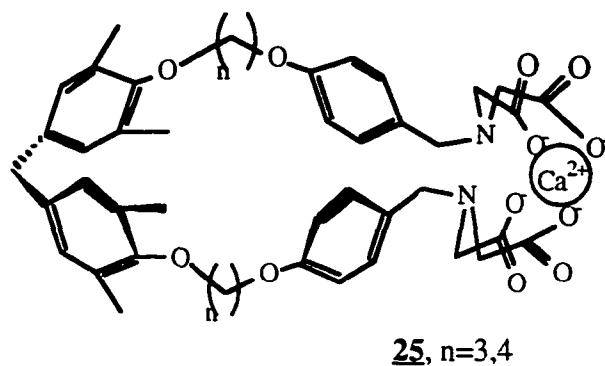
Schneider[87] studied the allosteric behavior of metallated cyclophanic hosts **28**. The copper and zinc complexes **28** bind dansylamide or naphthalene by one or two orders of magnitude weaker than the related Koga's host **4** (R = CH3). The explanation was based on the smaller contribution of the π-cation effect in the binding aromatic guests.

Recently Schneider[88] reported the synthesis and study of a more complex allosteric system **29**. The free ligand (L), forms complexes with both Zn(II) and Cu(II) in a M2L

stoechiometry. However, in the presence of naphthalenic fluorescent guests **G**, only ternary complexes MLG are formed indicating a negative cooperativity effect towards the second metal ligation.

Significant intensity changes in the fluorescence spectrum of mixtures of **G** and the free ligand occur only in the presence of the metal cations indicating the inclusion through a ring-contraction allosteric effect. The binding of the negatively charged guests **G** was found to be enhanced by the supplemental electrostatic interaction with the complexed metal. Allosteric systems similar to **29** may find applications in the detection of low concentrations of certain metal cations.

Another example of allosteric system is **31**, (Section III), where the metal center modulates the binding and the stability of certain substrates in aqueous systems is the self-assembled phospha-metalla-cyclophane developed by Lee and Schwabacher.[71]
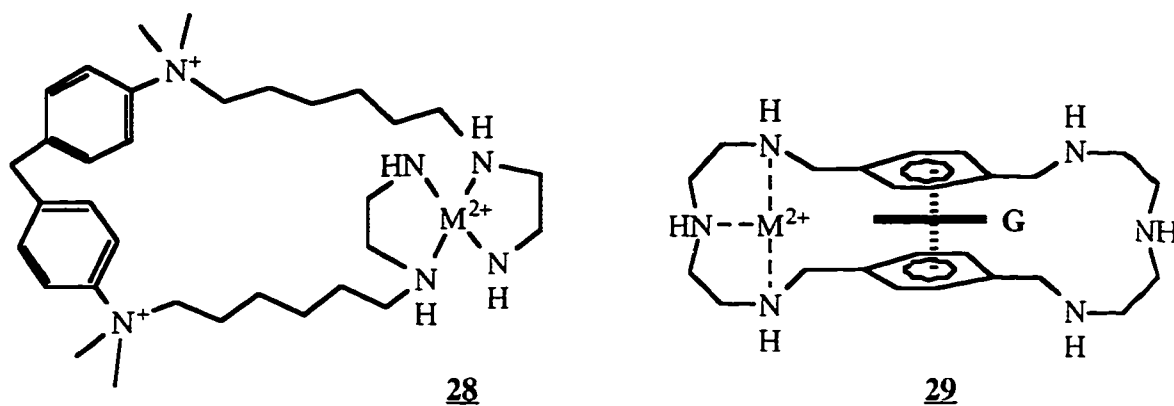
I.5 Biomimetic Catalysis

Artificial catalytic hosts are important models in the understanding of different biological catalytic phenomena. Due to specific characteristics (e.g. resistance to proteases etc.) artificial catalysts may improve, complement or substitute the mimicked enzymes in different applications or in biological systems.

The principle of enzymatic catalysis, as proposed initially by Pauling[89] over 40 years ago, is based on the differential binding of the transition state relative to the ground state. "The entire and sole source of catalytic power is the stabilization of the transition state; reactant-state interactions are by nature inhibitory and only waste catalytic power" [90] is one of the reformulations and generalizations of this principle which is not able to account for all the catalytic processes where the strong enzyme-substrate interactions were found. According to the relatively recently developed "split-site" biocatalysis model,[90] there are exceptions, where the substrate is tightly bound by the catalyst at the "binding site". The "catalytic power" is enhanced at the "catalytic site", which has a different spatial location, based only on the entropic effect of bringing the reactants together in the proper orientation (the effective of molarity is high). Then, the actual catalytic conversion takes place according to the classical transition state stabilization, at the "catalytic site".

Many of the synthetic catalytic hosts are acting in a "split-site" fashion. In the case of modified cyclodextrin catalysts, many examples may be found[91] where the inclusion site is located at a certain distance from the extracavity "catalytic site" usually attached to one of the rims.

Many of the cyclophanes presented in the previous paragraphs show catalytic actions (e.g. $\underline{10}^{92}$ in S_N2 methylations; $\underline{4}$ with attached pyridoxamine side-chain[93] in transaminations; aza-crowns[94] in enolizations). Beautiful examples of auto-catalysis are the biomimetic self-replicating nucleoside (Rebek[95, 96, 97, 98, 99]) or peptide (Ghadiri[100]) analogs.

30

Breslow used the inclusion complexes formed by β–Cd's with aromatic residues to construct an efficient metallo-phosphatase mimic.[101] The catalytic action is based on the appropriate positioning in **30** of an efficient catalytic group, the La-H_2O_2 complex relative to the substrate, cooperatively bound by 2 Cd-residues. The observed rate accelerations of $>10^7$ are significant for an artificial enzyme mimic (typical "natural" enzymatic rate enhancements[102] are 10^{10}-10^{15}). Product inhibition is avoided by canceling the cooperativity effect between the Cd "binding sites" upon the cleavage of the substrate.

Relatively few examples are known of metallo-phosphatase mimics. Bis-imidazolic clefts[103] or Cd's[11]) without metal centers exhibit smaller rate accelerations. Also, phosphatase mimics are less known among the antibody catalysts or imprinted metallopolymers, due to the difficult access to the corresponding pentavalent transition state analogs. In these cases, organic phosphates are used for antibody eliciting[104, 105] or template polymerizations,[106, 107] yielding esterolytic materials which usually are inhibited by phosphates.

Due to less complicated design, most of the known phosphatase mimics are organic chelates without hydrophobic binding site.[108, 109] Several examples will be given in Section IV.4.

II. SCOPE AND OBJECTIVES

The main scope of the present study is to gain more knowledge about how to design and study self-assembling hosts able to bind with high affinities and selectivities.

A self-assembling host which was designed, synthesized and studied in Dr. Schwabacher's group is the Co_2PBP_2 **31**. The comprehensive study of this host has shown that: (i) the self-assembling process yields the desired structure **31**; (ii) this host shows cooperativity and selectivity in the binding of naphthalene and indole species; (iii) this host is capable of size and shape recognition; (iv) compared with other synthetic, water-soluble hosts, the Co_2PBP_2 host presents one of the highest binding enantioselectivities reported in literature.

M_2PBP_2: **31**
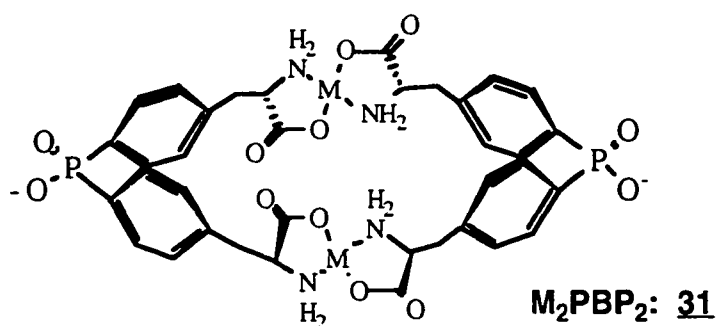
The following structural features of **31** determine several limitations on the performances of this macrocycle: (i) the negatively charged aminoacid chelating groups determine a negative cooperativity in binding anionic hosts; (ii) the relatively low stability constants of many aminoacid-metal chelates determine the dissociation of **31** in the conditions of the low dilution binding studies; (iii) the Co(II) complexes of the type **31** are paramagnetic, being sometimes difficult to study by NMR techniques; (iv) the chelated Co(II) is not oxidable to Co(III), preventing the access to the study of less transient macrocyclic species.

The question we decided to address is: can these limitations be removed by simply changing the nature of the chelating groups? The predictions were, that replacing the aminoacid groups of **31**, with polyamines, would provide the Schwabacher research group with a complementary, more stable cationic host. Cationic and anionic binding probes are necessary for the correct evaluation of the different concerted binding interactions present in these hosts and the biological systems they are mimicking.

Several study stages are necessary to accomplish the above mentioned objectives: (i) completing the binding study of the known Co_2PBP_2 with a set of significant guests; important structural and behavioral comparison elements with the newly designed macrocyle will be thus obtained; (ii) studying the ligand synthesis; (iii) studying the individual properties of the ligand and different metal macrocycles; (iv) performing the binding studies.

III. DESIGN OF THE MACROCYCLE

Several structural elements are important in the design of a macrocycle related to the M2PBP2 hosts **31**. The diarylphosphinate groups **32**.(Scheme 1) have the following desirable properties: (i) it is a hydrophobic collapse[39, 71] proof element; (ii) solubility in aqueous systems; (iii) external hydrophilicity; (iv) inter-convertibility between phosphinate-ester, phosphinate-salt and phosphonium-salt functional groups, which creates access to novel series of receptors with anionic, nonpolar or cationic character in the covalent connection point.

The chiral phenylalanine motif **33** will also be retained in a similar form in the new structure. Retaining the connectivity of the M2PBP2 macrocycles will allow the comparative evaluation of the effects of the new chelation group.

Micromolar range affinity for different metals and formation of positively charged complexes are the main requirements for a suitable chelating group. A group of choice may be the ethylenediamino **34** group: its metallic complexes have high stability constants and are usually positively charged. Such a macrocyclic binding site is expected to exhibit cooperativity in binding due to the convergence of the electrostatic interactions and ligation. The metallic complexes of ethylenediamine are formed in a large variety of configurations: planar, tetrahedral, octahedral etc. This can be regarded as a supplemental advantage, since different metals will generate, through a simple complexation reaction, macrocyclic hosts with huge differences in the cavity geometry and, consequently, in binding and catalytic activities.

The ethylenediamino group also provides easy access to kinetically locked or less labile macrocycles, when metals such as Co(III), Pd or Pt are used in the self-assembling process. The Co(III) octahedral complexes provide chelation sites for other slow exchanging ligands, which may induce structural changes or serve as catalytic sites in the resulting host.

PBP: **32**

M₂PBP₂: **31**

33

34

BDAP: **35**
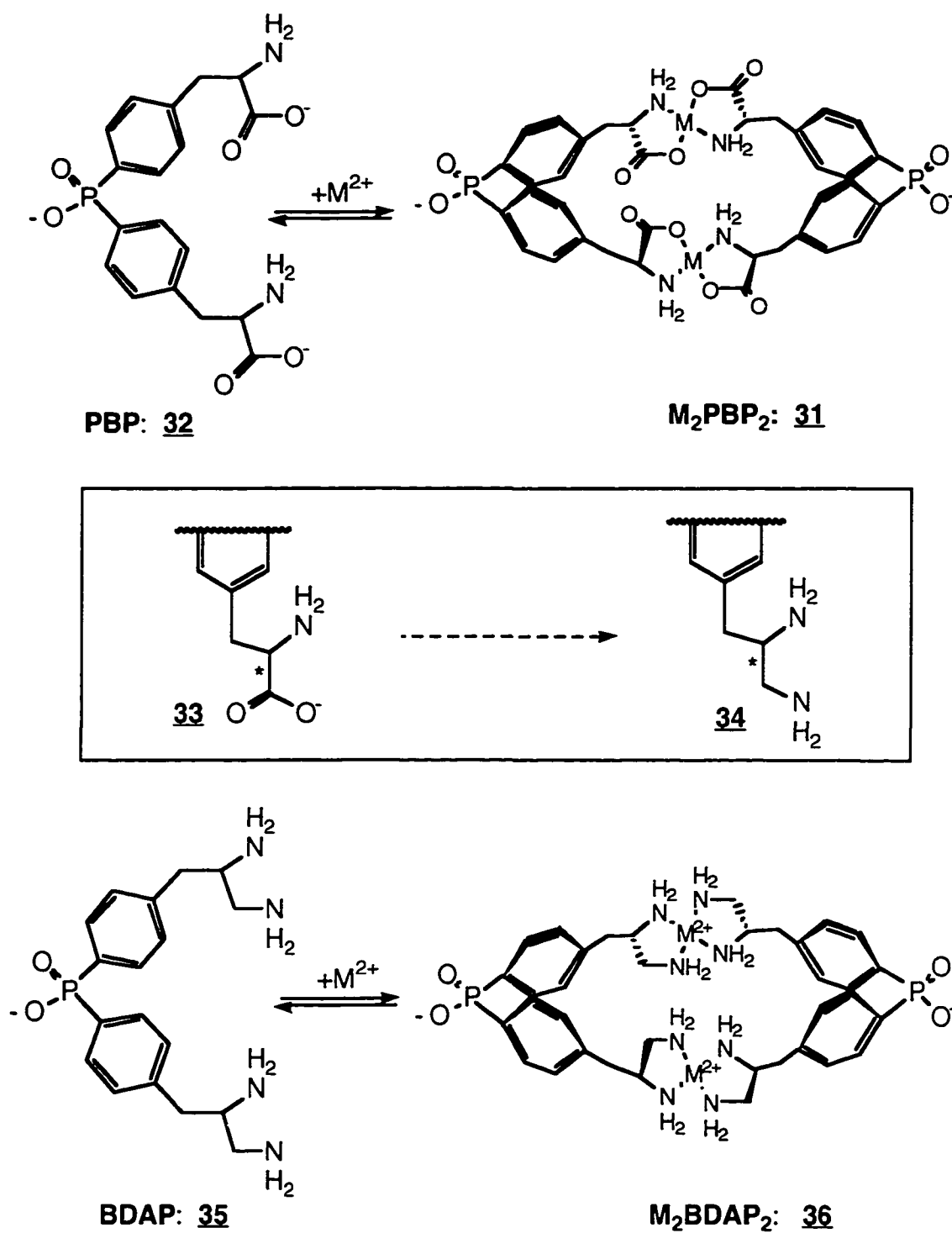
M₂BDAP₂: **36**

Scheme 1   Design elements for the generation of a cationic macrocylic binding site:

M₂BDAP₂

Aqua complexes of ethylenediamine type ligands with Co, Zn, Cu or other metals

are known to exhibit catalytic[109] activity as esterases and phosphatases[110, 111] or

proteases[109] and racemases.[112]

Therefore, a significantly different BDAP ligand, **35** was derived from the structure

of the PBP ligand **32** by making small structural changes **33** —> **34** (Scheme 1). The

stereochemistry of the chiral center was chosen (S) due to the natural availability of the

phenylalanine which will constitute the main building block for the synthesis of the ligand

(Scheme 1). The chiral centers will confer stereoselectivity for the hosts incorporating the

BDAP ligand, and in the same time represent sensitive probes in the determination of the

binding constants through circular dichroism. Obviously, the M_2BDAP_2 hosts will present

diastereoisomerism at the metal center. The importance of this feature is most relevant in

the case of the kinetically inert complexes, when these diastereomeric macrocycles may be

isolated and studied as separate entities.

IV. RESULTS AND DISCUSSION

IV.1 Synthesis of the BDAP Ligand

IV.1.1 Initial Synthetic Work

We decided to prepare the BDAP ligand **35** from protected PBP **38** previously

prepared in Schwabacher group.[71, 72, 113] The initial synthetic route for the preparation of

the BDAP ligand (Scheme 2) starts from the known[113] (L)- N-BOC-iodophenylalanine

methyl ester **37**.
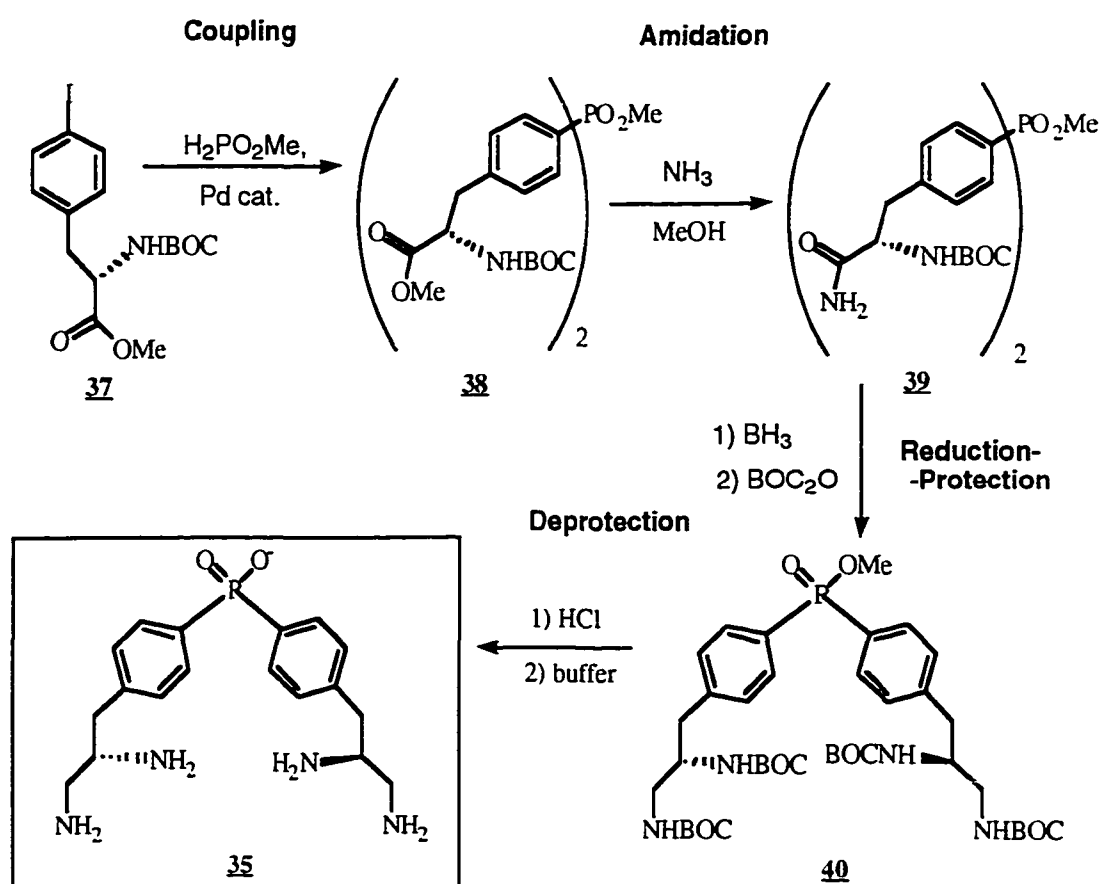
Scheme 2   Preparation of the BDAP ligand (Initial synthetic work)

The one pot coupling of **37** with methyl phosphinate, in the presence of a Pd(II)

catalyst yields diarylphosphinate **38**. The conversion to amide is easily achieved using the

general aminoacid amidation procedures.[114] The crucial step in this proposed scheme would

be a selective reduction of **39** which should affect only the amide residue. The protection of

the amine would make the purification of the final protected ligand **40** easier. The

deprotection of **40** is expected to be facile and quantitative, yielding the hydrochloride of

the ligand **35**, ready to be used in binding studies if dissolved in a borate ~pH 9 buffer, in

presence of an appropriate transition metal cation. This method offers the possibility of

orthogonal protection of the newly formed amino group (Scheme 2, step I.3).
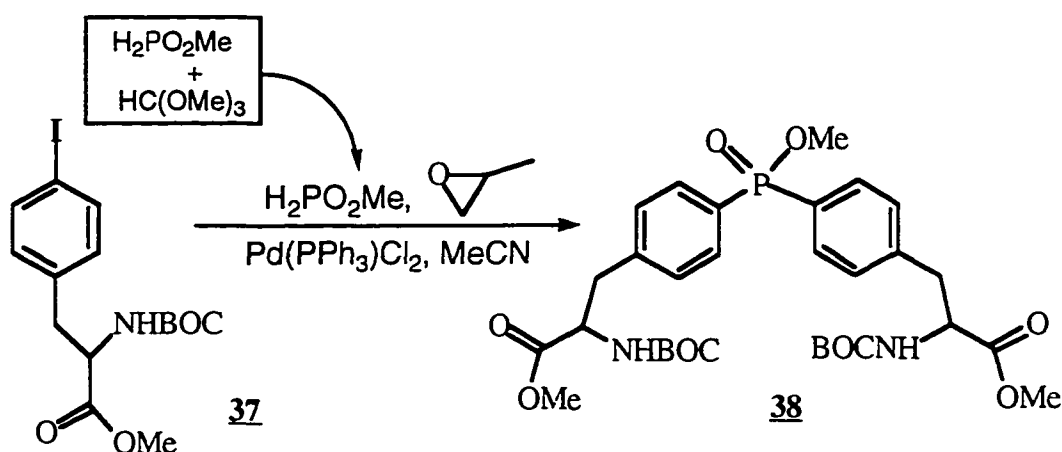
Scheme 3   The Pd catalyzed coupling between methyl-phosphinate and
             N-BOC-iodophenylalanine

IV.1.1.1 Coupling (Scheme 2)   The esterification mixture formed from the

reaction of phosphinic acid with trimethyl orthoformate[115] (Scheme 3) yields methyl

phosphinate which is used directly as a starting material in the one pot coupling[113] with the

aryl iodide (**37**, Scheme 3) to yield 57% isolated yield of symmetrical diarylphosphinate **38**.

However, the several flash chromatographic systems tested were unable to separate the

product from an impurity, which based on ^{31}P- and ^{1}H-NMR peak attributions, is a

dimethyl arylphosphonate. In previous studies,[71] this variable impurity could be removed by fractional crystallization, only after deprotecting **38** to PBP. In the present study another impurity was revealed in the ^{31}P-NMR taken in $CDCl_3$ solution of the product separated after the flash-chromatographic step. This impurity peak appeared as a shoulder, at 32.22 ppm near the product peak, at 33.00 ppm. The peak corresponding to the phosphonate impurity was also present at 20.85 ppm. One possible source for these impurities is the initial esterification mixture used as a starting material. Gallagher[116] reported that the methyl phosphinate is accompanied by significant amounts of phosphonate impurity.

IV.1.1.2 Amidation (Scheme 2)   The amidation step in methanol saturated with ammonia, followed the general amidation procedure.[114] The yield is 84% but again the flash chromatography was unable to separate a pure compound. The ^{31}P-NMR indicates that the impurities are in the same structural relationship as those present in the starting ester: a shoulder, at 36.67 ppm of the main product **39** peak, at 36.83 ppm and the 23.68 ppm phosphonate impurity peak.

IV.1.1.3 Reduction / Protection (Scheme 2)   Two systems were tested for the selective reduction of the amide group of **39**. The $NaBH_4$ and I_2 in THF[117] was reported to selectively reduce amides in presence of carbamates. However, in the case of the compound **39** or of the model methyl diphenylphosphinate, this reduction system affects the phosphinate group, causing the complete disappearance of the P-OCH$_3$ doublet and the appearance of a P-H type signal at 8.03 ppm, with J = 490 Hz. Next, the resistance of the methyl diphenylphosphinate towards the BH_3 in THF was explored and found to be satisfactory for reductions at room temperature. At the reflux temperature recommended[118] for the reduction of primary amides, the P-OMe groups were partially reduced. Some loss of the BOC groups was also observed. The reduction mixtures of the compound **39** were

quenched with aq. NH4Cl, to prevent acidolysis of the BOC protecting group. The crude

amine was extracted, and then protected with BOC2O, without further purification (Scheme

2). Extraction in ether of the protected product __40__ was followed by a flash chromatographic

separation step giving low yields in reduced products (all containing the -C__H__2-NHBOC

group).
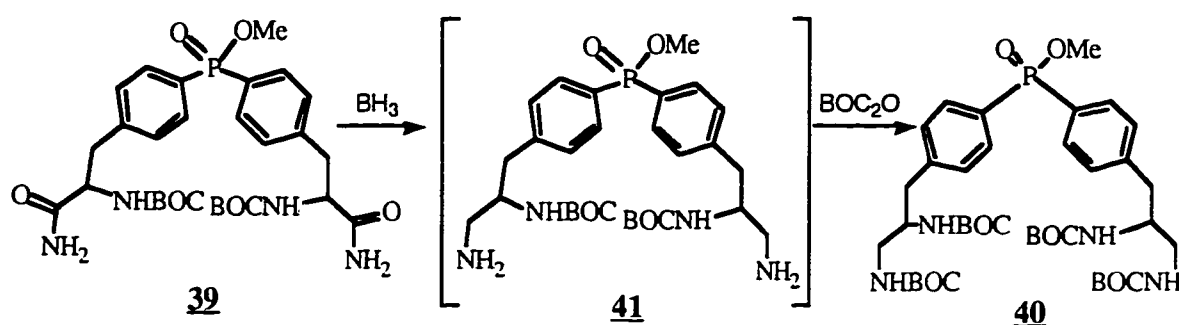
Scheme 4   The reduction and protection steps

In order to improve the overall yields, model phenylacetamide reduction/quenching/

protection sequences were studied. The purpose was to find the conditions to allow the

complete reduction of two amide groups, without affecting the BOC and P-OMe groups.

The quenching phase presents similar selectivity aspects: while a complete hydrolytic

decomposition of the amineborane complexes requires low pH values, the acid lability of

the BOC group prevents the use of strong acids. Finally, it was found that reduction at room

temperature followed by quenching of the reduction mixture in MeOH at 50°C for 14 hr is

an acceptable solution, yielding, after protection with BOC2O, 33% of N-BOC-

phenylethylamine. The procedure was repeated on the compound __39__ with an overall isolated

yield for the reduction, quenching, protection and separation, not exceeding 14%. Another

compound was isolated in comparable amounts, with ^{1}H-NMR signals having the same

chemical shifts and couplings. The only difference found was the lower integrals of the *tert-*

Bu proton peaks, suggesting that the compound might be a BOC protected amido-amine resulting after the protection of the incompletely reduced diamide **39**.

IV.1.2 The New Synthetic Route

The low yields and the several by-products resulting during the coupling and the reduction steps led to the consideration of several alternative synthetic routes. The simplest alternative, which benefited from the already gathered experience, uses the same basic steps but in a different order (Scheme 5).
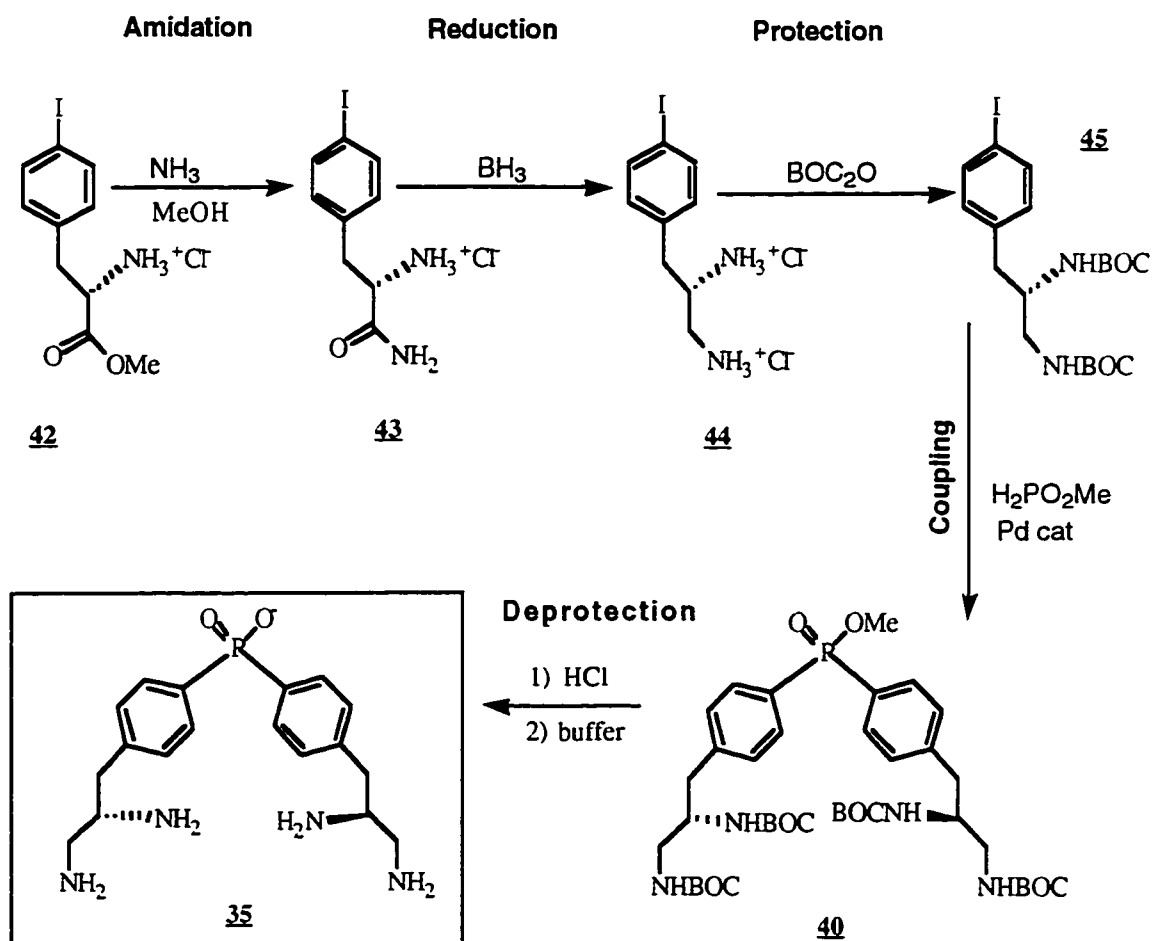
Scheme 5   New alternative for the preparation of BDAP ligand

The first step consists in the conversion[71] of the available L-iodophenylalanine methyl ester hydrochloride, **42** to amido-amine **43**, which may be next reduced in less selective conditions to diamine **44**. The key coupling step of this alternative, uses a protected diamine **45** yielding in one or 2 steps,[71, 113] the diarylphosphinate **40**.

This alternative also allows the easy preparation of unsymetrical diarylphosphinates by coupling the compound **45** with other aryl iodides. This would lead the preparation of larger families of ligands suitable to self-assemble to form macrocyclic hosts.

IV.1.2.1 Amidation (Scheme 5)   The amidation was performed in methanol saturated with ammonia in conditions similar with those established for the diarylphosphinates (Scheme 2). Two product crops are separated, one as a free amine, on crystallization from MeOH and one as a hydrochloride, **47** from MeOH-Et$_2$O with an overall yield of 82%. The crude amide can also be used directly in the next reduction step.

IV.1.2.2 Reduction (Scheme 5)   Reduction tests made on compounds **43** and **39** have shown that NaBH$_4$ and I$_2$ in refluxing THF[117] cleaves the iodine from the aromatic ring. Therefore, the alternative BH$_3$-THF[118] reduction system was tested on **43**. Working at room temperature, this system was found suitable for the complete and selective reduction of the amide group. The quenching step was also free of selectivity conflicts due to the absence of any acid cleavable protective group. Therefore, more vigorous reaction conditions were used, which drove the reaction to completion: (i) the borane reduction step at room temperature was continued with a heating step; (ii) the quenching was done by using HCl solutions. The separated yield for the dihydrochloride, precipitated from MeOH-Et$_2$O solutions with a stream of anhydrous HCl, was 59%. The crude free diamine is clean enough to be used directly in the next protection step.
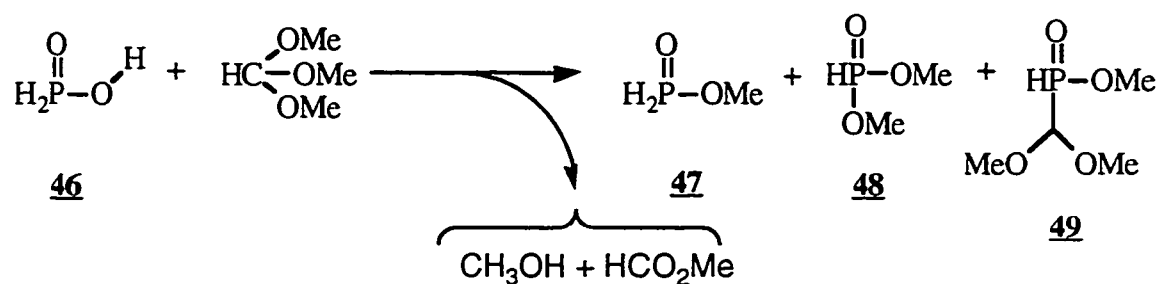
<u>IV.1.2.3 Protection (Scheme 5)</u>   The protection was performed following the

general procedure used for the production of iodophenylalanine methyl ester **37**[71] with the

only difference that K_2CO_3 replaces the less soluble Na_2CO_3 which was previously

observed in the case of **42** to lead to a urea side product. Pure product **45** was separated by

recrystallization from methanol with 79% yield.

<u>IV.1.2.4 Combined yields</u>   For the reduction-protection, when the crude diamine

44 resulted after the reduction was directly protected in the above mentioned conditions, the

combined yield of **45** from **43** was 51-59%. When amidation-reduction-protection were

performed without intermediate purifications, the 3 step yield for **45** from **42** was 46-52%.

<u>IV.1.2.5 Coupling (Scheme 5)</u>   The 1 step coupling of the newly prepared **45**

followed the same known procedure used in the coupling of **37** (Scheme 3). The resulting

crude product was even less pure than the corresponding **37**. The product and impurity ratio

obtained from ^{1}H-NMR integrals of P-OC$\underline{H}_3$ protons varies from batch to batch, from 3:2

to 2:3. For one of the "best" crude coupling mixtures the yield in product **40** was determined

by using an ^{1}H-NMR internal standard, to be 57%. However, another 37% of a related

compound containing POMe groups was also formed. Repeated flash chromatographic

separation steps were unable to resolve this mixture. Suspecting again, as in the previous

case (Scheme 2) that the impurities resulted from the side products detected in the

esterification mixtures of the phosphinic acid, an improvement of the purity of the starting

methyl phosphinate was considered necessary.

<u>IV.1.2.6 Improved preparation of methyl phosphinate</u>[119] (<u>Scheme 6</u>)   The [31]P-

NMR of the phosphinic acid esterification mixtures showed that methyl phosphinate is

accompanied by the impurity **49** (~10-15%) and unreacted **46** (1-4%). The impurity **48**

observed previously by Gallagher[116] was not seen in the freshly prepared esterification

mixtures used in these studies. However, dimethyl phosphonate **48** has been detected in

older esterification mixtures, and its formation may be accelerated during the coupling

conditions. The attack of the free dimethoxymethyl cation on a phosphorus (III) tautomer of

46 or **47** is the presumable source of the formation of the impurity **49** .

$$
\underset{\mathbf{46}}{\overset{O}{\underset{H_2P-O}{\parallel}}\overset{H}{}} \; + \; \underset{}{\overset{OMe}{\underset{OMe}{HC-OMe}}} \longrightarrow \underset{\mathbf{47}}{\overset{O}{\underset{H_2P-OMe}{\parallel}}} \; + \; \underset{\mathbf{48}}{\overset{O}{\underset{OMe}{\overset{\parallel}{HP-OMe}}}} \; + \; \underset{\underset{\mathbf{49}}{MeO \quad OMe}}{\overset{O}{\overset{\parallel}{HP-OMe}}}
$$

$$
CH_3OH + HCO_2Me
$$

Scheme 6   The esterification of phosphinic acid with trimethyl orthoformate

Table 2   The effect of the cosolvent on the distribution of the transesterification
products

Cosolvent	% Product, **47**	%**49**	%**46**
MeCN	74.8	23.5	1.7
none*	83.9±3.0	12.0±0.8	4.2±3.8
CH₂Cl₂	91.4	6.6	2.1
CH₃Cl	95.8	4.2	0
THF	91.3±8.3	3.3±0.6	5.5±7.7
THF-Toluene	95.9±0.6	0.6±0.5	3.6±1.2
Toluene	95.0±1.9	1.9±1.3	2.2±1.4

*excess of trimethyl orthoformate used as a solvent

Therefore, adding nonpolar, low dielectric constant cosolvents to the transesterification mixture was expected to repress this ionization process and the formation of **49**. Dilution of a mixture of **46** and trimethyl orthoformate at 0-5 °C with an equal volume of cosolvent yielded a solution about 1 M in **46** and 3-5 M in orthoformate. The yield of **47** is solvent dependent (Table 2). Mixing the components at room temperature seemed to have insignificant influence on product purity and yield. ^{31}P-NMR was used to monitor the composition of the transesterification mixture in time. In 1:1 THF / toluene, the ^{31}P-NMR resonance for unreacted phosphinic acid **2** gradually shifted from about δ 11 to about δ 8 over the course of the reaction as the concentration and solvent composition change. Other signals also shifted substantially. However, identification of ^{31}P resonances in this solvent was straightforward using proton coupled spectra: **49** (δ 30.1, dqd, J = 559,11.7,8.0 Hz), **46** (δ 8.7, t, J = 564Hz), **47** (δ 18.5, tq, J = 567, 12.9 Hz).

Solutions of methyl phosphinate in toluene / THF / trimethyl orthoformate can be kept at room temperature with relatively little decomposition. After 1 week, ^{31}P-NMR showed that the major component is still methyl phosphinate **47** (58%) with traces of phosphinic acid **46** (3%) and substantial amounts of methyl dimethoxymethylphosphinate **49** (9%) but also a significant amount of dimethyl phosphonate **48** has formed (δ 11.9, d sept, J = 699, 11.8 Hz, 30%). Since this side product was not observed in the first hours after mixing the reagents, it is recommended that the preparation of the ester to be made immediately before its use in the coupling steps. For a separate sample, a reaction a yield of 93% in methyl phosphinate was determined by ^{1}H-NMR internal standard method.

As expected, the use of nonpolar cosolvents repressed the formation of the phosphonate **49**. The best results were obtained by using THF - toluene mixtures (Table 2). The opposite effect was noticed when the more polar acetonitrile was used as a cosolvent. Moreover, assisting the carbocation formation by adding H_2SO_4 to the esterification mixtures of phosphinic acid, shifted the outcome of the reaction to the predominant

formation of byproduct **49**. In the case of toluene, a two-phase reaction mixture was observed at early reaction times, and **49** is probably formed in the more polar phase. This may be an explanation of the variable and slightly increased amounts of the impurity **49** found in toluenic esterification mixtures.

IV.1.2.7 Two step coupling (Scheme 7) The one step coupling starting from the improved quality methyl phosphinate solutions was retested. The same impurities were detected in both the crude reaction mixtures and in the product purified by flash chromatography, but in a smaller amount. Since in the production of the protected intermediate **38** corresponding to the PBP ligand **32**, a two step procedure[71] gave better purities of the products, this approach was also considered for the coupling of compound **45** (Scheme 7).

1st step coupling 2nd step coupling
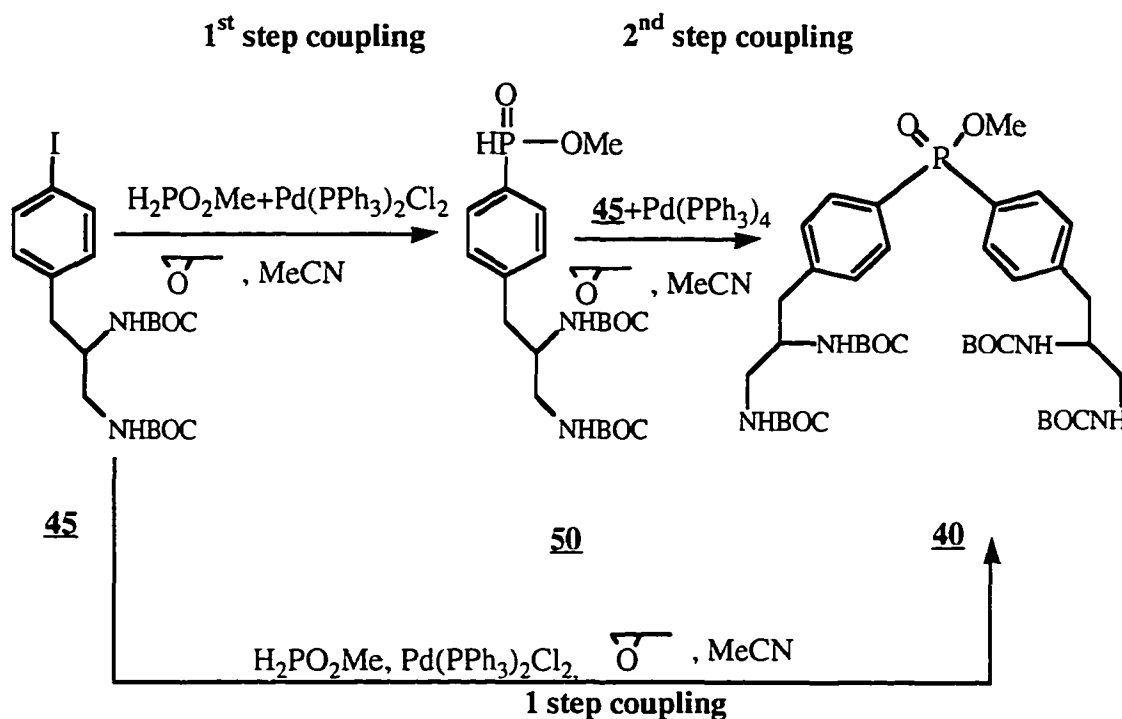
Scheme 7   Coupling alternatives: 1 step and 2 step Pd catalyzed couplings

Following the general procedure[71, 113] in the first step coupling, a relatively clean

crude monoarylphosphinate **50** was separated with 74% yield after the partition of the

reaction mixture between Et_2O-aq. $NaHCO_3$. Attempts to purify the product by flash

chromatography resulted in low yields and impure products, probably due to the lability of

the monoaryl substituted phosphinate group.[113] Therefore, the crude **50** was used as a

starting material in the second coupling step, catalyzed by Pd(0). This time, the resulting

crude diarylphosphinates were almost free of the previously mentioned impurity. After flash

chromatography followed by a crystallization from MeOH step, the ^{1}H- and ^{31}P-NMR

indicated that the compound was pure. The reaction yield was determined by ^{1}H-NMR

(internal standard) to be 86% (overall yield of isolated product **40** starting from **45** was

44%).

IV.1.2.8 Deprotection (Scheme 5) Treatment of the protected diarylphosphinate

40 with 10-20% aq. HCl at room temperature for 0.5-2hr resulted in the loss of the BOC

groups and only partial deprotection of the phosphinate group. Boiling the mixture for 30

min. yields quantitatively BDAP **35**. After evaporation, BDAP is precipitated from aq.

concentrated solutions with absolute EtOH. After drying, the yield in separated

$BDAPx3HClx4H_2O$ was 66%.

However, carefully acquired and processed NMR spectra showed that this product is

not totally pure. A broad "bump" in the aromatic area of the ^{1}H-NMR, at 7.45 ppm and a

shoulder in the ^{31}P-NMR at 23.48ppm (at 0.1 ppm upfield of the product signal) are

evidences that the separated BDAP contain another impurity (~5-8%) similar in structure

with the product. Two other weak impurity signals were detected in the crude BDAP, at

19.05 and 12.62 ppm. The latter signal disappears after the precipitation with EtOH and was

attributed to the 4-(2,3-diaminopropane)-phenylphosphonate, being close to the value of

13.7 ppm found for the phosphonate impurity from the PBP production.[71] Ion exchange on

Sephadex CM25, using aq. NH$_3$ and NH$_4$HCO$_3$ as eluents, separates also the 19.62 ppm

impurity but fails to affect the ratio between the product signal and the 23.48 ppm impurity

signal. During the ion exchange purifications, due to the presence of bicarbonate anion, the

^{31}P-NMR presented a series of peaks in the region where the product was expected to

appear. The formation of mono- or poly-carbamate derivatives of the BDAP due to the

presence of HCO$_3^-$ anion may constitute a possible explanation of these multiple signals.

After treating these samples with 1M HCl, when the presumed carbamates are expected to

decompose, a clean, single signal ^{31}P-NMR was obtained. Other purifications of BDAP on

Sephadex cation exchanger loaded with [Cuen$_2$]$^{2+}$ and elution with ethylenediamine or on

Dowex cation exchanger and elution with aq. or ethanolic HCl and/or NH$_3$ failed to change

the product-impurity ratio. Interestingly, it was found that the BDAP is retained very tightly

on Dowex cation exchangers, being eluted in very broad bands even when 4M aq.

concentrated HCl was used. Another than the expected ionic interaction, possibly a π–π

interaction is responsible for the retention of the ligand on the column.

IV.1.2.9 Preparation of *tert*-Butyl Phosphinate[119] Scheme 8)   Since the purity of

the BDAP ligand used in binding studies was considered to be critical, a new modification

of the coupling procedures studied until now (Scheme 8) was devised. It was thought that

the use of a *tert*-Bu group in the phosphinate residue, would improve the chromatographic

separability of the protected BDAP 35. The expected increase in resistance to basic

hydrolysis and higher susceptibility to acidic hydrolysis conditions are also features of the

tert-butyl phosphinates which could prove useful in the isolation / decomposition process.

The transesterification equilibria of methyl phosphinate with a series of alcohols has

been studied by Gallagher and Honegger.[120] However, no synthetic application of these

transesterifications was devised. A synthetic development where a transesterification in the

phosphinic ester series is used as a first stage in a tandem reaction leading to glycosyl

phosphinic acids was recently reported.[121]

In the present study, the transesterification was carried out in anhydrous *tert*-BuOH as a cosolvent, in conditions similar with those used in Table 2.*tert*-Butyl alcohol proved to be a superior solvent for the reaction of phosphinic acid with trimethyl orthoformate, since it formed only mixtures of **29** and **33** without contamination by **31**. Repeated addition of *tert*-butyl alcohol and evaporation under reduced pressure, produced a mixture, predominantly of *tert*-butyl phosphinate contaminated with methyl phosphinate.
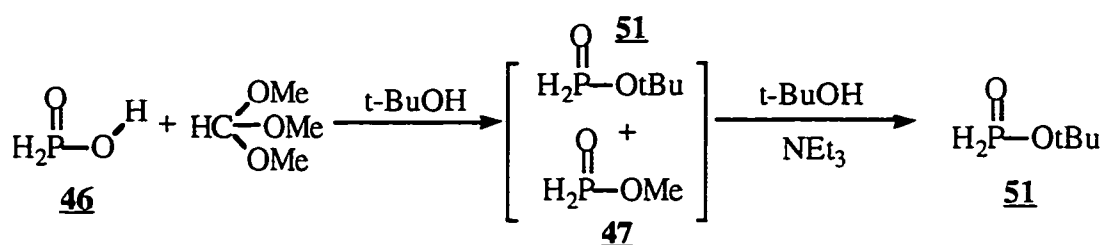
Scheme 8   Transesterification to *tert*-butyl phosphinate

This mixture, however, proved to be unsuitable for cross-coupling reactions with aryl iodides. Reaction of a 7:1 molar ratio of *tert*-Bu to Me phosphinates in CH_3CN with aryl iodide **45** and triethylamine under catalysis by $(Ph_3P)_2PdCl_2$, gave roughly a 1:1 mixture of methyl arylphosphinate and *tert*-butyl arylphosphinate. The methyl phosphinate **47** appears to react faster than *tert*-butyl phosphinate, consuming the limiting amounts of the aryl iodide before significant reaction with *tert*-butyl phosphinate takes place. Therefore, **51** free of any methyl phosphinate contamination is needed for practical use.

Consequently, after the completion of the ester exchange, triethylamine was added to prevent further reaction of the excess orthoformate with phosphinic acid (unreacted or formed through hydrolysis). At the same time, preferential acidic hydrolysis of the newly formed *tert*-Bu ester is avoided. Then, the volatiles were removed in vacuo. Repeated dissolution of the residue in *tert*-butyl alcohol and removal of volatiles in vacuo to drive the

transesterification further, toward the *tert*-butyl ester, led to a crude *tert*-butyl phosphinate almost free of methyl ester. Final dissolution in toluene and filtration through basic alumina removed the last traces of phosphinic acid **46** and methyl phosphinate **47**, providing a solution of *tert*-butyl phosphinate **51** suitable for the next coupling reaction.

IV.1.2.10 Synthesis of 53 through One Step Coupling (Scheme 9) The one step coupling of the aryl iodide **45** with 0.48 equiv. of *tert*-butyl phosphinate was carried out in conditions similar with those using methyl phosphinate.
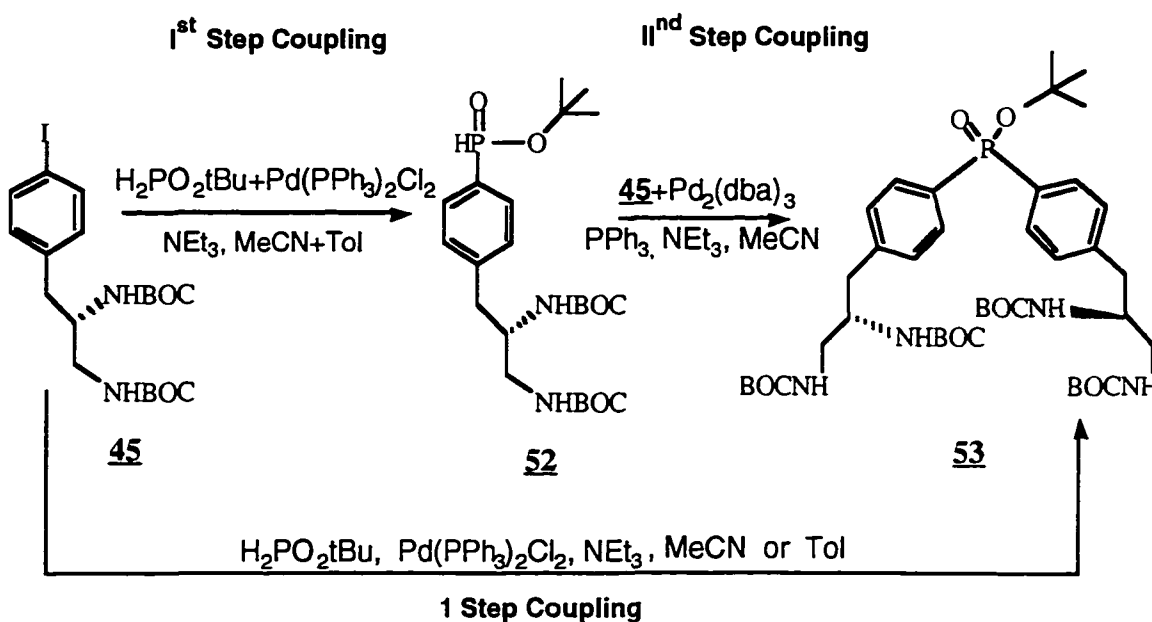
Scheme 9   Synthesis of **53** by one and two step Pd catalyzed coupling

Since the ^{1}H-NMR of the crude coupling samples run with NEt$_3$ instead of propylene oxide are cleaner, most of the samples were run in the presence of NEt$_3$.The coupling rates are slower than those of methyl phosphinates with **45** (Scheme 7) or **37** (Scheme 3). The coupling of BOC-iodophenylalanine **37** with *tert*-butyl phosphinate **51** was also found to be faster than with **45** (Table 3, entries 10 and 11)

Table 3: Optimization study of the one step coupling reaction (Scheme 9). The conversion of aryl iodides (ArI) **37** or **45** and the corresponding yields in *tert*-butyl monoarylphosphinate (mono), diarylphosphinate (bis) **40** or **53** were calculated from the ^{1}H-NMR data obtained by monitoring the aromatic and *tert*-butyl protons of these species in the crude reaction mixtures. Solvents: T = Toluene; An = MeCN. Catalysts: A =(4-Me$_2$NC$_6$H$_4$)$_3$P : Pd$_2$(dba)$_3$ = 1.6; B = (4-CH$_3$-C$_6$H$_4$)$_3$P : Pd$_2$(dba)$_3$ = 1.6; C = Pd(PhCN)$_2$; D = Pd$_2$(dba)$_3$; E = (C$_6$H$_5$)$_3$P : Pd(dba)$_3$; two additions of ArI and two separate heating cycles were done for the samples at entries 12 and 13

Exp.#	Cat.	ArI used	Equiv. **51**	Equiv. Pd(0)	Equiv. NEt$_3$	Solvent	Concn. [M]	Temp [°C]	Time [hr]	% Conv ArI	% Yield bis	% Yield mono	% Yield imp. I	% Yield imp. II
1	A	**45**	.48	.075	1.25	An+T	.19	80-90	6.0	64	51	9	0	4
2	A	**45**	.48	.075	1.25	An+T	.19	80-90	9.0	62	51	6	0	5
3	A	**45**	.48	.075	1.25	An+T	.19	80-90	11.0	65	54	5	0	5
4	A	**45**	.47	.063	1.25	An+T	.19	80-85	7.0	7	62	3	0	2
5	B	**45**	.48	.063	1.25	An+T	.19	80-85	8.0	64	50	10	0	5
6	C	**45**	.48	.063	1.25	An+T	.19	80-85	8.0	52	45	5	0	2
7	A	**45**	.48	.063	1.10	An+T	.23	85	5.0	3	50	1	0	2
8	B	**45**	.48	.063	1.10	An+T	.23	85	5.0	61	53	3	0	5
9	D	**45**	.48	.063	1.10	An+T	.23	85	5.0	41	0	0	6	5
10	A	**37**	.50	.100	2.00	An+T	.23	80-85	6.0	68	62	0	0	6
11	D	**37**	.50	.100	2.00	An+T	.23	80-85	6.0	48	24	16	0	8
12	E	**45**	.47	.100	1.14	T	~.24	80 / 85	1.5/3.5	60	3	33	3	1
13	E	**45**	.47	.088	1.14	T	~24	80 / 85	1.5/4.5	80	38	36	5	2
14	E	**45**	.42	.063	2.00	T	~.20	90	2.0	61	31	0	8	2
15	E	**45**	.42	.063	2.00	T	~.20	90	5.0	71	48	2	19	1

46

A limited optimization study (Table 3), was focused on the influence of the catalyst system, solvent and molar ratio of reagents on the conversion of the aryl iodide **45** and intermediate **52** and the yields in product **53** and impurities. These results were calculated from the integration data of the aromatic and *tert*-butyl proton peaks. In these calculation, the stoechiometry of the conversion of aryl iodide **45** to the product **53** was considered 1—> 2 while to the intermediate **53** and impurities 1—> 1. The maximum conversions of aryl iodide **45** reached 65% and those of the *in situ* formed monoarylphosphinate intermediate **52** reached ~90%.

Nevertheless, the separation of the product **53** from the crude reaction mixture was difficult due to the presence of unconverted monoarylphosphinates **52** and two other impurities which constantly appeared in P-OC$\underline{H}_3$ region of the ^{1}H-NMR spectrum at 1.515 and 1.494 ppm. The most common ratio between the product **53**, having the ^{1}H-NMR shift at 1.485 ppm, and the impurity peaks "1.515 ppm" and "1.494 ppm" ~1:0.15:0.05 and remains approximately constant during the reaction.

Only the 1.515 ppm impurity is easily separated by flash-chromatography with usual binary solvent mixtures. For the removal of the unconverted monoarylphosphinate **52** an extra-oxidation step with NaIO$_4$[122] of this impurity to the phosphonic ester **54** was introduced (Scheme 10). Oxidizing a synthetic mixture of **52** and excess of **53** shifted the P-OC$\underline{H}_3$ signal in the ^{1}H-NMR characterizing **53** from 1.570 to 1.515 ppm. This suggests that the previously observed 1.515 ppm impurity in different coupling mixtures might be an oxidation product structurally related to **54**. No further investigations were made to confirm this assumption.

Also, it was found that the oxidation step works best if it is performed after the flash chromatographic step, when the Pd catalyst residues are removed. Being polar, the oxidation product **54** was easily removed from the product by filtration through basic alumina.
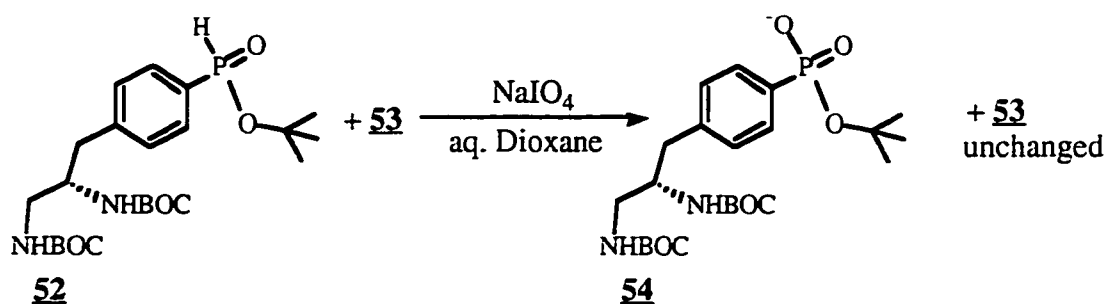
Scheme 10   Oxidation of monoarylphosphinates **52** is a necessary purification step

After the oxidation, the ^{1}H-NMR still contains an impurity peak at 1.494 ppm. A

more careful TLC screening for an optimum flash chromatographic eluent system led to use

of the Hexanes-CH_2Cl_2-MeCN-*tert*-BuOH solvent mixture which allowed a better

resolution of the 2 components having close Rf values (ΔRf = 0.06). The overall yield of

pure **53** after this separation was less than 10%, mainly due to a significant fraction of

product still contaminated. Even if not practical, this separation allowed the identification of

the structure of the impurity **55** which is responsible for the ^{1}H-NMR peak at 1.494 ppm

(Figure 2). The positive ion ESI-MS data is also consistent with the assigned structure **55**.

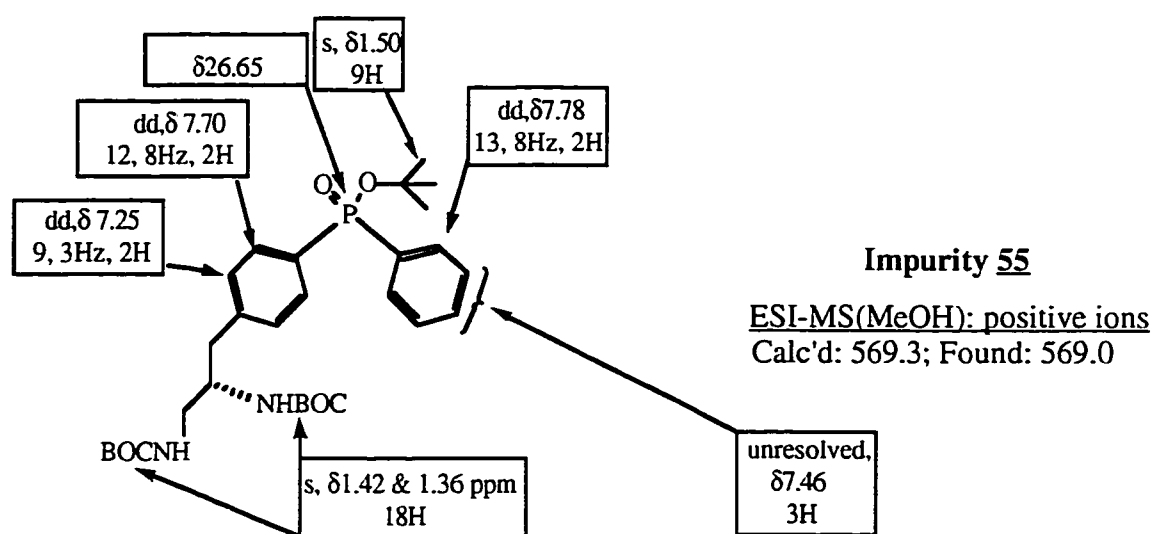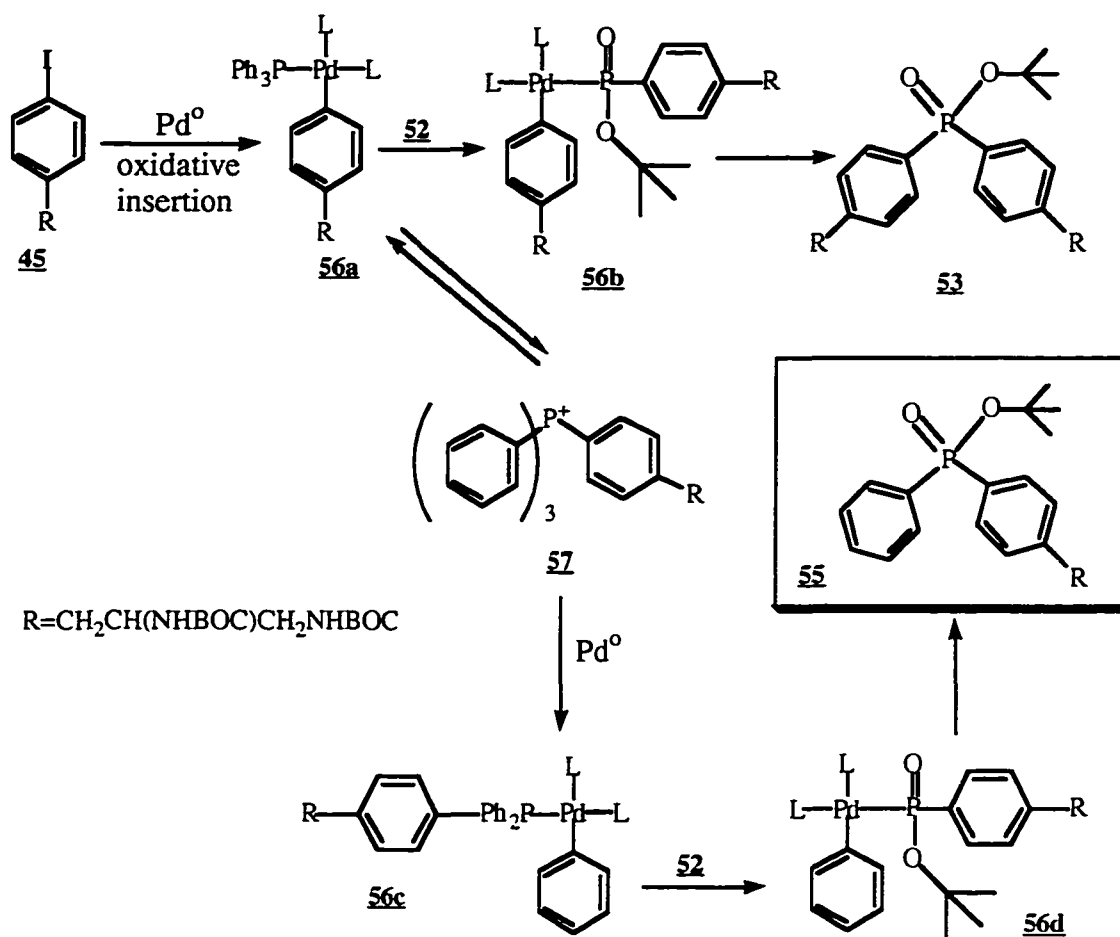**Impurity 55**

ESI-MS(MeOH): positive ions
Calc'd: 569.3; Found: 569.0

Figure 2 ^{1}H-,^{31}P-NMR and electrospray-MS data supporting the assigned structure **55**

R=CH$_2$CH(NHBOC)CH$_2$NHBOC

Scheme 11   A possible mechanism leading to the formation of **55**

The formation of compound **55** may be explained if a formal migration of a phenyl

group from the PPh$_3$ ligand is considered. A possible mechanism involves the formation of

the known tetraphenylphosphonium intermediate.[123, 124] The attack (Scheme 11) of the a

nucleophilic species derived from **52** on the phosphonium cation **57** or on the oxidative

insertion product **56 a** or **56 c** yields the product **53** or the impurity **55** respectively.

In order to avoid the formation of the byproduct **55**, the Pd(PPh$_3$)$_2$Cl$_2$ catalyst was

replaced with 1:2 mixtures of Pd(OAc)$_2$ with tris-tolylphosphine, benzonitrile or tris-

dimethylaminophenylphosphine ligands. In all these cases as well in the case in of using

Pd$_2$(dba)$_3$ the reactions were slowed down and the conversions of **45** and **52** were lower, but

the 1.485 ppm impurity related ^{1}H-NMR signal was not observed. Also, formation of *tert*-butyl {4-[(S)-N,N'-di-Boc-1,2 diaminopropyl]-phenyl} (4-N,N'-dimethylaminophenyl) phosphinate, a side product corresponding to **55** and generated through the presumed migration of fragments from tris-dimethylaminophenylphosphine ligand was not noticed. Among the new ligands tested, the best conversions in **45** and **52** (63 and 71%) were found for the tris dimethylaminophenylphosphine ligand.

IV.1.2.11 Synthesis of 53 through Two Step Couplings (Scheme 12)

The two step couplings using *tert*-butyl phosphinate were studied hoping to improve the overall coupling yield. After the first step coupling in presence of Pd(Ph$_3$)$_2$Cl$_2$ pure **52** could be separated with 75% yield. A flash-chromatographic step with an eluent containing NEt$_3$ which prevents decompositions of the product on the silica column was necessary. An impurity responsible for the P-OC$\underline{H}_3$ signal at 1.515 ppm in ^{1}H-NMR spectrum which also appears in the 2 step couplings (phosphonic ester? **54**), was efficiently removed form the mixture. Another impurity whose ^{1}H-NMR signals seems to indicate the structure of the reduced product 4-N,N'-di-Boc-1,2 diamino-3-phenyl-propane was isolated as a fraction containing ~12% of the weight of the initial crude reaction residue. At >2:1 molar ratios of **51** to **45** the contamination of the product with traces of diarylphosphinate **53** is avoided. One of the advantages of the use of *tert*-butyl phosphinate procedure, is that a pure mixture of solid diastereomers of **52** could be isolated after recrystallization from ether. The corresponding pure methyl phosphinates were never obtained, due to their partial decomposition during the flash-chromatographic procedures.

A parameter optimization study was done in order to increase the conversion of the monoarylphosphinate **52** as much as possible in the second step coupling. The slower catalytic system [Pd$_2$(dba)$_3$ + tris-dimethylaminophenyl-phosphine ligand] was used, since the triphenylphosphine caused the usual transpositions (Scheme 11). A propylene oxide and

triethylamine mixture was used as a proton scavenger system. Slightly increased

conversions were obtained when ~1equiv. of propylene oxide were added for each

equivalent of aryl iodide. This may be explained through the reaction of propyleneoxide

with any incidental traces of moisture at the beginning of heating period. Increasing the

temperature increased the conversion without affecting the side-reactions. However, at

temperatures exceeding 100 °C a decrease of the product yield and increased amounts of

impurities were observed. A minimum of 2 equiv. of **45** to each equiv. of **52** were needed in

order to maximize the conversions in **52**. When used as limiting reagent, the aryl iodide **45**

was totally consumed producing **53** without other visible side-products.
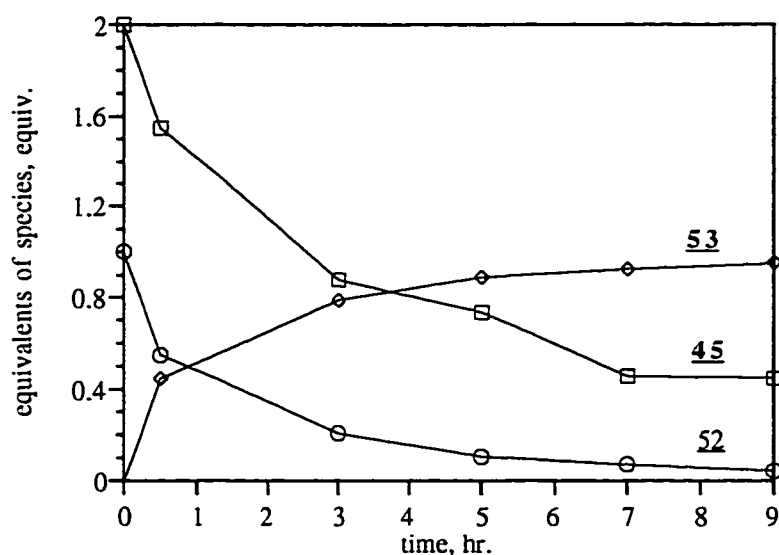

Figure 3   Variation of the number of equiv. of the remaining monoarylphosphinate **52**,
            aryl iodide **45** and formed diarylphosphinate **53** during the IInd coupling step

Time monitoring of the reaction in a NMR tube sealed under N_2 (Figure 3) showed

that most of the monoarylphosphinate **52** is converted into product but some of the starting

aryl iodide is involved in side reactions, contaminating the resulting reaction mixture.

Longer reaction times then 6 hours are not recommended. The concentrations of the

disappearing **45** and **52**, forming **53** were monitored by ^{1}H- and ^{31}P-NMR. Another side product with peak at 34.21 ppm which formed in the first hour of coupling and then its concentration leveled off at ~10% was also followed by ^{31}P-NMR.

The separation of the product remained a laborious process. A flash-chromatographic step, with eluents containing AcOH is needed for the resolution of **53** from the dimethylaminophenyl phosphine ligand and other impurities. The contamination with unconverted monoarylphosphinate **52** has still to be removed by a $NaIO_4$ oxidation step followed by filtration through basic alumina. The overall yield for the second step coupling, including the isolation / purification of the *tert*-butyl diarylphosphinate **53** was 57%. The combined yield, for both coupling steps, from the starting from the aryl iodide **45** is 43%.

From Figure 3, the conversion of **52** in **53** seems almost quantitative. Later, in gram scale couplings, it was found, that another byproduct (Figure 4, **58**) is formed having the -P-O-C(CH_3)$_3$ ^{1}H and ^{31}P-NMR signals overlapped with those of the product. Due to the larger scale flash-chromatographic separation, the impurity does not separate well. Changing the eluent system from Hexanes-EtOAc-AcOH = 26:7:3 to Hexanes-CH$_2$Cl$_2$-MeCN-AcOH = 40:20:10:4 improves the resolution of this impurity. With this eluent system, the impurity was separated from older, impure flash-chromatography fractions and crystallization mother liquors where it can be found in larger concentrations. Its ^{1}H-NMR shows common signals with those of the product **53** and several unusually broadened signals. The ESI-MS of the impurity suggests an isomer of the product **53** but this information must be regarded with caution due to difficulties of the ^{31}P- and ^{1}H-NMR detection of the contamination with product **53** of the isolated impurity **58**. Structure assignment was attempted only after the deprotection of this impurity with HCl to the tetraamine **59**. Although, the aromatic area of the ^{1}H-NMR spectrum is complex, a tentative peak assignment is given below, which needs further confirmation from a COSY experiment.
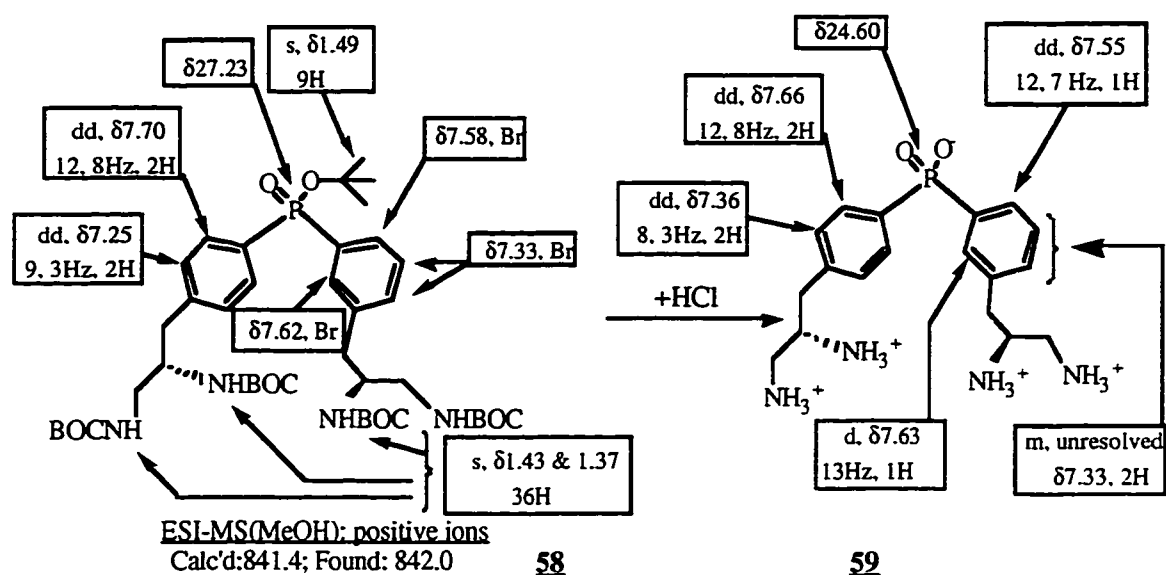
δ27.23

s, δ1.49
9H

δ24.60

dd, δ7.70
12, 8Hz, 2H

dd, δ7.66
12, 8Hz, 2H

dd, δ7.55
12, 7 Hz, 1H

δ7.58, Br

dd, δ7.25
9, 3Hz, 2H

dd, δ7.36
8, 3Hz, 2H

δ7.33, Br

+HCl

δ7.62, Br

''NHBOC

NH₃⁺

NH₃⁺

BOCNH

NHBOC NHBOC

NH₃⁺ NH₃⁺

s, δ1.43 & 1.37
36H

d, δ7.63
13Hz, 1H

m, unresolved
δ7.33, 2H

ESI-MS(MeOH): positive ions
Calc'd:841.4; Found: 842.0 **58**

59

Figure 4   ³¹P- and ¹H-NMR peak assignments for the protected **58** and deprotected **59** "iso-BDAP" impurity

Interestingly, all the aliphatic signals of the deprotected "iso-BDAP" **59** are overlapping, with the exception of a single benzylic hydrogen which is significantly downfield shifted. This shift and the upfield shifted proton ortho to the phosphorus on the "transposed" ring, at 7.55 may indicate that they are subjected to the influence of the ring current of the adjacent benzenic residue. Therefore, the relative orientation of the rings in the "iso-BDAP" is different from that in the BDAP, which suggests the existence of a slow rotational/conformational isomerism.

The equilibration rates between the different conformations in the protected compound **58** is slowed down to a degree which determines the observed unusually broad signals. The formation of the impurity **58** may also involve the participation of the tris- dimethylaminophenyl phosphine ligand **61** (Scheme 12). Next, the cation of phosphonium **60** may undergo the attack of the nucleophile derived from the phosphinate **52** at the most activated ring. The tentative ¹H-NMR peak attributions indicating a meta substitution of one of the benzenic rings is consistent with the possible attack of a nucleophilic species derived

from the monoarylphosphinate **52** at the electron deficient meta position of the

phosphonium species **60**. Considering the different fractions of impurity separated after the

flash chromatography of the mother liquors residues resulted from the crystallization of a

large batch of production of **53**, a formation ratio of **53** : **58** of 6:1 has been estimated.
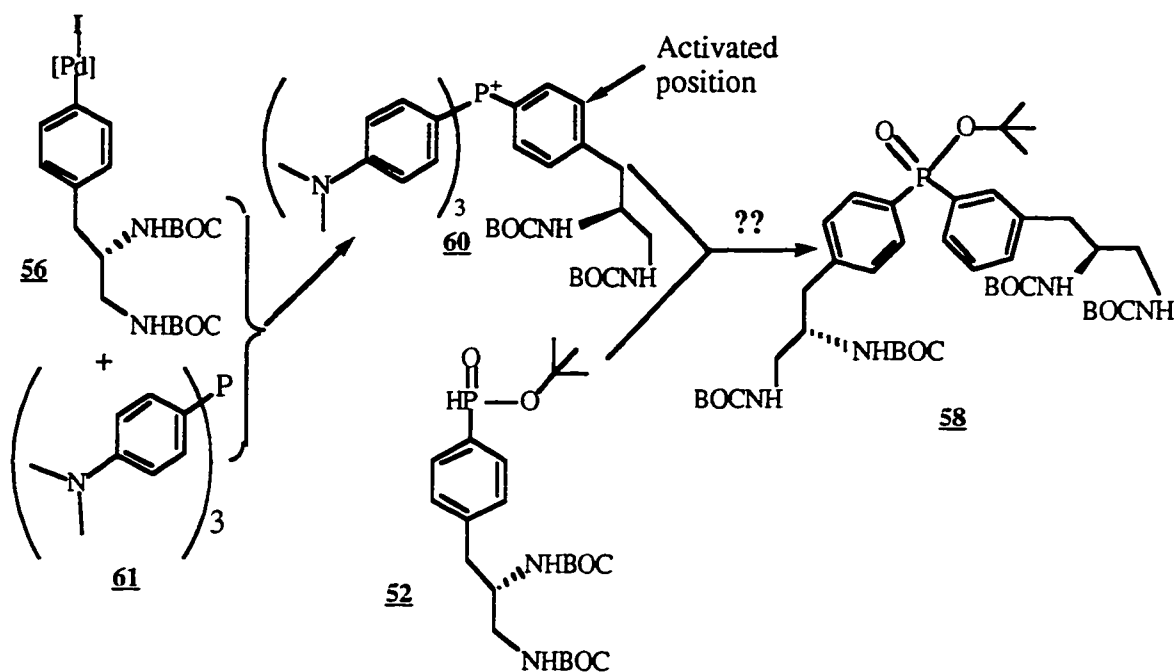
Scheme 12   Possible scheme for the formation of the impurity **58**

IV.1.2.12 Deprotection of 53 to the BDAP ligand, 35   The decomposition of the

tert-butyl diarylphosphinates takes place under mild conditions, at room temperature, due to

the acid lability of the protecting group on the phosphorus. The precipitation of the product

from aq. EtOH yielded pure products which after several days of drying, still contained

EtOH traces (less than 1equiv. of EtOH per product equiv.). Repeated freeze-drying of the

product from nanopure water completely removed the traces of EtOH. When the

deprotection took place in organic solvents (EtOH, CH_2Cl_2) saturated by bubbling

anhydrous HCl, slow precipitation from the solution took place. Even in these conditions,

the separated BDAP incorporated variable amounts of the solvent in which the deprotection took place. For completing the deprotection with aq. TFA, temperatures of ~60°C were necessary. Precipitation from aq. EtOH yielded the usual EtOH contaminated BDAP. However, after repeated lyophilizations, all the samples described above proved to be pure.

IV.2 Structural Studies on the BDAP Species

IV.2.1. The BDAP Ligand

NMR, IR, UV, MS and elemental analysis data support the assigned structure 35 of BDAP (see also Chapter V). The P-H couplings which generate the doublet of doublets splitting pattern for the aromatic protons in ^{1}H-NMR, correspond to those found in various diaryl phosphinates[71, 113] and in the ^{31}P-NMR spectra. Due to the presence of chiral centers, the methylene protons are not equivalent, causing two ABX and CDX (Pople notation) sets of splitting patterns in ^{1}H-NMR, (Figure 5).
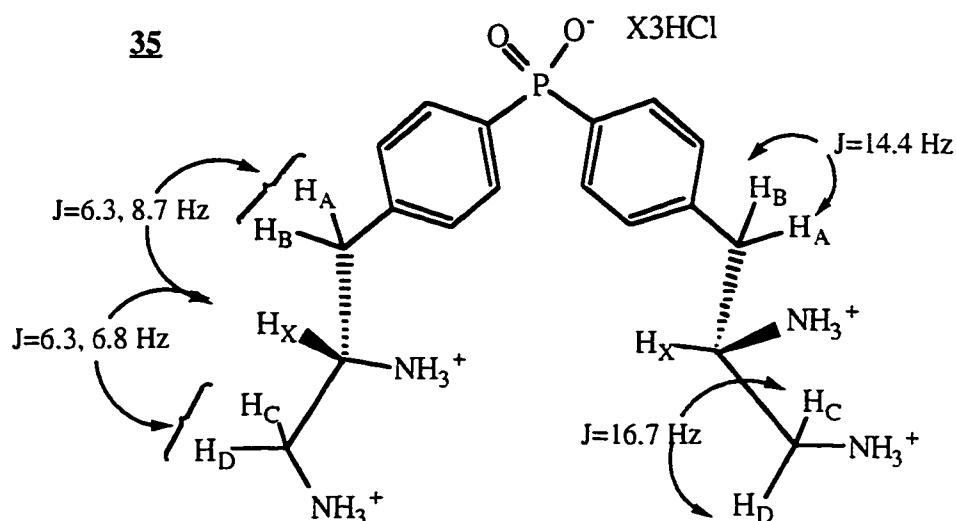

Figure 5   Coupling of the aliphatic protons in D_2O solution of BDAP (35), hydrochloride salt

Table 4 ^{1}H-NMR chemical shifts and coupling constants for acidic, basic and Zn-complexed BDAP species ("/" sign used for partial attributions; two sets of data given when two alternative attributions are possible). The case of the Zn complex is discussed in section 4.2.2.

Parameters for the aq. Species:		BDAP^{3+}	BDAP$^-$	BDAP$_2$Zn$_2$
Chemical shift [ppm]	H$_{A, B}$	3.23 / 3.04	2.93 2.68	2.86 2.60
	H$_X$	3.78	3.24	2.81
	H$_{C, D}$	3.40 / 3.35	2.95$^{(2)}$ 2.76$^{(2)}$	3.02$^{(1)}$ 2.31$^{(1)}$
Geminal couplings [Hz]	J$_{AB}$	14.4	13.4	12.8
	J$_{CD}$	16.7	13.0	10.4
Vicinal couplings [Hz]	J$_{XC, XD}$	6.3 / 6.8	8.2 / -	-
	J$_{XA, XB}$	6.3 / 8.7	8.6 / -	8.4

$^{(1)}$ Attributed on the basis of COSY experiment, Appendix, Figure A3
$^{(2)}$ Attributed on the basis of the titration of BDAP with ZnSO$_4$, Figure 7

The pH and concentration variations cause dramatic changes in chemical shifts and coupling constants which complicate even further the spectra. The differentiation of both sets of geminal protons increases as the pH increases. New, AMX like splitting patterns were observed in 0.1M borate solution, at pD = 9, (Table 4, Appendix, Figure A1).

A COSY experiment (Appendix, Figure A2) confirmed the initial observation that at pD 9, the ^{1}H-NMR signals at 2.95-2.93 ppm are coupled with all the other aliphatic signals

and therefore can be attributed to one of the protons situated on each of the C-1 and C-3 of

the 3-phenyl-1,2-diamino-propane residue of BDAP.

These pronounced spectral changes are more then a simple deprotonation effect due

to the increased pH values of the solutions. Partial or total deprotonation of the

ethylenediamino unit probably locks the structure in a limited number of more rigid

conformations. Similar effects take place when a metal ligates the ethylenediamino units

and will be discussed in the next paragraphs.

^{31}P-NMR data also provided evidence for the composition of the isolated form of

the BDAP. A sample with an estimated concentration of 2.5×10^{-2} M was titrated with HCl

and the chemical shifts were measured against an external standard of 85% H_3PO_4.

Downfield shifts were noticed when the sample was treated with increased amounts of HCl,

Table 5, indicating that the protonation of the phosphinate group takes place until the fully

protonated tetrahydrochloride with a maximum shift of >31.92 ppm is obtained. At ~pH 9

the phosphinate group is fully deprotonated, and the predominant species in the solution

contain ~2 of the amino groups deprotonated. Since the chemical shift of the isolated BDAP

hydrochloride is almost identical with that of species with free amino groups at pH 9, one

can conclude that: (i) the isolated, pure BDAP in solution, is not protonated on the

phosphinate group, the predominant species being somewhat less then a trihydrochloride.

(ii) the solid dissolved in water as sample #2, Table 5 is not a tetrahydrochloride, since no

protonation of the phosphinate group is indicated in the ^{31}P-NMR spectrum (iii) since for

1,2-propylenediamine pK_a values at room temperature are 9.8 and 6.9,[65] the solid BDAP

must be in the trihydrochloride form.

The elemental analysis of a well dried solid sample of BDAP also supported the

trihydrochloride, in a hydrated form: $BDAP(HCl)_3(H_2O)_4$. Supplemental evidence for this

composition was also obtained from UV linear fits of the absorptions at 230 nm of dilutions

of a BDAP sample obtained from the decomposition of an exact amount of pure, protected

BDAP -hydrochloride 35,sample. Assuming a 100% deprotection yield, an extinction coefficient of ε^{230} = $(2.51\pm0.02\times10^4)$ M^{-1} cm^{-1} was found. The same ranges of extinction coefficients were determined for solutions of pure samples of BDAP x 3HCl x $4H_2O$ in 0.1M HCl. Thus strong evidence was obtained for the well defined composition BDAP x 3HCl x $4H_2O$ by combining the results of individual ^{31}P-NMR, UV and elemental analysis.

Table 5 ^{31}P-NMR data and protonation forms for aq. solutions of BDAP (external standard of 85% H_3PO_4)

Sample Number	Species	$^{31}PNMR$ Shift [ppm]	Protonation degree, "n" for BDAPxnHCl
1	~1.5×10^{-2} M BDAPxnHCl in 0.2M borate buffer, (pD = 9)	23.57	<3
2	~2.5×10^{-2} M BDAPxnHCl, pH3-4	23.55	≤ 3
3	sample 2+1 eq.HCl 1M	25.27	3-4
4	sample 2+2 eq.HCl 1M	27.39	3-4
5	~2.5×10^{-2} M BDAPxnHCl, sample in 0.1M HCl	31.92	~4

Several other methods for the determination of the composition of the isolated BDAP failed to match the above results or the less accurate results of peak integration in ^1H-NMR. For pure BDAP samples, 2,4,6-trinitrobenzenesulfonate[125](TNBS) and ninhydrin[126] spectrophotometric amine quantitative analyses gave repeatedly concentrations in BDAP x 3HCl of only 65-80%. UV monitoring of the TNBS samples in time revealed

that in the BDAP case, the nucleophilic substitution with amino groups is not complete, within the reaction time recommended in the standard procedure. For the ninhydrin method, the extinction coefficients at λ_{max} = 570 nm per amino group for both the ethylenediamine or BDAP were found to be ~20 times lower than those reported by the authors.[126] However, the results corresponded to a 99% pure sample of BDAP x 3HCl x 4H$_2$O when the fits were repeated at λ_{max} = 406 nm and were based on a ethylenediamine calibration curve.

A VIS spectrophotometric complexonometric titration of a ~5 mM BDAP in aq. 0.1M borate solution with aq. CuSO$_4$ failed to give consistent results due to the precipitation at different points of the titration of insoluble cooper complexes, while the ~10 mM ethylenediamine control remained in solution and gave good correlation results. However, titrating lower concentrations of BDAP ligand was not attempted due the lack of sensitivity determined by the low extinction coefficient (ϵ^{612nm}) of the cooper(II) -ethylenediamine complexes.

IV.2.2 BDAP Labile Complexes

The extent and the outcome of the self-assembling process is strongly dependent upon the pH, concentrations of different species and the nature of the metal used for the construction of the chelation bridge.

A fair estimation of the concentration and pH ranges where the BDAP - M complexes are soluble can be extrapolated from existent literature data.[65] The pK_{a1} and pK_{a2} values for the ethylenediamine are 7.1 and 9.9 and for 1,2 propylenediamine 6.9 and 9.8 at 25 °C in a 0.1M ionic strength solution. Other important stability constants with ethylenediamine and hydroxide ligand are given in Table 6. Since most of the metal hydroxides mentioned in the Table 6 also have low solubility products (e.g. K_{sp} = 2.2x10^{-20} for Cu(OH)$_2$ and K_{sp} = 1.8x10^{-14} for Zn(OH)$_2$), the presence of insoluble species must be

taken into account, especially at high pH values and concentrations of metal ion. The precipitation aspects are more complex, if one takes into account factors as insoluble mixed ligand complexes or aging of the precipitates or irreversible precipitation. Another aspect, this time favorable to the ethylenediamino chelation process is the contribution of the effect of molarity in the last cyclization step, when the desired cyclic M_2BDAP_2 forms.[52, 127]

Table 6   Logarithms of stability constants for metal complexes given for 0.1-1M ionic strengths[65] $logK_{1-3} = log(K_1 \cdot K_2 \cdot K_3) = -(pK_1+pK_2+pK_3) = -pK_{1-3}$; the stabilities of 1,2 propylenediamine complexes are similar (+/- 0.1 pK units)

metal center	en			OH^- ion		Notes
	$logK_1$	$logK_{1-2}$	$logK_{1-3}$	$logK_1$	$logK_{1+2}$	
Co(II)	5.6	10.5	13.8	3.9	4.5	oxidatively unstable
Co(III)	-	34.7	48.7	13.52	-	-
Cu(II)	10.5	19.6	-	6.3	12.6	stable $Cu(OH)_2$
Ni(II)	7.4	13.5	17.7	3.7	8.0	$OH^-:-pK_{1-4}=28.3$ stable $Ni(OH)_4^{2-}$
Pd(II)	-	-	-	12.4	25.2	en:-$pK_2 = 18.4$
Zn(II)	5.7	10.6	13.2	5	8.3	$OH^-: pK_{1-4}=18.0$ stable $Zn(OH)_4^{2-}$

Due to these multiple complex equilibria, an quantitative comprehensive simulation was not attempted but some pH limits were estimated for the preliminary self-assembling and binding experiments. A simulation of the independent effect of pH on the species which participate in the auto-assembly process is shown in Figure 6. Only the independent

processes of ligand protonation, metal ligation in soluble and insoluble hydroxides was taken into account. Analysis of the concentration profiles and the precipitation limits shows that only a narrow pH range of 8.2-8.5 would keep enough of the free metal and ligand in solution for the chelation to take place. In reality, this range broadens, due to the essential contribution of the chelation process. Therefore, in most of the experiments with Zn_2BDAP_2, a borate buffer media, at pH = 9-9.5 and concentrations of the complex lower than 1mM were used successfully.
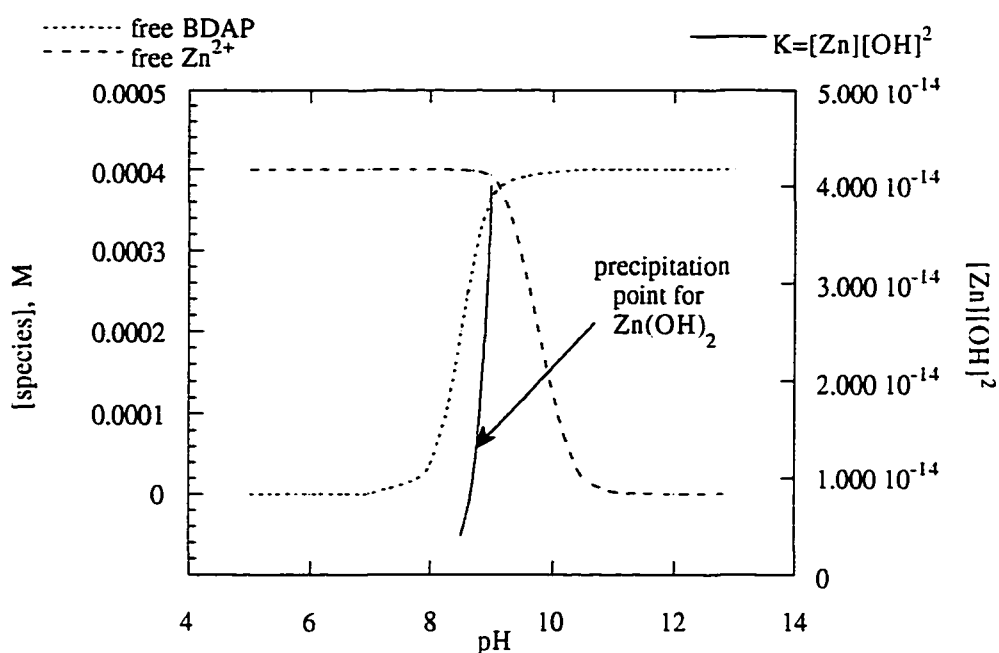
Figure 6   Concentration profiles of BDAP (...) and Zn (—) as a function of the pH of the buffer. Chelation was not considered. Variation of the effective solubility product, K (___); Precipitation of $Zn(OH)_2$ occurs when $K > K_{sp} = 1.8 \times 10^{-14}$

The constitutional and structural differences between the ethylenediamine and BDAP ligands were revealed experimentally when the limits of solubility of the complexes were tested. While all the complexes prepared in 0.1M borate buffer at concentrations of Co, Zn, Ni, Cu, and Zn ions under 1.2 mM and in presence of 2 equivalents of

ethylenediamine were soluble, some of the corresponding BDAP complexes have shown limited solubilities in the same concentration range. The Cu and Zn complexes in 0.1M borate buffer, were all soluble at a concentration under 1.2 mM metal in presence of 1.4 equivalents of BDAP. In the same conditions, Ni, Co(II), and Pd cations precipitated. Cutting all concentrations to 1/2 left only the Co(II) insoluble.

The reason of using excess of ligand is to favor the formation of macrocyclic species instead of oligomeric ones and to avoid precipitation.[71] UV analysis of the remaining solutions after partial precipitation of the Ni and Co species revealed that the precipitates contain 60-67% of the ligand. Evidence of oxidative complexation of Co(II) in presence of BDAP ligand are discussed in section IV.2.3.

Direct evidence for the macrocyclic self-assembly of the $Co(III)(CO_3)$, Cu(II), Pd(II) and Zn(II) M_2BDAP_2 type complexes was searched in mass spectroscopy. Mild ionization techniques, such as electrospray (ESI) and fast atom bombardment mass spectrometry(FAB) were reported for the detection of molecular ions of metal mediated self-assembled labile macrocycles[71] or [2]-catenanes.[82] ESI ionization technique was reported[128] to be also used in the observation of cobalamin-dependent methionine synthase holoenzyme. Therefore, there are enough reasons to believe that this method would prove useful in the detection of the self-assembly and also in substrate binding, in the case of the high affinity host-guest complexes.

In our hands, in neither Co_2PBP_2 nor the M_2BDAP_2 case, no proof of monocharged ionic species was obtained using ESI or MALDI-MS. However, multiply charged M_2BDAP_2 species and fragments were found in the Co-carbonato, Pd and Zn cases, consistent with the complexation with a 1:1 ligand to metal ratio (see Chapter V).

Due to the better solubility and uncomplicated NMR spectral features, most of the structural and binding studies were made on the Zn_2BDAP_2 receptor. Relatively simple to follow upfield shifts are produced by complexation, in the aromatic area. The shifts are

dependent on the BDAP : Zn ratio, representing an average between the complexed and

uncomplexed ligand and are characteristic of a fast complexation equilibria. The shifts in

the aliphatic area of this self-assembled host are not all in the same direction, complicating

even more an already complex spectral area. A titration of the ligand with $ZnSO_4$ solution

revealed the following aspects (Figure 8): (i) all the shifts are linear, characteristic of a high

affinity constant self-assembling process; (ii) when excess of Zn is present, the shifts level

off, indicating essentially a 1:1 complexation process; (iii) the "equivalence point" of the

titration is indicating an approximate concentration of BDAP of 94%; (iv) the large shifts

especially in the aliphatic region are those expected for a complexation process where the

metal center binds to aliphatic amino groups; (v) the small aromatic shifts suggest that the

aromatic phosphinate group does not interfere in the macrocyclization, by Zn ligation.
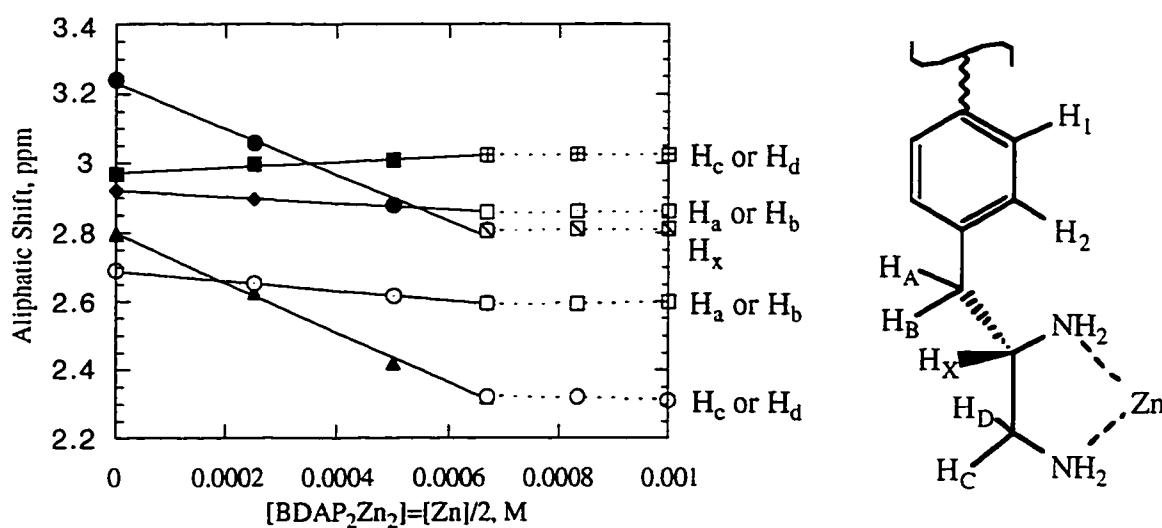
Figure 7 ^1H-NMR titration of 5.4×10^{-4} M BDAP ligand with 1.0×10^{-1} M $ZnSO_4$ in 0.1M borate pD = 9 buffer the maximum shifts: for aromatic protons (not shown): $H_1 = -0.009$ and $H_2 = -0.065$ppm; for aliphatic protons: $H_x = -0.433$, H_C and D = 0.456 and +0.070 ppm, H_A and B = -0.052 and -0.104 ppm. Attribution of H_C and D signals is based on the COSY experiment (see Appendix, Figure A3)

As expected, the maximum shifts in the aliphatic region are those of the H_X, H_C and H_D protons. As a result of the chiral environment, one of the H_C or H_D protons is more sensitive to chelation than the other.

A COSY experiment (Appendix, Figure A3) was performed to check the partial assignments based on the titration experiment. Strong couplings between the 2.60 and the 2.81-2.86 ppm signals and the lack of strong coupling between 3.02 and 2.86 ppm confirms the above assignments. The relatively strong coupling between the 2.31 and the 3.02 ppm signals constitutes evidence to assign the 3.02 ppm peak to one of the H_C or H_D protons. Next, based on the proton correspondence chart established during the titration experiment, (Figure 7), the signal at 2.95 ppm from the NMR spectrum of BDAP in borate buffer could be attributed to one of the H_C and H_D protons. This way all the constitutionally different protons could be attributed, as shown in Table 4.

Circular dichroism (CD) spectra of the free BDAP ligand and its Zn and Co(III)-carbonato complexes were also acquired. Significant changes in the ellipticity were noticed when 0.8 equiv. of $ZnSO_4$ were added to a millimolar range concentration of free BDAP ligand (Figure A4). Due to the large difference of $\Delta\theta = (1.867 \pm 0.005) \times 10^{-6}$ deg $M^{-1}cm^{-1}$ in ellipticity between 232 and 248 nm, the method was considered sensitive enough to be used at the determination of the concentrations of the Zn_2BDAP_2 macrocycle where its dissociation becomes significant. The absolute values of the ellipticities E at different wavelengths for solutions of Zn_2BDAP_2 in the $1.4 - 45 \times 10$ M^{-5} range were decreasing linearly with the concentration, suggesting that no dissociation of the macrocycle occurs at these ranges of concentration. The linear fit the data (Figure 8), also allowed the calculation of the specific molar ellipticity of the Zn_2BDAP_2 at $\lambda_{max} = 232$nm of $\theta = (-1.864\pm0.007) \times 10^{-6}$ deg $M^{-1}cm^{-1}$. Best linear fits however were obtained using differences in ellipticities, ΔE, measured at wavelengths with the most pronounced Cotton effect, such as 232nm and 248 nm. Fits of ellipticities at lower wavelengths than 225 nm were less accurate, contrary

to the expectation that the high Cotton effect will increase the sensitivity of the

measurement. Probably the strong background UV absorption of the BDAP ligand

interferes in this case.

Under 1.4×10 M^{-5} concentration, the dispersion of the ellipticities was too large to

be fitted. Therefore a low concentration dissociation limit could not be established with the

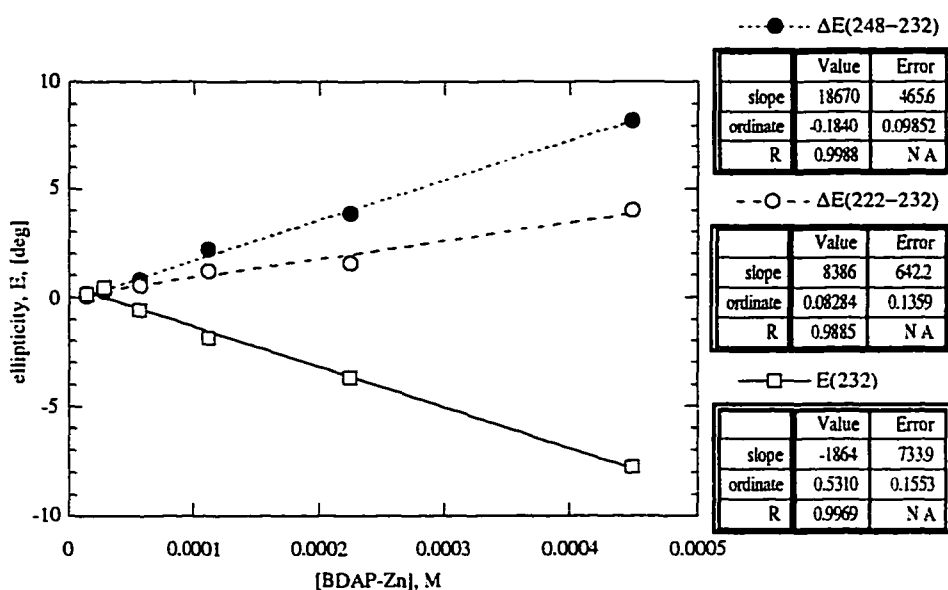0.1cm light path cell used in these series of experiments.

···●··· ΔE(248–232)

	Value	Error
slope	18670	4656
ordinate	-0.1840	0.09852
R	0.9988	N A

--O-- ΔE(222–232)

	Value	Error
slope	8386	6422
ordinate	0.08284	0.1359
R	0.9885	N A

—□— E(232)

	Value	Error
slope	-1864	7339
ordinate	0.5310	0.1553
R	0.9969	N A

Figure 8   [Zn₂BDAP₂] range where no dissociation occurs at Zn/BDAP molar ratio of

0.85. From the slope of the E(232nm) fit, θ^{232nm} = $(-1.864 \pm 0.007) \times 10^{-6}$ $M^{-1}cm^{-1}$ was derived; the most accurate fit is E(248-232nm) = f(BDAP₂Zn₂)

The fact that the macrocyle does not dissociate at concentrations greater then 1.4×10

M^{-5} is an important result, even if further studies using a 1cm cell would probably lower

this concentration to a more exact limit. The experiment proves that the Zn₂BDAP₂ host can

be used without the interference of any dissociation process at dilutions of 10 -100 μM and

above, thing which was not possible in the Co₂PBP₂ host case.[71]

A less accurate value for the molar specific ellipticity of the BDAP-Co carbonato complex was estimated for λ_{max} = 232.5 nm at -2.6x10^{-6} M^{-1}cm^{-1} and for visible region, for λ_{max} = 504nm to θ = -8.6x10^{-4} deg.M^{-1}cm^{-1}. Interpretation of CD spectra in the UV and the visible regions (Appendix, figure A4) could lead to important configuration assignments for both Co(III) and carbon chiral centers.[129] The CD maxima in the visible area of the Co macrocycle could also allow convenient determinations of weaker binding constants with aromatic guests.

IV.2.3 Synthesis of BDAP$_2$Co$_2$(CO$_2$)$_2$

Mixtures of Co(II) salts in the presence of ethylenediamine are reported[130] to oxidize at room temperature when exposed to air with the formation of a pink precipitate containing Co(II) and Co(III) complexes. The behavior of the BDAP ligand is analogous, leading to the formation of precipitates which remain insoluble even in hot, concentrated HCl. The addition of 0.8 equiv. of CoCl$_2$ to a deaerated 0.1mM aqueous solution of BDAP in anaerobic conditions, leads to the slow formation of a white precipitate which is soluble in 1M HCl. This white precipitate remains soluble in acid even after being exposed to air. However, even at further dilution, these white suspensions, which presumably contain Co(II) oligomeric species, remain insoluble. A more directed assembling was attempted by templating the formation of the cyclic BDAP-Co dimers starting from labile Co$_2$PBP$_2$ complexes. To 1 equiv. of the soluble Co$_2$PBP$_2$ complex (~0.5mM concentration in aq. 0.1M borate, preformed from 2 equiv. of PBP and 1.6 equiv. of Co(II)), 2 equiv. of BDAP ligand was added. Thus, BDAP was expected to form a stable complex, by displacing the lower affinity, the labile PBP chelating group. Moreover, the process was expected to proceed as a successions of stepwise equilibria, resulting in the selective formation of the cyclic Co$_2$BDAP$_2$ host, mainly based on the effect of molarity which should be similar with

that determined for the macrocyclization of Co_2PBP_2 (EM = 0.062 M). However, the templating conditions tested in both aerobic and anaerobic conditions failed to yield soluble precipitates. Suspecting that the main difficulty in the formation of a BDAP-Co cyclic dimer is the concurrent formation of insoluble linear oligomeric aggregates, a more controlled synthetic route was designed. The synthetic studies started from the known syntheses of Co(III)-ethylenediamino complexes.

Soluble ethylenediamino complexes with the general formula $Co(III)L_2en_2$ are generally[131] prepared in 1 step, from a mixture of a Co(II) salt and the appropriate ligands[132,133] in presence of air or H_2O_2. Next, by heating the complexes with new ligands, the"L" ligands can be selectively substituted.[134,135] In presence of excess of ligand L, the slow equilibrium between the cis /trans configurations can also be shifted.[136, 137] However, the application of these methods for the synthesis of the cyclic BDAPCo complexes is still missing the high dilution conditions which would favor the formation of the highly desired cyclic complexes. Selectivity for cyclic complexes can be achieved by working in solid phase or in dilute solutions,[138] at concentrations lower than the effective molarity (EM[52, 127]) which characterizes the ring closure of the BDAPCo dimers. A two step procedure favors this type of selectivity by forming first the Co_2BDAP complex and allowing it to react at low concentrations with another equivalent of BDAP (Scheme 13). It is well known that even in the absence of a particular strain, the EM values for the formation of rings larger than 10 are relatively low.[138] As an estimate, the EM = 6.2×10^{-2} M value for the equilibrium cyclization of Co_2PBP_2[71] can be used. Working at concentrations lower than 10^{-2} M should provide a reasonable basis for selectivity. Additional use of a naphthalene template[60] may result in supplemental enhancement of the EM for the cyclization. The "wrong" alternative is the 1 step procedure (Scheme 13), where 3 intermediates are formed in approximately the same amounts. Even at high dilutions, in a next complexation step, this
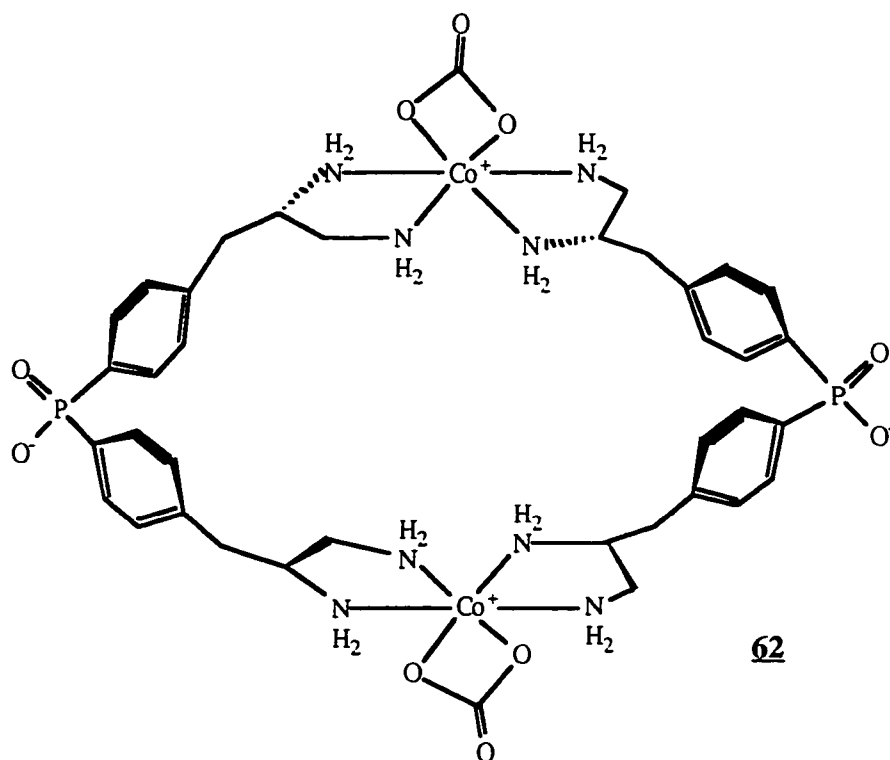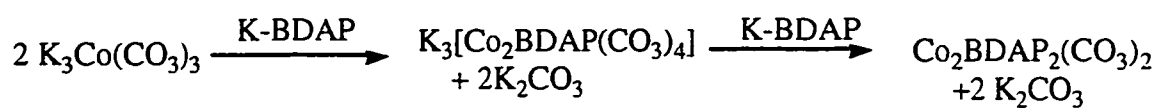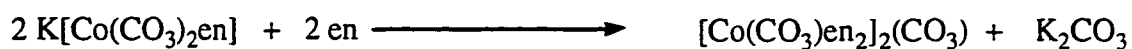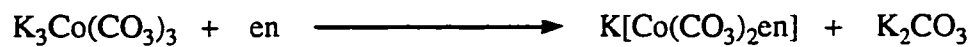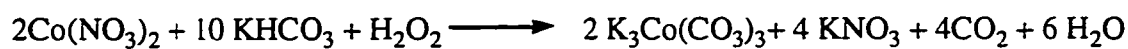
mixture should statistically yield a mixture of 4 : 5 of complexes incorporating two BDAP

residues, which are susceptible to oligomerize or cyclize respectively.

The 2-step selective cyclization route can be conveniently followed by using the

versatile carbonato- Co complexation method[139] which is well known for the preparation of

[Co L_{1-4} en$_{1-2}$] type complexes (Scheme 14). The labile tris carbonatocobalt green complex

$K_3[Co(CO_3)_3]$[140, 141] can undergo step-by-step ligand substitutions. The conversion to the

blue, $K[Co(CO_3)_2en]$ mono-ethylenediamino-carbonato complex[141] proceeds fast, at room

temperature, in highly concentrated solutions. The second ethylenediamine substitution does

not take place in the mentioned conditions, being much slower.[142]
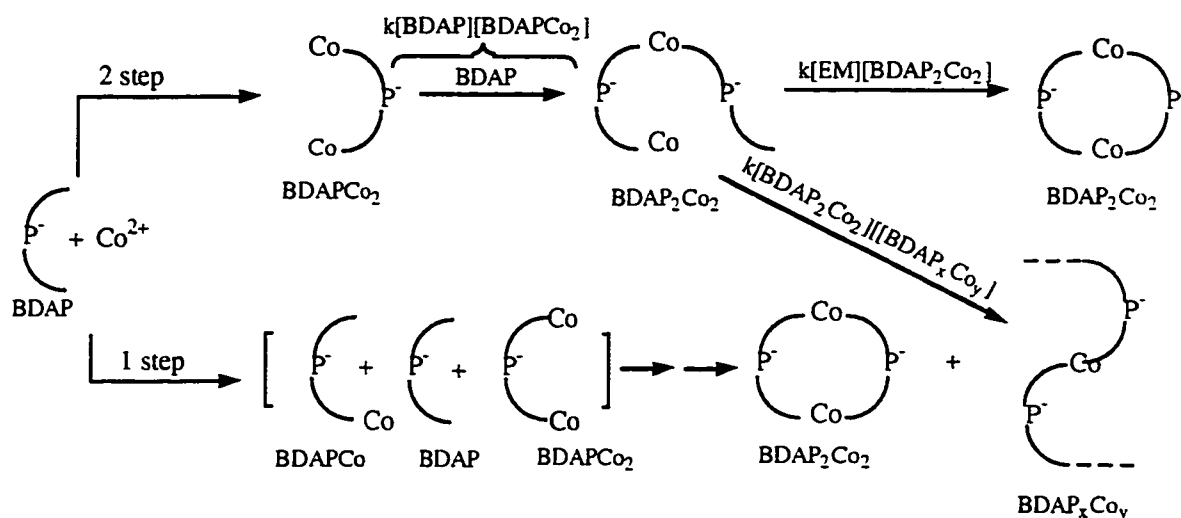
Scheme 13   Alternative schemes for the preparation of cyclic Co_2BDAP_2 complexes

Actually, the second substitution has not been studied for preparative purposes,as a

separate step, because of the lack of practical interest. The pink $[Co(CO_3)en_2]Cl$ is usually

prepared directly from the green tris carbonato-cobalt complex[143] or from ethylenediamine-

monocarbamates[144] formed *in situ* by bubbling CO_2 in a cold solution containing H_2O_2,

ethylenediamine and Co(II).

$$2Co(NO_3)_2 + 10 \, KHCO_3 + H_2O_2 \longrightarrow 2 \, K_3Co(CO_3)_3 + 4 \, KNO_3 + 4CO_2 + 6 \, H_2O$$

$$K_3Co(CO_3)_3 + en \longrightarrow K[Co(CO_3)_2en] + K_2CO_3$$

$$2 \, K[Co(CO_3)_2en] + 2 \, en \longrightarrow [Co(CO_3)en_2]_2(CO_3) + K_2CO_3$$

$$2 \, K_3Co(CO_3)_3 \xrightarrow{\text{K-BDAP}} \begin{array}{c} K_3[Co_2BDAP(CO_3)_4] \\ + 2K_2CO_3 \end{array} \xrightarrow{\text{K-BDAP}} \begin{array}{c} Co_2BDAP_2(CO_3)_2 \\ +2 \, K_2CO_3 \end{array}$$

62

Scheme 14   The proposed preparation of the $BDAP_2Co_2(CO_3)_2$ complex follows well

known route for the preparation of bis-ethylenediamino-carbonato-cobalt

In the next paragraphs a similar procedure starting from the "green solution" of $K_3[Co(CO_3)_3]$ will be described for the preparation of $BDAP_2Co_2(CO_3)_2$ complexes. The outcome of this preparation will be a mixture of diastereoisomers **62** presenting optical activity due to the fixed configuration of the ligand's chiral carbon. In addition to the more selective cyclization route, there are several other advantages offered by the structure **62**.

A third step of carbonate ligand substitution is possible, especially in acidic conditions.[145] Preparative applications for the synthesis of bis-ethylenediamino cobalt complexes with acetylacetone,[146] cis-diaqua-,[110]cis-dibromo- cis and trans-aquabromo-[147] sulfate, thiosulfate p- nitrophenyl methyl-phosphonate (which is slowly hydrolyzed to methyl phosphonate) and phosphate[131] are known.

The initial studies were made on the ethylenediamine model compounds. A key synthetic step, the preparation of the bis-ethylenediamino-carbonato-cobalt starting from mono-ethylenediamino-carbonato-cobalt is not mentioned in literature. The reaction, run at high [Co(II)] concentrations (~0.5-1 M) and a slight excess of ethylenediamine yielded a product with ^{1}H-NMR, UV spectra and the color matching that of an authentic sample of $[Co(CO_3)en_2]Cl$.[142]

Within the same range of concentrations, the reaction of Co(II) with ethylenediamine, H_2O_2 in CO_2 saturated aqueous solutions was successfully adapted for the monoethylenediamino-carbonatocobalt synthesis. Next, the studies were focused on adapting these preparative methods to the milimolar range of $[Co^{2+/3+}]$ concentrations. The low concentration preparation of $K[Co(CO_3)_2en]$ *via* the ethylenediamine-monocarbamate method[142] yielded mixtures of mono- and bis-ethylenediaminocarbonatocobalt complexes even when the starting Co(II) and ethylenediamine were used in ratios higher than 1. The lack of selectivity in this case is probably due to a 70°C heating period which is necessary for any complexation to take place.

The preparation at ~10mM concentrations of the K[Co(CO$_3$)$_2$en], starting from 1eq. K$_3$Co(CO$_3$)$_3$ and 1.1 equiv. ethylenediamine in 0.1 M KHCO$_3$ aqueous solutions proved also unsuccessful. At these concentrations,~10 times more diluted then those recommended in literature, impure complex mixtures are formed, also accompanied by large amounts of precipitates. Suspecting that the main problem is the instability of the tris-carbonato complex, tests were repeated at higher KHCO$_3$ content. The rates of ligand exchange were slowed down but the yields were almost quantitative and the UV of the product corresponded to that of the authentic compound.

As an alternative, the solid phase synthesis of [Co(CO$_3$)en$_2$]Cl proved also successful. After the preparation in solution phase, the [Co(CO$_3$)$_3$]$^{3-}$ was retained on a Dowex 1X4 anion exchange column. Heating the beads loaded with tris-carbonatocobaltic complex with ethylenediamine, changes the color of beads from green to blue (characteristic for [Co(CO$_3$)$_2$en]$^-$ anion which is still retained). After the complexation with ethylenediamine, the remaining dark-brown beads still contained Co residues, but a 80% conversion of the ethylenediamino ligand to a UV spectroscopically pure [Co(CO$_3$)en$_2$]$^+$ complex was obtained.

Table 7 UV characteristics of Co(III) complexes, used in the Equations 1-4

Complex	λ (nm)	ε(M^{-1}cm^{-1})
K$_3$Co(CO$_3$)$_3$	640*	155
	440*	166
[Co(CO$_3$)$_2$en]$^-$	640	43
	568*	158
	512	66
[Co(CO$_3$)en$_2$]$^+$	568	39
	512*	134

* indicates a maximum in absorption at the specified wavelength

All the above reaction mixtures were monitored by UV. From the extinction coefficients determined at different wavelengths for authentic samples of $K_3Co(CO_3)_3$, $K[Co(CO_3)_2en]$ and $[Co(CO_3)en_2]Cl$, (Table 7), 2 sets of 2 equations (Equations 1-4), each with two unknowns (the concentrations of the complexes) were derived.

$$[KCo(CO_3)_2en] = -20.88 \left(\frac{A^{640}}{155} - \frac{A^{440}}{166} \right) \qquad \text{Eq.1}$$

$$[K_3Co(CO_3)_3] = \frac{A^{640}}{155} - [KCo(CO_3)_2en] \frac{43}{155} \qquad \text{Eq.2}$$

$$[KCo(CO_3)_2en] = -0.2785 \left(\frac{A^{512}}{134} - \frac{A^{568}}{39} \right) \qquad \text{Eq.3}$$

$$[Co(CO_3)en_2]^+ = \frac{A^{512}}{134} - [KCo(CO_3)_2en] \frac{66}{134} \qquad \text{Eq.4}$$

This simple set of equations are assumes that only two components contribute to the spectra, therefore constituting simplification of the real mixtures. The compositions derived with these equations and the ratio of absorptions A^{512nm} / A^{568nm} (which is $= 3.4$ for a pure sample of $[Co(CO_3)en_2]^+$) were the optimization tools used in monitoring the 2 step syntheses of the derivatives of bis-ethylenediamino-carbonato-cobaltic complexes.

Monitoring the first and second complexation steps with the model ethylenediamino ligand, the following preliminary observations were made: (i) the first step complexation is much faster than the second one; (ii) in the first step of complexation, concentrations of $KHCO_3$ of 0.7 M or higher are necessary to avoid the precipitation by-products; (iii) the $KHCO_3$ inhibits weakly both steps of the complexation; (iv) in the slower, second step complexation, the rate doubles if the $KHCO_3$ concentration is reduced 10 times (from 0.7 M to 0.07 M) without significant precipitation by-products; (v) $Ca(ClO_4)_2$ can be used to

reduce the concentration of free carbonate species, without affecting the concentrations of the carbonato-complexes; (vi) the green solution of $K_3Co(CO_3)_3$ described in the literature as unstable can be stored for weeks in refrigerator by simple dilution in 2 M $KHCO_3$.

Considering the simple model of a second bimolecular reaction, with no other competing reactions, concentration profiles from the first and the second step complexations were fitted using the Kaleidagraph® software package for Macintosh. Some of the equations which formed the basis of this fit are:

For starting material profiles: The second order kinetics for the conversion of $K_3Co(CO_3)_3$ to $K[Co(CO_3)_2en]$, (Equation 5) integrated and rearranged in the form: $K_3Co(CO_3)_3] = f(t)$, (Equation 6):

$$-\frac{d[K_3Co(CO_3)_3]}{dt} = k\,[K_3Co(CO_3)_3]\,([en]_0 - [K_3Co(CO_3)_3]_0 + [K_3Co(CO_3)_3])$$

Eq.5

$$[K_3Co(CO_3)_3] = \frac{[en]_0 - [K_3Co(CO_3)_3]_0}{\exp\left(k\,t\,([en]_0 - [K_3Co(CO_3)_3]_0) + \ln\frac{[en]_0}{[K_3Co(CO_3)_3]_0}\right) - 1}$$

Eq.6

For product profiles: The second order kinetics for the conversion of $[Co(CO_3)_2en]^-$ to $[Co(CO_3)en_2]^+$, (Equation 7), integrated and rearranged in the form: $[Co(CO_3)en_2]^+ = f(t)$, (Equation 8):

$$\frac{d[Co(CO_3)en_2]^+}{dt} = k\,([KCo(CO_3)_2en] - [Co(CO_3)en_2]^+)\,([en]_0 - [Co(CO_3)en_2]^+)$$

Eq.7

$$[Co(CO_3)en_2]^+ = \frac{[en]_0 - [KCo(CO_3)_2en]_0 \exp \mathcal{A}}{1 - \exp \mathcal{A}}$$

Eq.8

where:

$$\mathcal{A} = kt\left([en]_0 - [KCo(CO_3)_2en]_0\right) + \ln\frac{[en]_0}{[KCo(CO_3)_2en]_0} \qquad Eq.9$$

The initial concentrations of the reactants and the rate constant were the parameters used for the fit (Figure 9) of the equations 5-8. The difference found between the rate constants characterizing the first ($k^{56\,C} = 5.1\times10^{-2}M^{-1}s^{-1}$) and the second complexation step ($k^{56\,C} = 4.5\times10^{-3}M^{-1}s^{-1}$) represents a minimum. Since the second step complexation was run at 10 times lower concentrations of $KHCO_3$ and considering the inhibitory effect of $KHCO_3$, the calculated 11 fold difference in the rates is probably even larger (~20 fold).
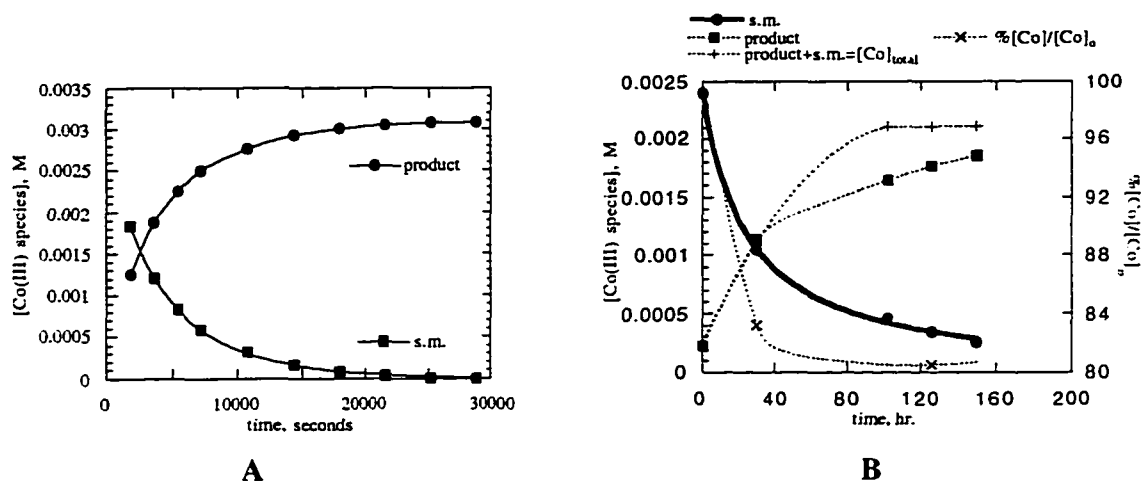
Figure 9   (A)   Concentrations of starting material, $[Co(CO_3)_3]^{3-}$ and product $[Coen(CO_3)_2]^-$ in the first step of the complexation, at 56°C, 0.7M $KHCO_3$

                    (B)   Concentrations of starting material $[Coen(CO_3)_2]^-$ and product $[Coen_2(CO_3)]^+$ in the second step of complexation, at 56°C, 0.07M $KHCO_3$; Also represented: the profile of the sum of concentrations of $\{[Coen(CO_3)_2]^- + [Coen_2(CO_3)]^+\}$ species and the % of $[Co(III)]$ recovery in the two complexes. The dotted curves are not representing the result of a curve fit calculation, they serve only to identify the points from the same profile

These determinations confirm the assumption that the competition between the two complexation steps is not significant. In the first stages of the second complexation step, some of the $Co(III)$ is lost relative to the initial, total balance of Co. These losses may be due to the thermal instability of the $[Co(CO_3)_2en]^-$ complex at prolonged heating times in presence of low concentrations of $KHCO_3$.

Since the only successful method for the low concentration preparations of mono- and bis-ethylenediamino complexes started from the green $[Co(CO_3)_3]^{3-}$ anion in solution or solid phase, the next studies for the preparation of $Co_2BDAP_2(CO_3)_2$ were focused on these 2 methods. Substituting the model ethylenediamine ligand with BDAP in the solid phase synthesis alternative, did not result in the release of the neutral $Co_2BDAP_2(CO_3)_2$ from the beads. The pink colored beads seemed to retain the desired complex, possibly through the same mechanism which takes place when the free BDAP ligand subjected to ion exchange on Dowex resins.

On the other hand, the slow and laborious high dilution, solution preparation of $Co_2BDAP_2(CO_3)_2$ proved successful. The first step was performed in 3-8 mM solutions of $[Co(CO_3)_3]^{3-}$ with 0.5-0.55 equiv. of BDAP and was complete within ~1 hr of heating. The second step was run at the same concentrations of $KHCO_3$ while the solutions were still blue or purple (conversion <50%). Then, a partial precipitation of ~90% of the $KHCO_3$ with $Ca(ClO_4)_2$ increased the reaction rate without affecting too much the stability of the remaining $[BDAPCo_2(CO_3)_4]^{3-}$. No rate enhancement were noticed due to the EM or when 0.25eq. of $ZnSO_4$.were added for each $Co(III)$,equiv., to template the cyclization.

At conversions ~80%, the second substitution step is stopped. Higher conversions are achievable, but also insoluble by-products are formed lowering the actual yield. The purification of $Co_2BDAP_2(CO_3)_2$ was made by passing the solution from the reaction through a K^+ loaded cation exchanger which is expected to retain all cationic impurities, $BDAP^{n+}$ and uncyclized products terminated in free BDAP ligands. Next, passing the

solution through a HCO_3^- loaded anion exchanger cleans the solution from unreacted

$[Co_2BDAP(CO_3)_4]^{3-}$, uncyclized products terminated in bis-carbonato-cobaltic BDAP

residues and other anionic impurities. The major, pink colored fraction which passed

through the columns unretained, was presumed to contain the desired macrocyclic complex

62. Two other colored complexes, violet and pink-orange are retained on this column. The

violet fraction is eluted at low concentrations of a $KHCO_3$ gradient and has the UV

absorption maxima at 536nm. Using the equations 1-4 the estimated ratio between the bis-

ethlyenediamino- and mono-ethylenediamino-carbonato-cobalt residues is 48:52 which

would approximately correspond to a monoanion **63**, which is restricted from cyclization

due to some intramolecular interaction.

63
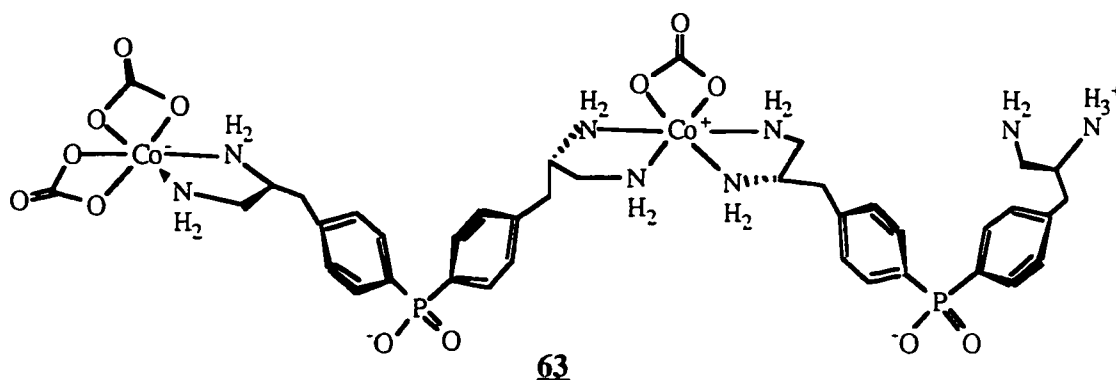
Acquiring mild ionization mass spectrometric evidences[82, 128] to support the

assigned structure **62** was problematic. The lability of the carbonate residue from these

complexes was revealed by submitting for ESI-MS an authentic sample of $[Co(CO_3)en_2]Cl$.

The weak molecular ion (Calc'd for $[en_2Co(CO_3)]^+ = 239.1$; Found 239.4 (30%)) was

accompanied by several intense fragment peaks. The most intense peak was found to be a

fragment missing a molecule of H_2CO_3 from the coordination sphere (Calc'd. = 177.1;

Found 177.4 (100%)). This fragmentation pattern implies that it is unlikely to find

unfragmented intense m/z peaks in the MS of the corresponding BDAP complexes.

Thus, as expected, no monocharged molecular ion corresponding to

$[Co_2BDAP_2(CO_3)_2]X^+$ at the calculated value for $C_{38}H_{52}N_8O_{10}P_2Co_2$ of m/z = 960.2 was

detected in either MALDI- or ESI- mass spectroscopy. The aqueous analytes contained also

K^+ and HCO_3^- ions at an almost neutral pH. Therefore, the carbonate species may be lost

from the coordination sphere or the counterion species. The following reasonable peak

attributions were made based on the association and fragmentation patterns described above.

No molecular peak for the BDAP ligand was detected in any of the spectra. Even if the

results are consistent with the fragmentation pattern observed for the $[Coen2(CO_3)]^+$ model

they remain inconclusive regarding the cyclic nature of the isolated compound.

Table 8　　　Attributions of the ESI-MS negative and positive ion peaks found for
different samples of $Co_2BDAP_2(CO_3)_2$ corresponding to the molecular ion
with the formula $C_{38}H_{52}N_8O_{10}P_2Co_2$ Calc'd: 960.2

Ionization Mode	Found		Attribution		
	m/z	%	Species	Charge	Calc'd m/z
Positive ions sample I & II	301.1	24	M+ H$^+$-CO$_3^{2-}$	+3	300.4
	481.2	9	M+2H$^+$	+2	481.1
Positive ions sample III	235.1	100	M+H$^+$+K$^+$ -CO$_3^{2-}$	+4	235.5
	291.1	53	M+4H$^+$+2KHCO$_3$	+4	291.0
	373.2	48	M+2H$^+$+2K$_2$CO$_3$ +H$_3$O$^+$	+3	373.1
	551.2	12	M+2H$^+$+KHCO$_3$- -H$_2$CO$_3$	+2	550.1
Negative ions sample III	353.6	100	M+K+CO$_3^-$-2H$^+$	-3	352.4
	451.5	32	M-Co^{3+}+H$^+$	-2	451.1
	549.5	17	M+K$_2$CO$_3$-2H$^+$	-2	548.1

The IR spectra of the solid $KHCO_3$ and $BDAP_2Co_2(CO_3)_2$ was taken in Nujol mull

and the absorptions found at 1633, 1307 and 831 cm^{-1} are close to those reported in the

literature for carbonato-complexes[148] and $[Co(CO_3)en_2]Cl$.[139] Several other diagnostic

absorptions could not be detected due to the overlap of the characteristic absorptions of the

excess of free bicarbonate (around 1415cm^{-1}). The proton and phosphorus NMR spectra are

characteristic for a mixture of isomers. Due to the high carbonate content, ^{13}C-NMR or an

elemental analysis were not possible. Indirect proof of a cyclic structure was found in the

binding studies (Section IV.3).

IV.3 Binding Studies

The binding abilities of the hosts incorporating the BDAP ligand 36 are studied next.

The purpose of the following binding studies is to detect and evaluate the strength of

binding between the self-assembled hosts and a relatively large variety of anionic and

neutral guests (Scheme 15).

M$_2$BDAP$_2$: 36 (Host)   M$_2$BDAP$_2$:Guest 64 (Complex)
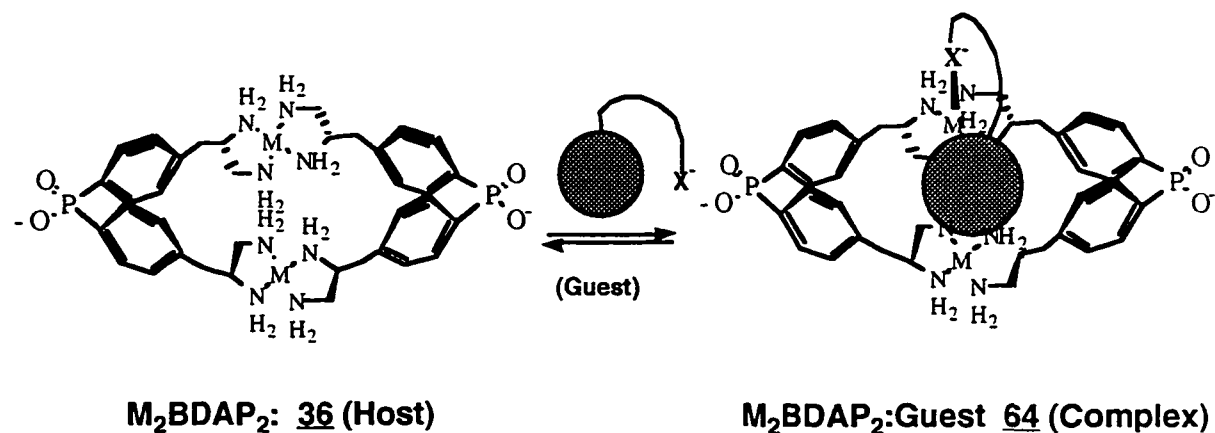
Scheme 15   Model of the binding of an anionic guest by the self-assembled M$_2$BDAP$_2$
host

For the evaluation of the binding strengths, the dissociation constants K_D (Equation 10) will be determined:

$$H + G \rightleftharpoons H{:}G \qquad\qquad K_D = \frac{H \bullet G}{H{:}G} \qquad\qquad \text{Eq. 10}$$

The determination of the K_D values allowed to evidence the cooperativity and selectivity in binding of the host. for guests containing certain structural features (Tables 9, 10, 11). The cooperativity between the inclusion of the aromatic moiety in the host cavity and the electronic interaction of the functional group X with the positively charged metal center is expected to result in enhanced stabilities of the H:G complexes **64**. This synergetic enhancement will be evaluated by calculating the value of the effective molarity[52, 127] (EM):

$$EM = \frac{K_D^X \bullet K_D^A}{K_D^{obs}} \qquad\qquad \text{Eq. 11}$$

IV.3.1 Detection of Binding: Transport Experiments

The carrier (host **36**) mediated transport of hydrophobic guests through aqueous membranes is a fast qualitative screening method for the detection of binding. The different metal cation containing self-assembled hosts M_2BDAP_2 can be qualitatively classified into strong, medium or weakly binding hosts. The experiments were performed in "H shaped tubes" (Figure 10), designed originally by Murakami and Snyder.[149]

Due to the hydrophilic exterior surface of the M_2BDAP_2 host, the solubility and partition constants of the bound guest in the aqueous phase is expected to increase. This determines increased transport rates of the guest between the "Source" and the "Receiving" isooctane layers. The experiment started by adding the guest in the "Source Phase" and

BDAP ligand in the aqueous phase. A background transport rate of the pyrene, which essentially is limited by the solubility of the free pyrene was determined this way. The rate of accumulation of the guest in the "Receiving Phase" can be monitored by UV spectrophotometry. Then, different metal cations were added in the aqueous phase. The self-assembling of the host M_2BDAP_2 **36** was expected to increase the transport rate due to the enhanced solubility of the host-guest complex **64**.
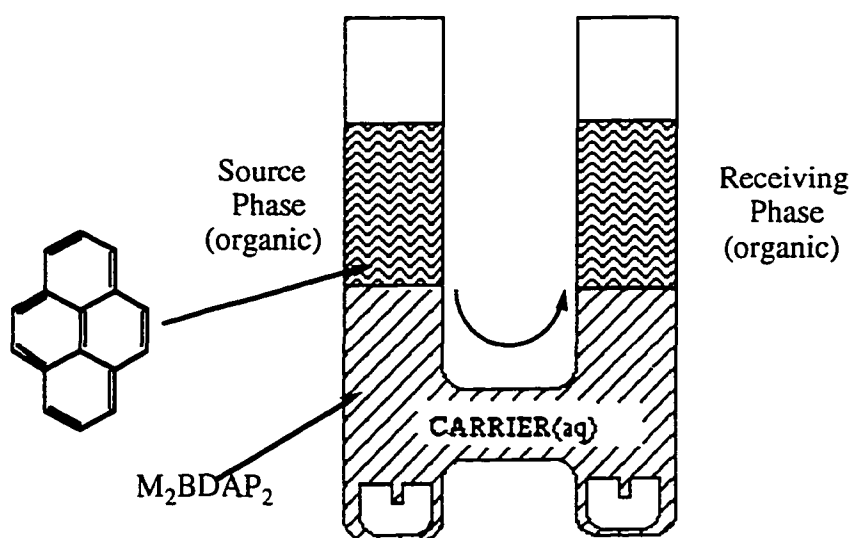

Figure 10   The Murakami[149] "H shaped tube" used in the transport experiments. Perfect mixing (at constant magnetic stirring rates) is assumed to take place in each of the phases

Pyrene was chosen as a guest due to its low solubility (low background transport rate) and high mediated transport rate found in previous Co_2PBP_2 mediated transport experiments.[71] The cations Cu, Pd, Zn, Ni and Co were chosen initially for the self-assembling process of the host.

The slopes representing the rate of the absorbance increase of pyrene in the receiving phase are with 95% confidence limit in the ranges 0.0062±0.0001 and

0.00081±0.0005 respectively. Since the two ranges do not overlap, the slight increase in the transport rate of pyrene of 1.3 can be considered as meaningful.

In theory, larger transport rate increases may be achieved by increasing the concentration of the host in the aqueous layer. However, this was not possible due to the formation of small amounts of precipitates at concentrations of M_2BDAP_2 larger than 0.5 mM. When partial precipitation occurred, the stirring rate changed and the results were found to be non-reproducible. Only in the Zn_2BDAP_2 case, evidence for binding pyrene was obtained by using this screening method, and therefore, the first ^1H-NMR binding experiments were focused on this host.

—●— [BDAP]=0.54mM
slope=0.00616Au/hr

-- □ -- [Zn2BDAP2]=0.53mM
slope=0.00810Au/hr
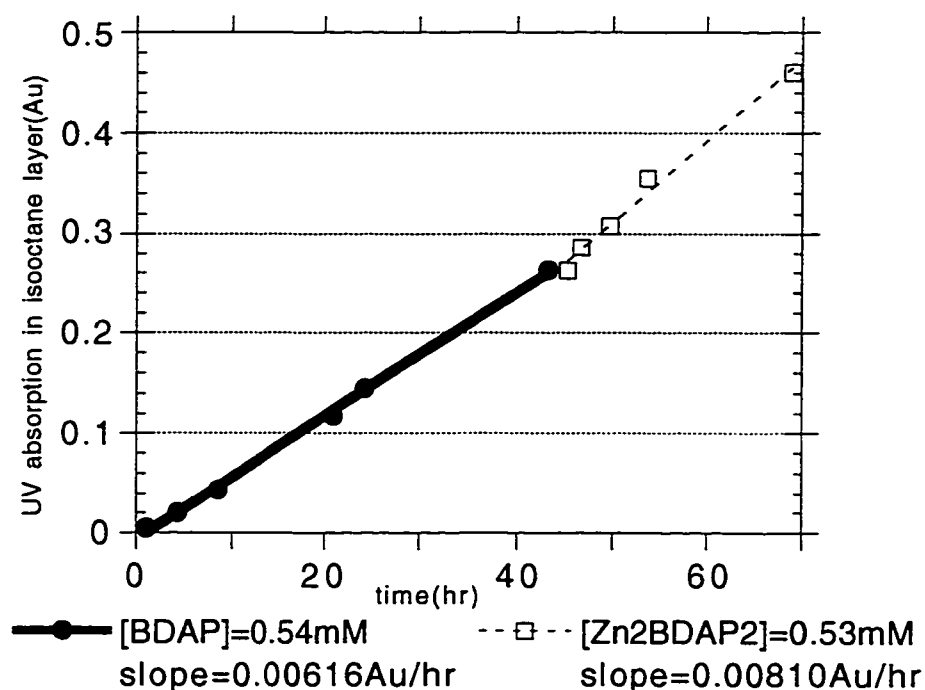
Figure 11   Transport rate of pyrene from the isooctane source phase, through aqueous

0.1 M borate membranes to the isooctanic receiving phase. Experiment done

in the presence of the ligand 35 only(—) or of the self-assembled Zn_2BDAP_2

host 36, M=Zn^{2+} (....)

IV.3.2 NMR Binding Studies

Among the variety of methods available for the evaluation of intermolecular associations, the ^{1}H-NMR titrations are the most complete and less subjected to misinterpretations.[150] For a fast equilibrium host-guest system (Equation 10), the observed chemical shift, δ_{obs} is a weighted average of the two states of the probe-proton: the "unbound" = "initial" state and the "bound" state:

$$\delta_{obs} = \delta_0 \cdot (H_0 - H \vdots G) / H_0 + \delta_{bound} \cdot (H \vdots G) / H_0 \qquad \text{Eq. 12}$$

where H_0 is the initial concentration of the host being titrated. Rewriting the equation 12 and substituting the $H \vdots G$ term with known terms from the expression of the equilibrium constant, one can derive the equation which is used for the determination of the dissociation constant, K_D.
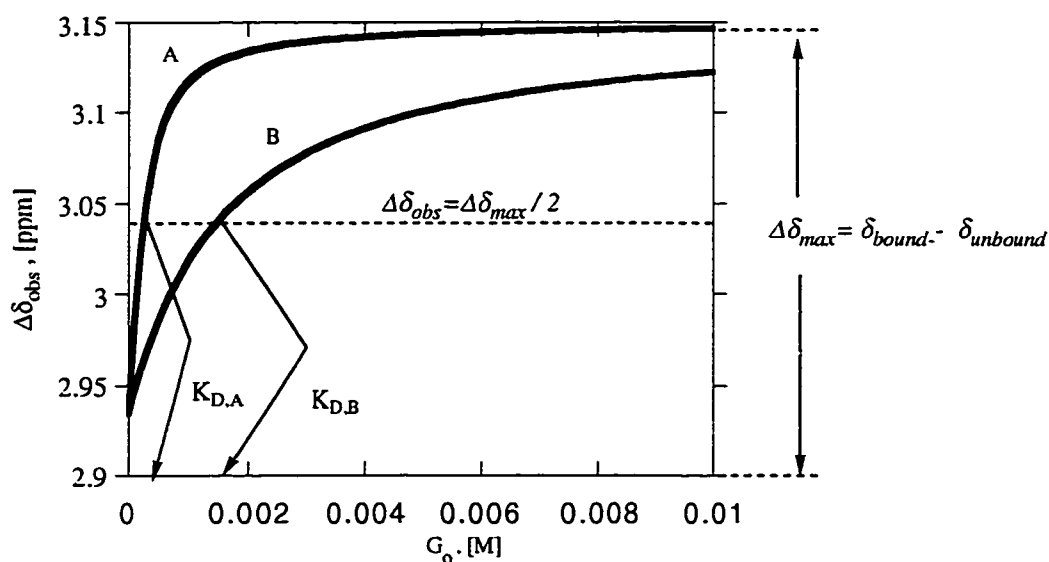
Figure 12   Binding isotherms for a strong association (A; $K_D = 1.4 \cdot 10^{-4}$M); for the same $\Delta\delta_{max}$ and δ_0 values, a relatively weaker association was simulated (B; $K_D = 1.4 \cdot 10^{-3}$M)

$$\delta_{obs} = \delta_o + \frac{\Delta\delta_{max}}{2H_o}\left(S - \sqrt{S^2 - 4H_o G_o}\right)$$ Eq. 13

where S and $\Delta\delta_{max}$ are expressed as: $S = H_o + G_o + K_D$, and $\Delta\delta_{max} = \delta_{bound} - \delta_0$ (the maximum extrapolated shift for fully complexed host).

The plot from Figure 12 corresponds to equation 13 and illustrates several important physical identities: (i) one can justify the use of dissociation constants as being the concentration of the guest when the system contains equal concentrations of bound and free host, i.e. $\Delta\delta_{obs} = \Delta\delta_{max}/2$; (ii) the curved region of each plot is the one which defines the most sensitively the strength of the binding process; the "linear" regions correspond to the "saturation" of the minor components and are less informative.

In an analysis-review on the systematic error sources in the NMR determination of binding constants, Wilcox[150] redefines an important criterion to meet when choosing the "titration points". These data points should be situated in the "curved" area of the binding isotherm, which is best defined as the 20-80% saturation interval of the minor component with the major component of the equilibrium.

When limited amounts of host are available, it is convenient to follow the titration at a constant host (H_o) concentration. For the determination of strong associations, an alternate dilution protocol is also available, at constant H_o / G_o ratio. However, this method may require longer NMR acquisition times especially for the last, low dilution data points.

The binding results derived from a selected series of NMR titrations are presented in Table 9, 10 and 11. Some of the headings are detailed below:

IV.3.2.1   Titration Conditions   All the binding data were determined at constant host concentration: a M_2BDAP_2 (M = Pd^{2+}, Zn^{2+}, $CoCO_3^+$) host solution is titrated with a solution containing the same concentration of host and excess concentration of guest. Since

in aqueous solution the chemical shifts are pH dependent, the solutions were buffered with sodium borate at 0.1M ionic strength. In several cases, parallel control experiments were run to determine whether the aggregation or the ligation to the metal of the guest may constitute concurrent equilibria within the concentration ranges used for a specific titration. As ligation sensors, solutions of en₂M were used, at concentrations twice as high as the correspondent M_2BDAP_2 (M = Pd^{2+}, Zn^{2+}, $CoCO_3^+$).

	Value	Error
$\Delta\delta$	0.062	0.005
K_D	0.0026	0.0006
δ_a	7.644	0.001

	Value	Error
$\Delta\delta$	-0.040	0.004
K_D	0.0038	0.0009
δ_a	7.296	0.001
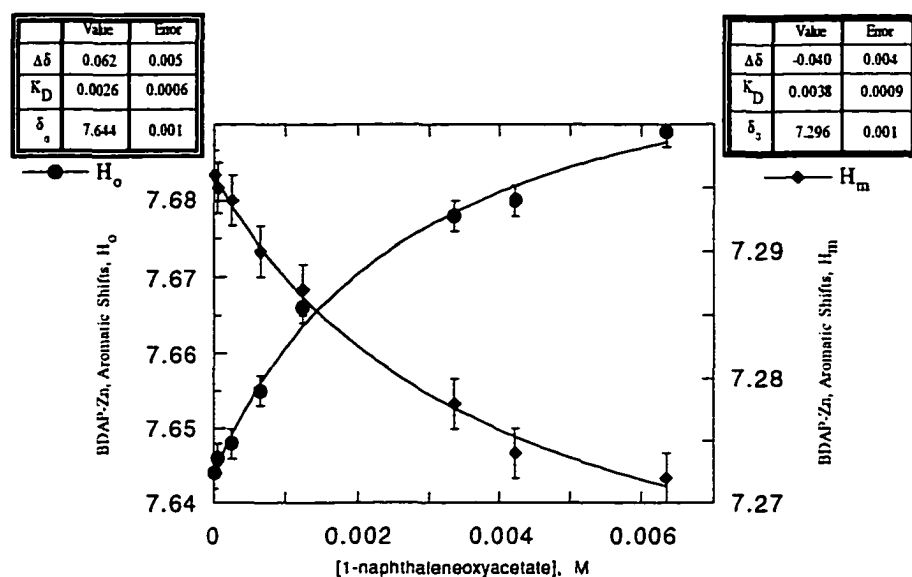
Figure 13   Fitted variation of the chemical shifts of the aromatic protons of the Zn_2BDAP_2 host during the titration with 1-naphthaleneoxyacetate in 0.1M aq. borate. The concentration of the host was kept constant at [Zn_2BDAP_2] = 1.5×10^{-4}M

IV.3.2.2 Number of Fits   The aromatic or aliphatic protons of both the M_2BDAP_2 (Figure 13 and Figure 14) or the guest (Figure 15) may be chosen as probes for binding constant determination. The measured NMR shifts were fitted with the equation 13 using the KaleidaGraph™ software, for Macintosh. However, simulations show that the value of the binding constant is affected only ~1% vs. ~10-15% depending on whether the calculation was based on the fits of the protons of the M_2BDAP_2 or guest respectively.
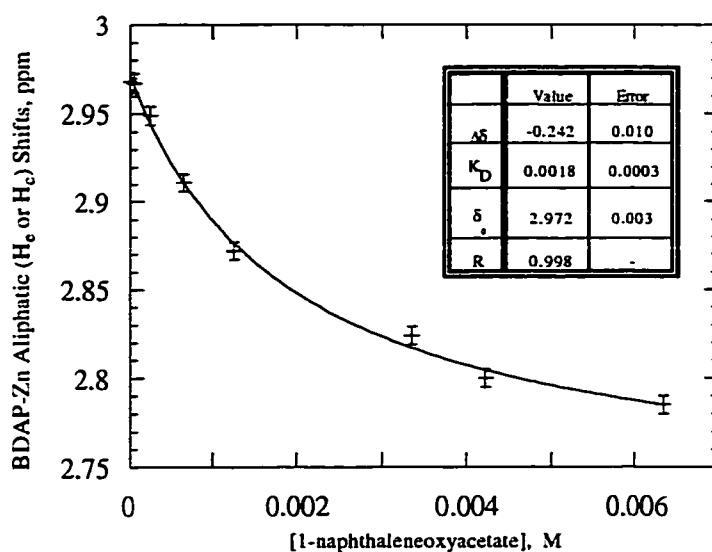
Figure 14   Fitted variation of the chemical shift of the aliphatic proton -C$\underline{H}_2$-NH$_2$ of the host during the titration with 1-naphthaleneoxyacetate in 0.1M borate. The concentration of the host was kept constant at [Zn$_2$BDAP$_2$] = 1.5x10^{-4}M
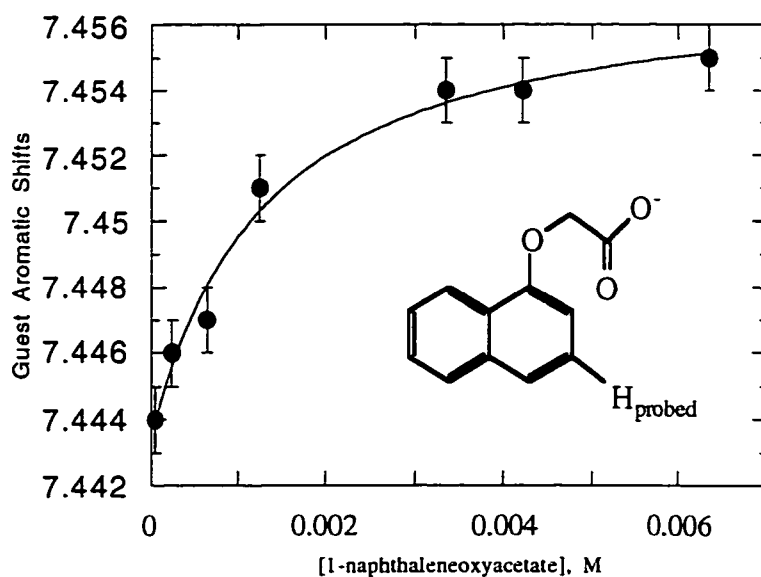

Figure 15   Fitted variation of the chemical shift of the aromatic proton of the guest during the titration with 1-naphthaleneoxyacetate in 0.1M borate. The concentration of the host was kept constant at [Zn$_2$BDAP$_2$] = 1.5x10^{-4}M

Therefore, unless the accuracy or the number of fits of the M_2BDAP_2 are not enough for the determination of the dissociation constants within reasonable error limits, fitted data from the guest's protons were not included. In most of the cases, the "guest fits" were calculated to check if they give consistent results with the other fits obtained from the host and the guest protons. Also non-monotonic fits for these guests may indicate that the aggregation is a significant process, along with the binding.

IV.3.2.3 Calculations and Error Ranges

For each titration case, all the observable protons of the M_2BDAP_2 host which are not excessively broadened were fitted. The shifts of the aliphatic protons of the host are the most difficult to follow. The complex splitting and peak overlapping characterizing the spectrum of the free BDAP is further complicated by peak broadening, especially in the case of tightly bound complexes. In these "difficult" cases, or when monitoring of the aromatic protons of the host is prevented by the overlapping of the guest protons, it was necessary to include in the final binding constant calculation the results from fitting observable guest protons. Also, it was necessary to decide whether the guest fits are not affected by other interferences and if they are consistent with those obtained from the host. Even in these cases, the weight of the final K_D result remains based mainly on the individual fits obtained from the host. Multiplets, generated by coupled protons were fitted only once, avoiding this way biased results. The reason of deriving the results from as many as possible individual fits is to narrow down the error range of the final, average dissociation constant value. This value was calculated by standard statistical methods[159] for a small number of samples, within the 95% confidence limit.

IV.3.2.4 Concentrations

In several cases, the selection of a concentration range for the macrocycle and guest which meets the 20-80% saturation criterion was prevented by

the solubility limits of certain guests, or the low sensitivity of the NMR determination when the ratio required G_O / H_O was too high (>100). Therefore, in addition with the error ranges, sturation ranges are also reported in Tables 9, 10 and 11 to allow the evaluation of the quality of the data.

IV.3.2.5 The $\Delta\delta_{max}$ values and the binding conformations in host-guest complexes

Conclusions on the topology and relative conformations of the host-guest complexes can be made using information from NOE or NOESY type of experiments or from the more accessible $\Delta\delta_{max}$ values. The values result from the 3-parameter fit of the equation 13. For homogeneity reasons, in the Tables 9, 10 and 11 are presented the values which were recalculated, using two parameter fits. For the third parameter, K_D, the average value of the independent dissociation constants calculated from each valid fit considered for that experiment was used.

Excepting the formation of Zn_2BDAP_2-AMP complex **64 k** (Table 9), the $\Delta\delta_{max}$ proton shifts in the carbonato-Co, Pd and Zn host molecules have the same direction when complexed with any of the guests (Table 9 and 10, and Figure 16-A), - all $\Delta\delta_{max}$ are negative, except for the proton H_1).

Most of the guests which were studied, have shown negative $\Delta\delta_{max}$ shifts of the aromatic protons. Based on the sign and value of the observed $\Delta\delta_{max}$ shifts, a relative conformation (topology) of the inclusion complex was derived and is depicted in Figure 16-B. This cavity inclusion arrangement is also supported enthalpically: the electron rich areas of the guest are nearby the positive metal centers and the arrangements of the quadrupoles of the aromatic rings from the guest and host are complementary.

As mentioned previously, $\Delta\delta_{max}$ values derived from the guest provide less accurate information for the quantitative calculations, but contain information on the geometric arrangement inside the host-guest complex. Two limiting relative conformations are

possible: equatorial and axial (Figure 17). Upon analyzing the $\Delta\delta_{max}$ values, several of the host-guests complexes could be categorized as having pseudo-axial or equatorial conformations.

As noticed in the Co_2PBP_2 binding studies,[71] the 1-substituted naphthalenes prefer orientations closer to equatorial, while the 2-substituted ones are adopting a large range of pseudoaxial orientations. The preference for one or another of the conformations is determined by steric requirements and by the maximization of the number of interaction points or surfaces.
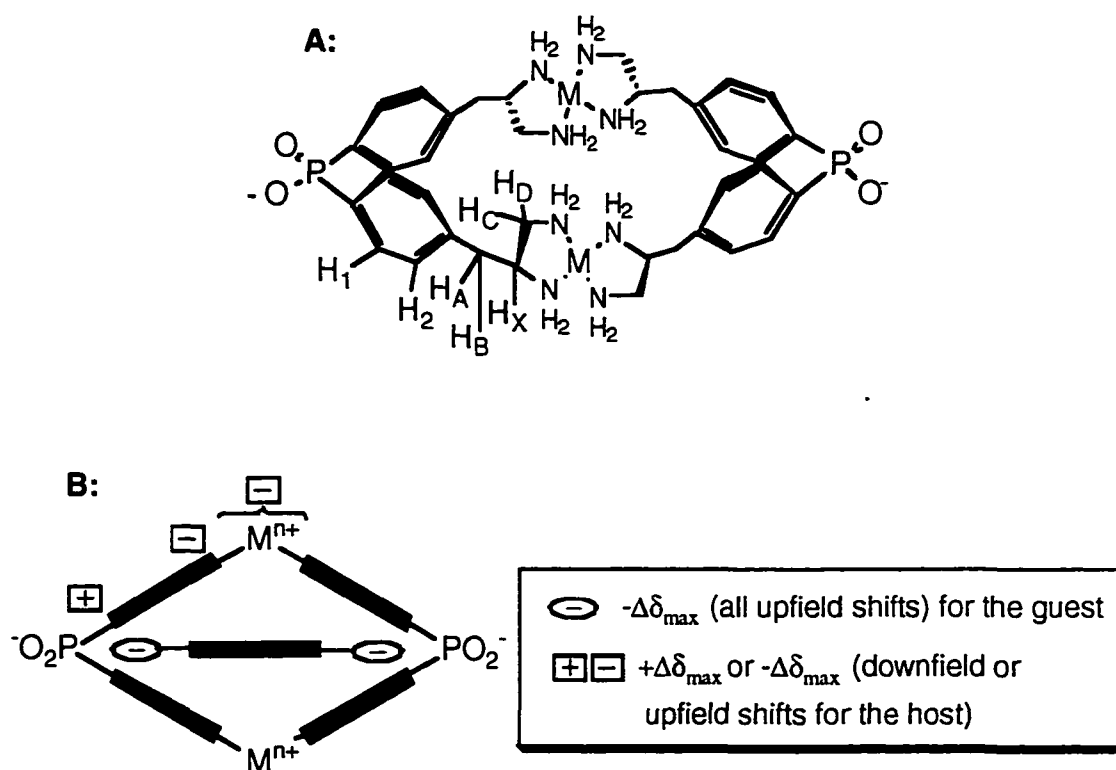
Figure 16   A: Aromatic (H_1, H_2) and aliphatic (H_A, H_B, H_C, H_D, H_X) protons monitored during the titration experiments

B: Presumed relative conformation of the host-guest complex based on the effects on the ^{1}H-NMR shifts, $\Delta\delta_{max}$. Only the aromatic frame (■■) is shown.
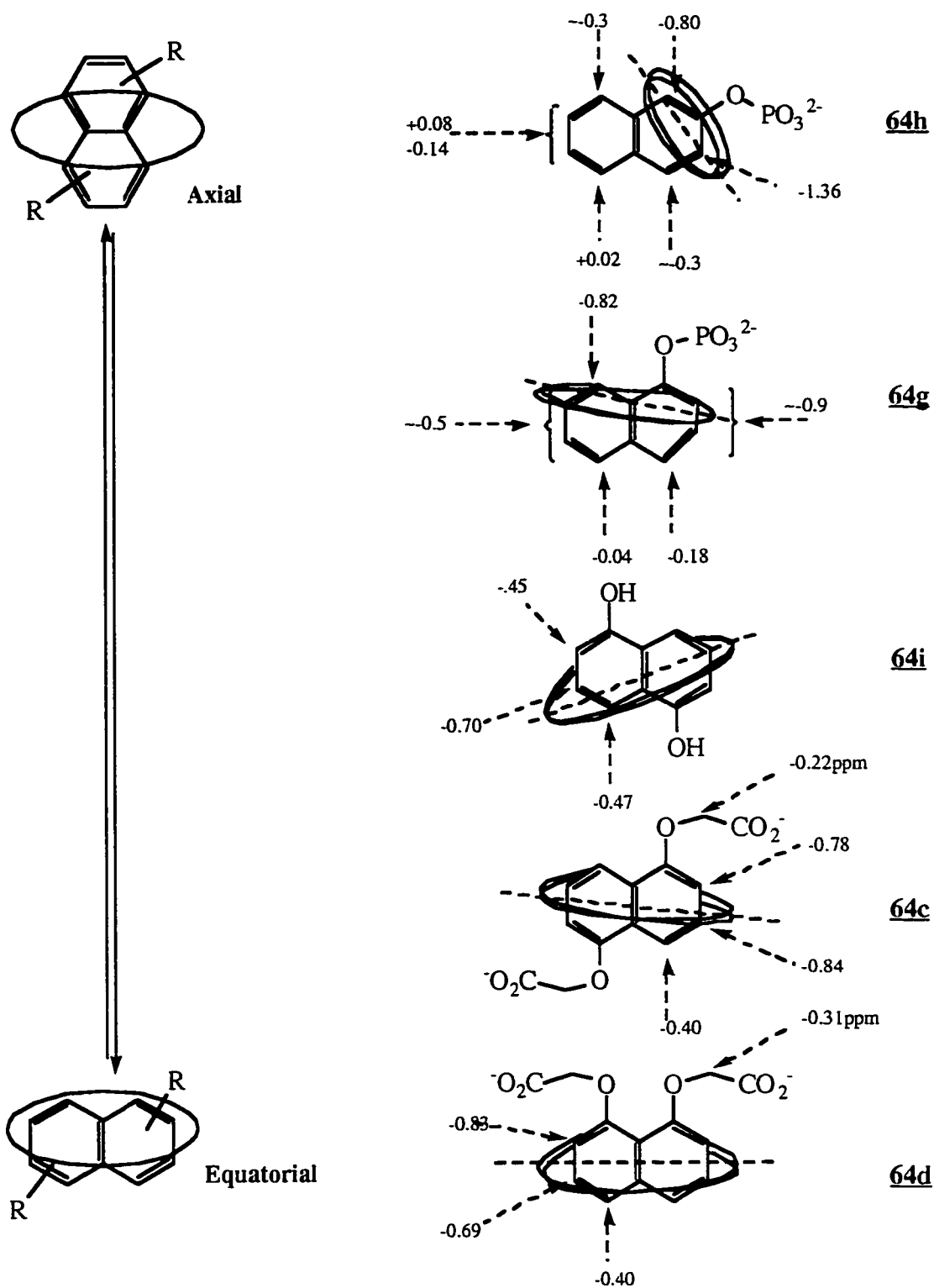
Figure 17   Different degrees of pseudo-equatorial or axial host-guest orientations

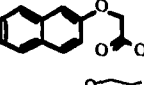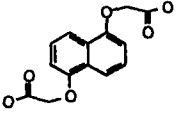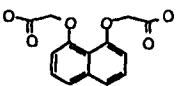Table 9   Complexes **64 a-j** of the Zn_2BDAP_2 self-assembled host
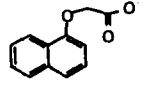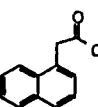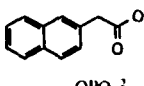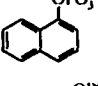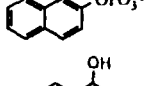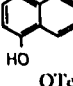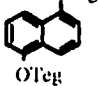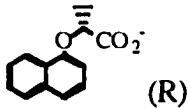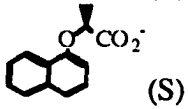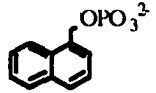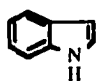
COMPLEX		RESULTS			CONDITIONS		
Host	Guest	$K_D[M]$	$\Delta\delta_{max}$ H1	$\Delta\delta_{max}$ H2	Qual. points[1]	Total points[2]	Sat'n interval
64 a		$(2.1\pm1.4)\times10^{-3}$	0.058	-0.032	5	8	2-79%
64 b		$(3.6\pm0.7)\times10^{-3}$	0.031	-	6	10	12-93%
64 c		$(1.4\pm0.2)\times10^{-3}$	0.133	-0.022	5	6	30-67%
64 d		$(2.4\pm1.6)\times10^{-4}$	0.105	-0.056	5	9	37-90%
64 e		$(2.2\pm0.7)\times10^{-3}$	0.068	-0.015	5	7	8-83%
64 f		$(8.1\pm4.3)\times10^{-3}$	0.080	-0.016	5	7	8-64%
64 g		$(2.1\pm1.3)\times10^{-4}$	0.098	-0.060	6	8	18-91%
64 h		$(2.5\pm0.5)\times10^{-4}$	0.059	-0.108	6	8	19-90%
64 i		$(3.6\pm1.0)\times10^{-4}$	0.058	-0.046	5	7	21-83%
64 j		$(5.3\pm2.0)\times10^{-3}$	0.049	-0.015	5	9	4-59%

Table 9 (continued)
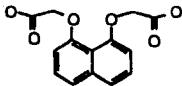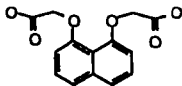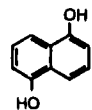
COMPLEX		RESULTS			CONDITIONS		
Host (metal)	Guest	$K_D[M]$	$\Delta\delta_{max}$ H1	$\Delta\delta_{max}$ H2	Qual. points[1]	Total points[2]	Sat'n interval
__64 k__	AMP	$(7.6\pm2.0)\times10^{-4}$	-0.042	-0.135	5	6	7-80%
__64 l__	CO_2^- (R)	$(3.8\pm0.4)\times10^{-3}$	0.106	-0.019	4	6	11-77%
__64 m__	CO_2^- (S)	$(3.9\pm1.0)\times10^{-3}$	0.108	-0.024	4	6	14-68%
__64 n__[3]	OPO_3^{2-}	$>4.5\times10^{-3}$	-	-	-	-	-
__64 o__[3]	indole	$>1.5\times10^{-2}$	-	-	-	-	-

[1]Points within optimum sensitivity, 20-80% saturation range

[2]Total number of experimental titration points

[3]No shifts observed at guest concentration ranges $\leq K_D$

Table 10   Complexes **64 p-r** of the M_2BDAP_2, host., with $M=Pd^{2+}$ or $[Co(CO_3)]^+$
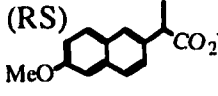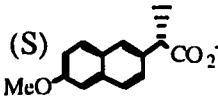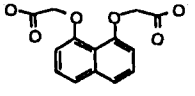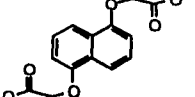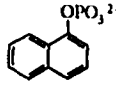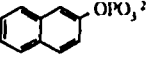
COMPLEX		RESULTS			CONDITIONS		
Host M=metal	Guest	$K_D[M]$	$\Delta\delta_{max}$ H1	$\Delta\delta_{max}$ H2	Qual. points[1]	Total points[2]	Sat'n interval
64 p[3] M=Pd^{2+}		$(2.4\pm0.4)\times10^{-4}$	0.139	-0.081	6	8	25-92%
64 q M=[Co(CO$_3$)]$^+$		$(4.9\pm2.8)\times10^{-4}$	-	-0.47	4	6	34-77%
64 r M=[Co(CO$_3$)]$^+$		$(8.2\pm2.4)\times10^{-3}$	-	-	3	7	4-50%

[1]Points within optimum sensitivity, 20-80% saturation range

[2]Total number of experimental titration points

[3]Several Pd-BDAP complexes were formed - see text and Figure 20

Table 11   Complexes **64 s-x** of the Co$_2$PBP$_2$ host

COMPLEX		RESULTS					CONDITIONS	
Host	Guest	$K_D[M]$	$\Delta\delta_{max}$ H1	$\Delta\delta_{max}$ H2	$\Delta\delta_{max}$ Hα	$\Delta\delta_{max}$ Hβ	Points[1]	Sat'n interval
64 s	(RS)	$(5.9\pm1.8)\times10^{-2}$	2.60	1.05	-30.79	6.11	7/9	8-74%
64 t	(S)	$(6.2\pm2.4)\times10^{-2}$	2.59	1.04	-26.12	15.48	7/9	10-77%
64 u[2]		$(1.9\pm0.4)\times10^{-4}$ (integration[2])	1.51	0.93	-[3]	-0.56	-/9	-
64 v		$\sim1.1\times10^{-4}$	-[3]	-1.38	-[3]	-[3]	5/10	10-96%
64 w	OPO$_3$[2]	$(7.4\pm2.2)\times10^{-3}$	0.100	0.20	-0.906	0.51	5/9	3-54%
64 x	OPO$_3$[2]	$(3.9\pm3.0)\times10^{-3}$	0.018	-[3]	-0.233	0.131	6/8	8-83%

[1]Number of points in the 20-80% saturation range / total number of titration points

[2]Slow host-guest complexation equilibrium

[3]All the other signals from the host protons broadened on complexation

93

IV.3.2.6 Discussion   The binding to the M_2BDAP_2 receptors is expected to be

driven entropically by the hydrophobic inclusion effect and enthalpically by a combination

of 3 main groups of interactions: (i) forces which contribute to the inclusion: Van der

Waals, inter-aromatic $\pi-\pi$ and cation-π interactions; (ii) electrostatic attraction between the

positive centers located on the host and the negatively charged guests; (iii) coordination of

guests as ligands to the metal centers on the host. Since most of the tested guests (Tables 9,

10 and 11) are naphthalene carboxylate and phosphate derivatives, all 3 binding interactions

should converge resulting in high affinity constants. An uncharged guest should bind

primarily through hydrophobic effect and nonpolar interactions. As a reference, several

available naphthalene diols, carboxamides or methanols were considered but failed the

solubility requirements.

Therefore, the 1,8-bis-tetraethyleneglycol naphthalene derivative corresponding to

the complex **64j** was synthesized being considered soluble enough for the purpose of this

study. This choice is arguable however, since hydrophobically driven "wrapping" of the

tetraethyleneglycolic side-chains around the complex[61, 151] or weak ligation to the metal

centers might lead to increased binding constants. The high aggregation tendency of the 1,8-

bis-tetraethyleneglycol-naphthalene, estimated to a dimerization constant of~7x10^{-2} M may

also be a result of the supplemental binding capabilities conferred by the TEG chains. Also,

the binding in complex **64j** seems surprisingly strong compared to the dianionic guest which

forms the complex **64 c** . Therefore, the dissociation constant of complex **64 j** should be

considered an underestimate. Therefore, its use as a reference will allow the estimation of

the lower limits of the effective molarities (EM)[52, 127]. This reference value will also be

useful in the estimation of the higher limits of the cooperative contribution of the charge in

the binding of naphthalenic anions.

The small differences in naphthalene-monocarboxylate binding (complexes **64 a, b,**

e, f by Zn_2BDAP_2 hosts are due primarily to stereochemical aspects. Unlike in the case of

Co_2PBP_2 complexes[71] the length of the side-chain in 1-substituted naphthalene

monocarboxylic guests (Table 9, complexes **64 a, e**) is not essential in binding. Branching

of the side-chain was also found to have no significant importance in binding (Table 10,

complexes **64 l, m**). The 2-substituted analogs bind weaker, especially when the side chain

is shorter, suggesting a stereochemical host-guest misfit. Compared to the binding of the

neutral guest in the complex **64 j** the effect on the cooperativity of the negative charge of

naphthalene mono-carboxylates seems negligible.

The differences in the binding of 1,5 -and 1,8-naphthalene-bis-oxyacetates to the

Zn_2BDAP_2 host, (complexes **64 c, d** Table 9) cannot be explained unless the stereochemical

aspects in a multipoint binding are addressed. Due to the higher symmetry, D_{2h} vs. C_{2h}, the

1,8-isomer has fewer stereochemical requirements to fulfill, in order to achieve a multipoint

binding conformation. The weaker binding in the case of the 1,5-isomer may be due to the

additional requirement of matching the "thickness" of the guest (distance between the 1, 4

or 5, 8 naphthalenic positions) with the distance between the Zn atoms of the host. The

relative conformation estimated for the 1,5-guest in the complex **64 c** (Figure 15) is

pseudoequatorial which also indicates a smaller inclusion-contact surface then in the case of

the "pure" equatorial inclusion, found in the case of the 1,8 isomer, in complex **64 d**.

The measure of the cooperativity between the inclusion forces and the ligation /

electrostatic interactions can be estimated quantitatively by calculating the EM values. As

reference values, the K_D of the complex **64 a** and the Zn-acetate K_D of $7.9 \times 10^{-2} M$,[65] -

corrected with the statistical factor of 3 which takes into consideration the availability of

only 1/3 of the Zn-atom binding sites - were taken. The calculated effective of molarity,[52, 127] EM in the formation of complex **64 d** is only 2.1 M. Even if modest, this value indicates

cooperativity and seems a closer-to-reality estimation than that calculated by using the

binding constants of complexes **64 a** and **64 j** which gives only EM = $3.0 \times 10^{-1} M$. The 7

fold difference between these estimations of the EM values may represent an estimation of the magnitude of the side-chain effect in the reference complex **64 j**.

The comparable affinities for 1,8-naphthalene-bis-oxyacetate of the non-ligating carbonato-Co or Pd and ligating able-Zn macrocycle (complexes **64 d, q**, Tables 9, 10) suggest that the negative charge or perhaps a H-bonding and not the ligation is mostly responsible for the cooperative binding. If this is true, it is possible that the difference in binding between complexes **64 c, d** to be a result of the more favorable ionic interaction when the negative charges are concentrated on only one side of the guest.

Naphthalene phosphates binding (Table 9, complexes **64 g, h**) is 200-300 stronger in the case of the complexes Zn_2BDAP_2 compared with the Co_2PBP_2 complexes **64 w, x** Table 11). This behavior was expected, being due to the favorable ionic interactions and, maybe, to the ligation between the phosphate anion and the metal centers. Again, taking the formation of complex **64 j** as a reference, and different approximations or extrapolations for the inorganic hydrogen phosphate dianion affinity for Zn (Table 12), low values of the effective molarity were found.

The validity of the alternative calculation "C" (Table 12) of the EM value is based on a dissociation constant Zn - naphthyl phosphate with a barely acceptable error range. This is partially due to the lack of sensitivity characterizing the results of titrations with low saturations of the host. On the other hand, this value may be the closest to the reality since it characterizes the ligation of an organic phosphate to a bis-ethylenediamino center. This value was corrected with a statistical factor of 1/2, taking into consideration that the ligation of the second naphthyl phosphate has only one Zn-ligation site available in the Zn_2BDAP_2. In conclusion, due to the underestimation of the dissociation constant of the complex **64 j**, it can be stated with enough confidence that the effective molarity in the phosphate binding is at least 0.39 M.

Longer side-chains terminated in phosphate groups, as in 1-naphthylmethyl

phosphate **64 n** do not increase the binding as expected. A test titration of 1-

naphthylmethylphosphate failed to find evidence of dissociation constants smaller than

$4.5 \times 10^{-3} M$. A higher concentration of this guest will be necessary to be used in order to

determine the exact value of this dissociation constant.

Table 12   Evaluation of the effective molarity value for the ligation of 1-naphthyl
phosphate. EM = $K_D^{phosphate} \cdot K_D^{64 j} / K_D^{64 g}$

Alternative Calculation	Method for $K_D^{phosphate}$ evaluation	K_D $\times 10^3 [M]$	Statistical correction factor	EM [M]
A	Literature data[65] for Zn-HPO_4^{2-} ligation	4.0	3/2	0.15
B	Titration of a **64 a** complex[a] with Na_2DPO_4	4.3	1	0.11
C	5 parameter fit (Equation 15)[b] for the formation of **64 h**	31±41	1/2	0.39

[1] Zn_2BDAP_2 host 79% saturated with 1-naphthoxy acetate;

[2] Zn_2BDAP_2 host titrated with large concentrations of 1- and 2-naphthyl phosphates (see Figure 19 and corresponding comments below)

However, a biologically important substrate, the adenosine-monophosphate (AMP)

64 k binds almost as well as the naphthalenic probes even if the phosphorus-aromatic

moiety distance is larger then in 1-naphthylmethyl-phosphate. Since most of the $\Delta\delta_{max}$

shifts in the aromatic area are significantly smaller than those from the aliphatic area of the

AMP guest (Figure 18), it is possible that the actual inclusion process is that of the ribose

residue in the Zn_2BDAP_2 macrocycle. The distinctive, small and reversed in sign $\Delta\delta_{max}$

value of the H_1 protons may also support this assumption. The failure in detecting any

spectral shifts during the NMR or CD titration of Zn_2BDAP_2 with indole **64 o**, allows the

assumption that indole and the structurally related adenine residue bind very weakly, with
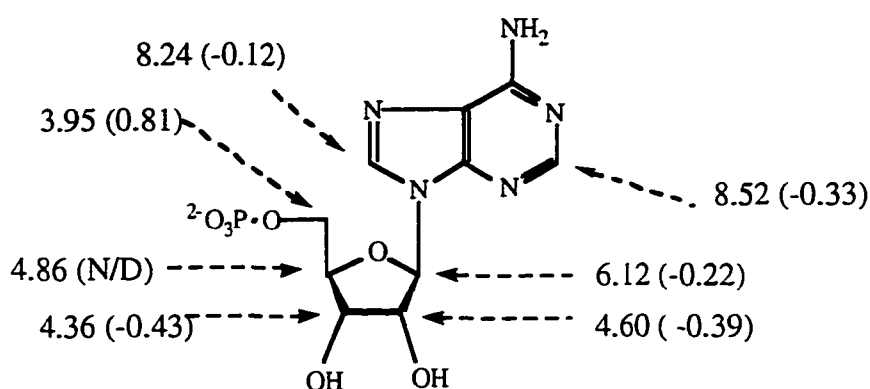
$K_D > 1.5 \times 10^{-2}$ M.

Figure 18   Proton shifts[63] of the AMP guest $\delta_0(\Delta\delta_{max})$ values in ppm calculated for the
binding to the Zn_2BDAP_2 host in 0.1M borate (complex **64 k**); N/D = could
not be determined

An outstanding affinity was measured for the **64 i** complex. The naphthalenediol

substrate at pH 9 should be mostly uncharged. The comparable stability of the complexes

64 j, r compared with the ~15 -22 times higher stability found for complex **64 i** suggests

that complexed Zn can act as a binding site for the hydroxylic group. Hydrogen bonding

with an amino group of the BDAP ligand, or a metal assisted deprotonation of the phenol

which favors supplemental ionic interactions or naphtholate ligation to Zn are other

hypotheses which need to be verified. Unfortunately, obtaining supplementary evidences

from the binding experiments of α-naphthol and 2,6-naphthalenediol with the Zn_2BDAP_2

is difficult due to the precipitation which occurs when mixing the host and guest solutions.

Another target of this project was to detect enantioselective binding of different

chiral substrates. The (R) and (S) (1-naphthyl)-oxy-1-propionic acids failed to be

differentiated by the Zn_2BDAP_2 host (64 l, m), while the Co_2PBP_2 macrocycle presented a

9 fold selectivity for the (S) enantiomer. Among the possible explanations is the positioning

of the chiral center substituted with the extra methyl group outside the constricted area of

the complex, where the binding interactions and steric repulsions take place . The low

$\Delta\delta_{max}$ (Figure19) found for the methyl group and the comparable binding strengths found in

all the naphthyl-oxy-acetate complexes 64 a, l, m suggest also that the methyl group is

located outside the binding zone.
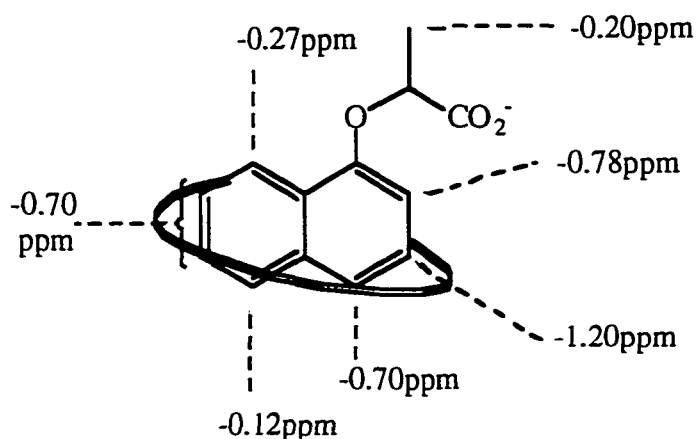
Figure 19   The $\Delta\delta_{max}$ values for the observable shifts of the guest from complexes
            64 l, m suggest that the methyl group attached to the chiral center does not
            interfere in an equatorial binding position

Enantioselection for the chiral naproxen pain reliever drug was not found for any of

the hosts Co_2PBP_2 and Zn_2BDAP_2.(complexes 64 s, t). A racemized (±) naproxen was used

as a substitute for non available (-) enantiomer. The binding constant of both naproxen

species, determined with approximation for the Zn_2BDAP_2 host is 1.2×10^{-2} M and is within

the range of the affinities found for complexes 64 s, t. These unusually weak binding

constants (one order of magnitude lower than the related β-naphthylacetic acid[71]) are probably due to a sterical misfit.

The lack of stereoselective recognition in the case of naproxen and (1-naphthyl)-oxy-1-propionic acid does not mean that the BDAP based hosts are not stereoselective in general. Studying the binding conformations of different achiral guest may offer the information necessary to choose better guest candidates for stereoselective binding. The topology of the complexes of Zn_2BDAP_2 (Figure 17) suggest that chiral derivatives of 2-substituted naphthyl acetate or naphthylmethyl phosphate might be better candidates for stereoselective binding. Due to the same topological considerations, chiral (1-naphthyl)-1-propionic or the (1, 8-naphthyl)-bis-1-propionic acids could also be considered in future stereoselective studies. The latter candidate could also show an interesting case of diastereoselective resolution based on the hinderance of the cooperativity in binding by the methyl residues in the R, S isomer.

In the binding experiment of Zn_2BDAP_2 with 1- and 2-naphthyl phosphates (Figure 20), the lack of "saturation" and the linear dependence which characterizes the final titration points deviates from a simple 1:1 binding isotherm. This suggested that a second binding process, possibly a phosphate group which ligates the metal, competes at high guest concentrations with the usual inclusion complex.

A titration of a mixture of $1.5 \times 10^{-4}M$ Zn_2BDAP_2 host with $6.4 \times 10^{-3}M$ 1-naphthyloxyacetate (79% saturation of the host) with sodium phosphate produced comparable shifts of the host protons, confirming the phosphate ligation assumption. The titration of Zn_2BDAP_2 with naphthyl phosphates was redone at lower guest concentrations and as expected, the titration points fitted the theoretical 1:1 host-guest complexation model (Table 9).

The data from the titration with high guest concentration could also be fitted using a supplemental linear parameter (k = slope), which characterizes the phosphate-metal ligation

at low saturation of the host with the second guest molecule. The dissociation constants

calculated this way, for 1- and 2-naphthyl phosphate are $2.4\pm0.7\times10^{-4}$ M and $2.2\pm0.7\times10^{-4}$

M respectively. Even if their error ranges are higher, these values are very close to those

found in the "low concentration" phosphate titrations and used in Table 9.
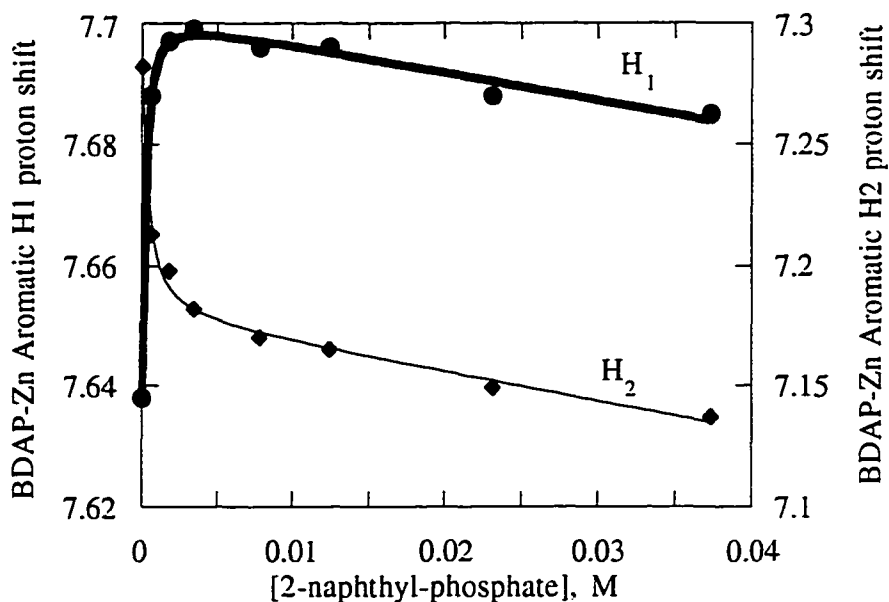
Figure 20 Zn_2BDAP_2 titration with high concentrations of 2-naphthyl phosphate
reveals a second parallel lower affinity binding process, which can be fitted
with the Equation 14

$$\delta_{obs} = \delta_0 + \frac{\Delta\delta_{max}}{2H_0}\left(S-\sqrt{S^2-4H_0\bullet G_0}\right)+k\bullet G_o \qquad \text{Eq.14}$$

$$\delta_{obs} = \delta_0 + \frac{\Delta\delta_{1\,max}}{2H_0}\left(S_1-\sqrt{S_1{}^2-4H_0\bullet G_0}\right)+\frac{\Delta\delta_{2\,max}}{2H_0}\left(S_2-\sqrt{S_2{}^2-4H_0\bullet G_0}\right)$$

Eq. 15

A more complete 5 parameter fit for the formation of **64 h** was made by using

equation 15, which combines the effects on δ_{obs} of both binding processes. This fit allowed

an approximate characterization of the binding of the second 2-naphthyl phosphate group to

the Zn_2BDAP_2 host: $K_D = (3.1 \pm 4.1) \times 10^{-2}$ M, $\Delta\delta_{max} = -0.044$ and -0.091 ppm (for the H1

and H2 protons respectively).
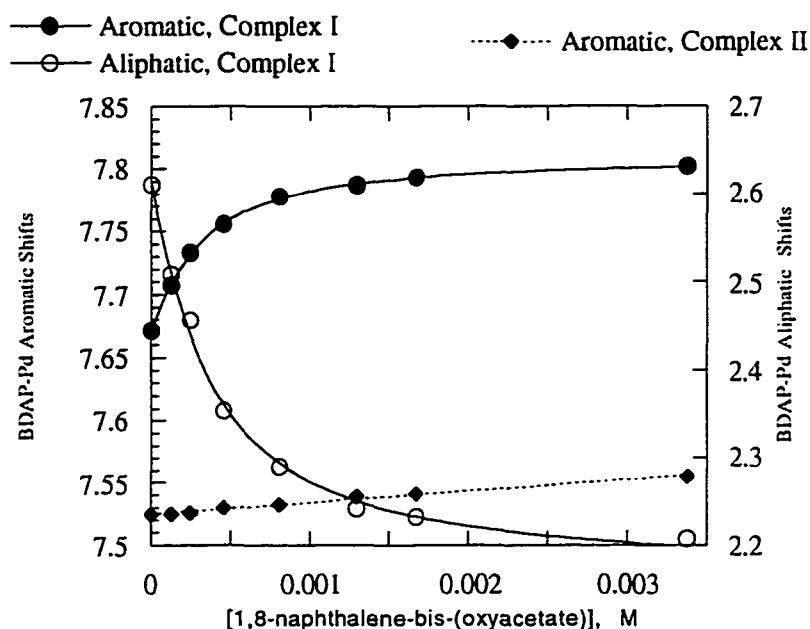
Figure 21   Shifts of the H_1 in Complex I and II and a non-attributed aliphatic proton
from Complex I, when a solution of 7.4×10^{-4} M BDAP and 5.9×10^{-4} M of
Na_2PdCl_4 equilibrated at 90°C is titrated with 1,8-naphthalene-bis-
oxyacetate

The titration of Pd_2BDAP_2 host with 1,8-naphthalene-bis-oxyacetate revealed the

different binding affinities of the slowly equilibrating BDAP-Pd species existent in aq.

solutions. As mentioned in section IV.2.2 a slow equilibrium of at least two complexes is

formed when milimolar range concentrations of BDAP in 0.1 M borate are treated at room

temperature with 0.8 equiv. of sodium tetrachloropalladate. In the aromatic area of the NMR

spectrum, the downfield shifted H$_1$ signal was attributed to Complex I and the upfield

shifted H$_1$ signal to Complex II. When titrated with a 1,8-naphthalene-bis-oxyacetate guest,

the downfield variation of the H$_1$ signal of the hosts are different (Figure 21). Complex I

binds stronger and is mostly saturated with guest at the end of the titration, while Complex

II presents only small linear shifts which characterize a week binding. An aliphatic signal

was also possible to be fitted and was attributed to Complex I, without being attributed to a

specific proton.

Interestingly, after the titration, leaving the mixture of host and guest to rest for 5

days at room temperature, shifts the initial equilibrium of Complex I / II = 2.7 to a molar

ratio of 25. This slow equilibrium displacement which favors the formation of Complex I, is

the opposite to the equilibrium displacements noticed for the BDAP-Pd mixtures alone,

which at longer times and higher temperatures favor the formation of Complex II (section

IV.2.2). This considerable shift could be attributed to a templating effect of the guest on the

formation of the stronger binding Complex I.

IV.3.2 Circular Dichroism (CD) binding studies

Interpretable changes in CD spectra of chiral hosts are induced upon binding of

achiral guests. Recently, Dougherty[57] has used the CD technique to evaluate the binding

constants of the derivatives of host **19** with a series of water soluble guests. Further, using

coupled-oscillator calculations on the acquired CD data, valuable insights in the reciprocal

host-guest orientations were obtained. The CD is a valuable way to probe noncovalent

interactions in diluted solutions, where the NMR method has certain limitations. Also this

low dilution technique helps in overcoming other frequent problems which arise during

binding studies such as low host or guest solubility and low critical aggregation

concentrations.

Several methods are available for the calculation of K_D constants from CD data. The classical approach, is to titrate the host at constant concentration with increasing concentrations of guest. This method developed by Rosen,[152] ignores any changes in the CD due to the concentration variations of the guest and is based on a laborious linear regression method. Dougherty[57] developed his own, more general method based on error minimization multifit calculations, which takes into consideration the influences of increased concentrations of guest and is not limited by the need to use constant concentrations of host. The method used in this project neglects the influence of guest concentration and is similar to the one presented in the NMR studies, based on the equation 13. The advantage over the other methods presented above is that it employs a convenient and available numeric method of calculation which allows the calculation of K_D with errors much smaller than the error ranges inherent with the experimental technique.

The titration of Zn_2BDAP_2 with 1,5-cis-cyclooctanediol constitutes an example where the CD method allowed the calculation of a very weak binding constant. The lack of magnetic anisotropy of the guest, as well as the large excesses of guest needed to saturate ~80% are factors which reduce considerably the sensitivity of the NMR method.

The changes in the CD spectra were recorded over a range of relatively high concentrations of 1,5-cis-cyclooctanediol (Figure 22, Figure A5). The two extremes of the spectra are around 249 and 234nm and an isosbestic point around 244nm. No corrections where made in terms of activities for the possible trespass of the critical aggregation concentration. The fit of the ellipticities measured between 250-245 nm during the titration is presented in Figure 22. Obviously, the errors of the fit increase as the measurement is made at a lower wavelength. Below the presented wavelengths the considerable dispersion of the experimental data is so large that no fit is possible and, moreover, the ellipticity variations became non-monotonic or even statistical. One reason for this might be the coexistence of several chiral complexes, but the limitations in the sensitivity of the method

seems to be a more plausible reason. The CD and the conformations of the host for this particular case of titration are relatively insensible to the interactions with the guest. Therefore, at lower wavelengths, where the UV absorption of the host becomes considerable, the range of the measurement errors become comparable with the binding-induced CD changes.
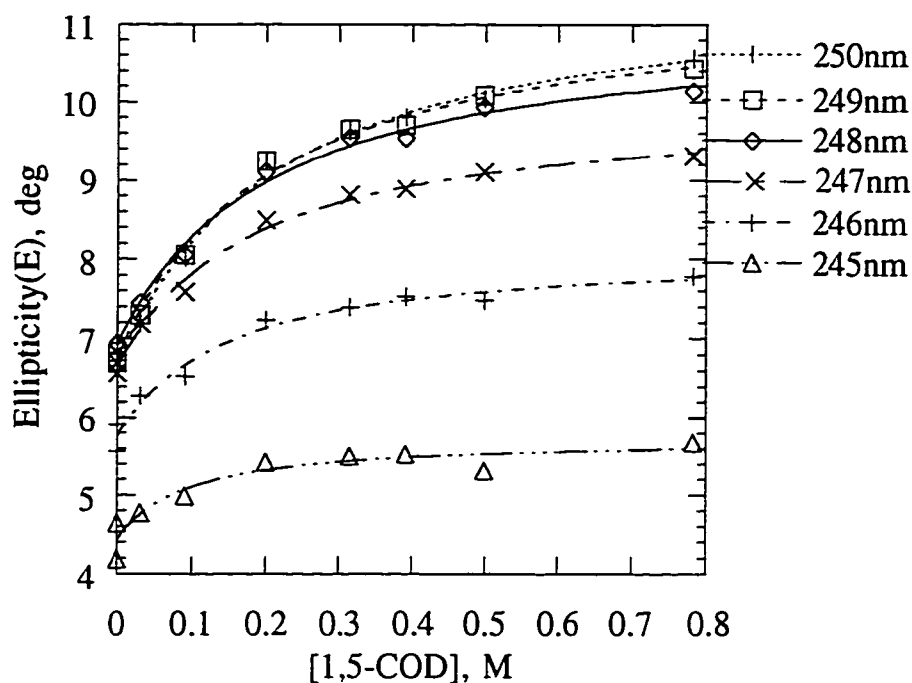
Figure 22   Curve fitting of the ellipticities measured at 250-245nm for a 5.92×10^{-5}M of Zn_2BDAP_2 in 0.1M borate titrated with a mixture of 5.92×10^{-5}M of Zn_2BDAP_2 and 7.82×10^{-1}M of 1,5-cis-cyclooctanediol in 0.1M borate

Several alternative combination of fits and background noise compensation calculations were attempted. The most consistent results were obtained by individually fitting ellipticities measured at 6 wavelengths between 250 and 245nm after subtracting the isosbestic point. The calculation of the average $K_D = (3.0 \pm 0.1) \times 10^{-1}$M and error ranges

follows the same statistical methods as those presented for the NMR studies. This experiment indicates that the CD titration method is appropriate for the determination of the binding of aliphatic substrates (even when this is relatively weak) to our self-assembled hosts. The titration data and results for the Zn_2BDAP_2 host with 1-naphthyl phosphate gave a dissociation constants $K_D = (1.3\pm0.2)\times10^{-4}$ M and 2-naphthyl phosphate gave $K_D = (1.9\pm0.3)\times10^{-4}$ M respectively. These values are relatively close and within the error ranges of determined in the NMR titrations (Table 9, complexes 64 g, h, where K_D is $(2.1\pm1.3)\times 10^{-4}$ and $(2.5\pm0.5)\times 10^{-4}$ M respectively). The large CD (Appendix, Figure A11) changes which were observed monitored and fitted with narrower error limits than in the case of the corresponding ^1H-NMR titrations are indicating that the CD method is a sensitive probe for high affinity binding. However, CD present limitation when weak binding of UV absorbing substrates is needed. In an attempt to use indole in the same titration conditions, the increasing UV background absorption due to high guest concentrations made any monitoring of the small binding-induced CD changes undetectable.

IV.4 Preliminary Hydrolysis Studies

The zinc, cobalt and copper alkanediamino complexes are known to have esterolytic activities. Therefore, for certain substrates and conditions, the corresponding BDAP complexes are expected to exhibit at least comparable levels of activities.
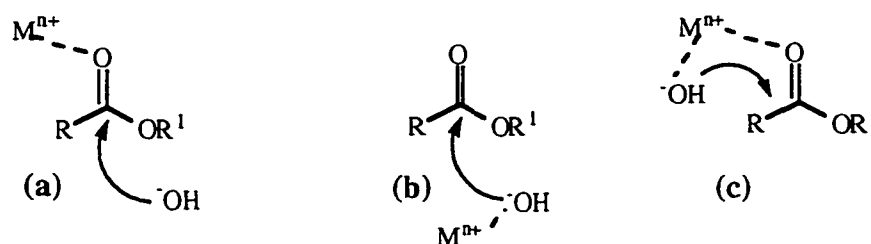

Scheme 16   Possible metal hydroxide hydrolytic mechanisms[109]

In aqueous solutions, a metallic aqua-complex may catalyze the hydrolysis of an ester[109] by a Lewis acid (a), metal hydroxide (b) or combined (c) mechanism (Scheme 16).

Substitutionally labile Zn complexes **65** are able to catalyze the hydrolysis of R = CF_3 carboxylic esters[109] through a metal hydroxide mechanism but fail to hydrolyze the corresponding acetates.
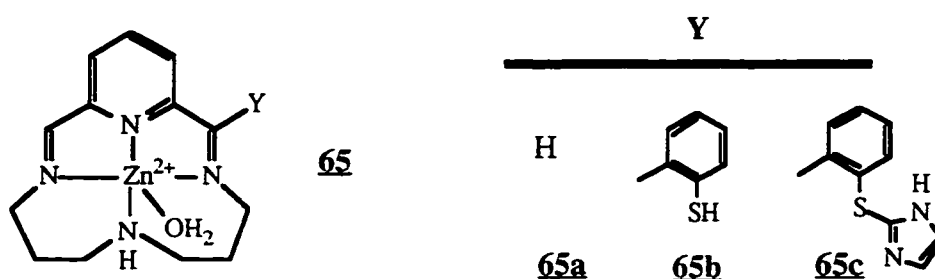
This limitation is due to the short lifetime of the tetrahedral intermediate **66** (Scheme 17). Electron withdrawing groups (R = -CF_3) or an appropriately positioned proton donor Y group[153] (**65 b** or **c**) may contribute to the stabilization of **66** and the continuation of the actual cleavage step.
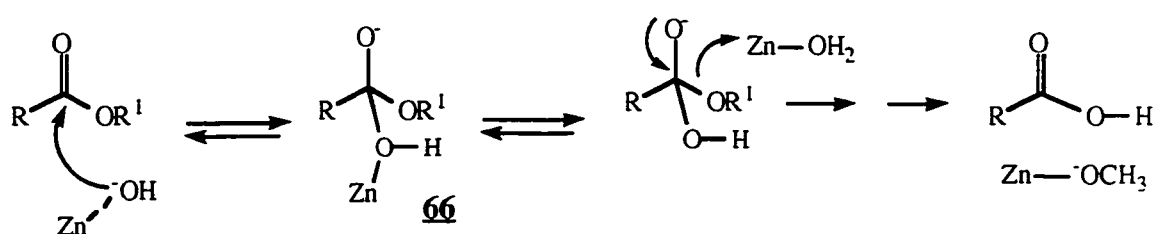
Scheme 17   Hydrolysis of carboxylic esters by a Zn-hydroxide catalyzed mechanism[109]

Breslow studied the effect of the assistance of Y groups in phosphate cleavage[153] and found that it is enhanced by a factor of 9, in **65b** or 20, in **65c** relative to the control **65a**. The Cu(II) analog of **65 a** is a better catalyst, since the formation of a tetrahedral intermediate **66** through a 4 membered ring closure[109] (Scheme 18) is a favored process.

Supplemental rate accelerations were achieved by Breslow and coworkers,[108] by tethering

to this catalytic site **67**, two Cd groups acting cooperatively as binding sites which

encapsulate the R and R[1] groups and hold the ester in an appropriate orientation for the

subsequent cleavage step.
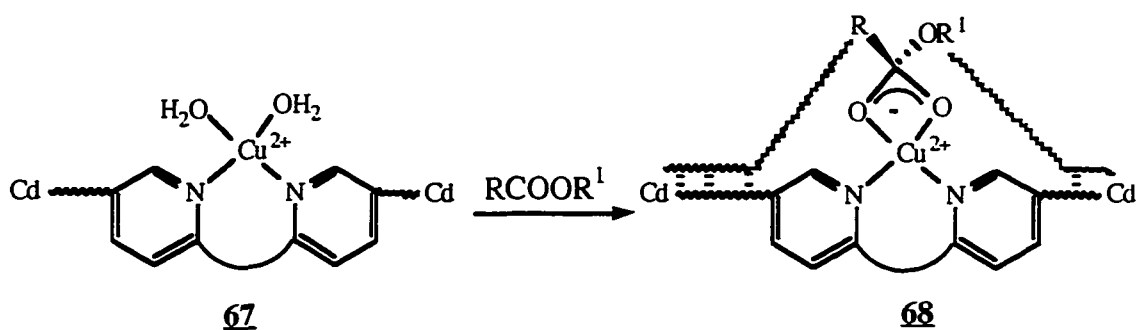
Scheme 18   Split-site mode of the cleavage of carboxylate esters[108]

However, simpler ligands such as triazacyclododecane **69**,[153] tetraazacyclododecane

70[154] and tris-(aminoethyl)amine **71 a** or tris-(aminopropyl)amine **71 b**[109] were also found

to form chelates of Co(III) and Zn(II) which are efficient in the phosphate, carboxylate or

other related hydrolytic cleavages.
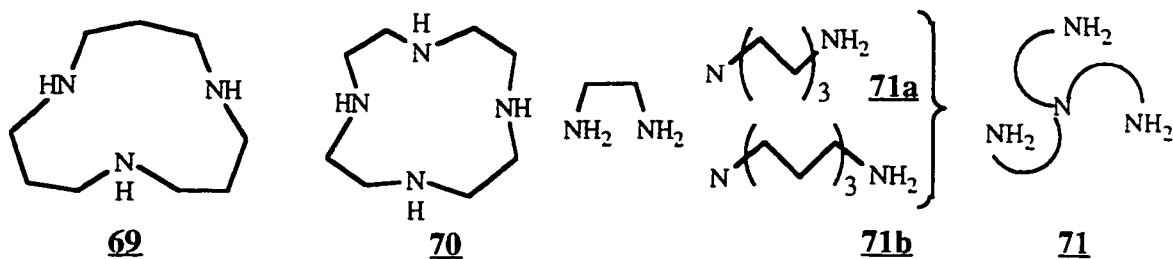
In the case of the Co chelates of **71** the esterolytic efficiency was dependent on the

size of the chelate cycle (Scheme 19). The formation of the 4 membered intermediates **72** or

73 is favored in the case of the 6 membered opposite cycles of the **71 b** ligand.[109, 155]

A preliminary study was done by ^{1}H-NMR spectroscopy as part of the present

research. Its scope was to reveal any hydrolytic rate enhancement for the naphthalenic

substrate **76** in presence of Zn$_2$BDAP$_2$ (Scheme 20). Unfortunately, this substrate has the

disadvantage of being unstable and sparingly soluble in borate solutions which affect

negatively the results of an ^{1}H-NMR study. An HPLC study[71] - which was not available at

the time when this part of the research was done- could have been more appropriate.
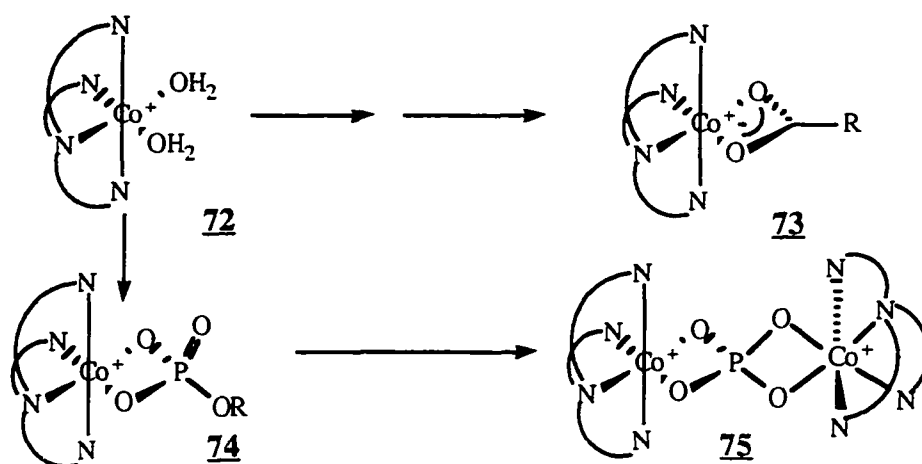
Scheme 19   Intermediates in the cleavage of carboxylic **73** and phosphoric **74** monoesters

As a control, a Znen$_2$ chelate was used which did not seem to affect the background

hydrolysis rate of the substrate in 0.025M aqueous borate (Scheme 20). A ~10 fold excess

of catalyst (~20 fold for the control) were used relative to the substrate, which allows for the

time being to ignore any product inhibition effect.
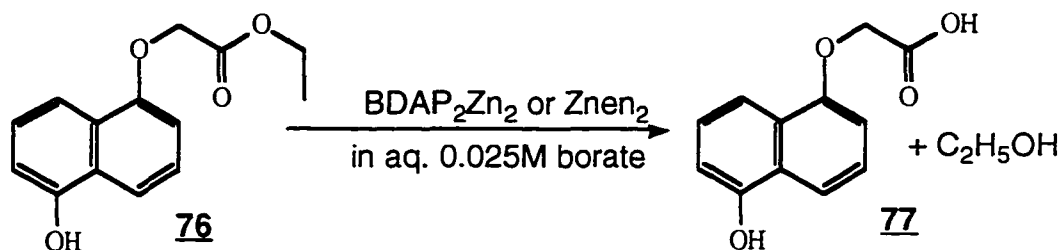
Scheme 20   Catalytic hydrolysis of ethyl-1-(5-hydroxy-naphthalene)-oxyacetate

The only proton of the probe which was monitorable was the $C\underline{H}_3$-proton of the esteric substrate and the alcoholic product. The ratio of the signal heights for $C\underline{H}_3$-(alcohol) / {$C\underline{H}_3$-(ester) + $C\underline{H}_3$-(alcohol) }was plotted against the time (Figure 23). Unfortunately, the initial rates, which would constitute the best proof of the catalytic rate enhancement in the case of Zn_2BDAP_2 host could not be determined. In the first 20 minutes of hydrolysis, ~25% of the ester is hydrolyzed in the presence of the Zn_2BDAP_2 which constitutes a x2 .5 rate enhancement relative to the $Znen_2$ control. The available data points cannot be fitted to a first order hydrolysis kinetics. This suggests a more complex kinetics where the hydrolysis slows down after the initial stages. A reason for this may be the partial precipitation which became visible in both samples after the first two hours of hydrolysis.

♦   Zn-BDAP sample, 2.27mM

□   en-control sample, 4.54mM
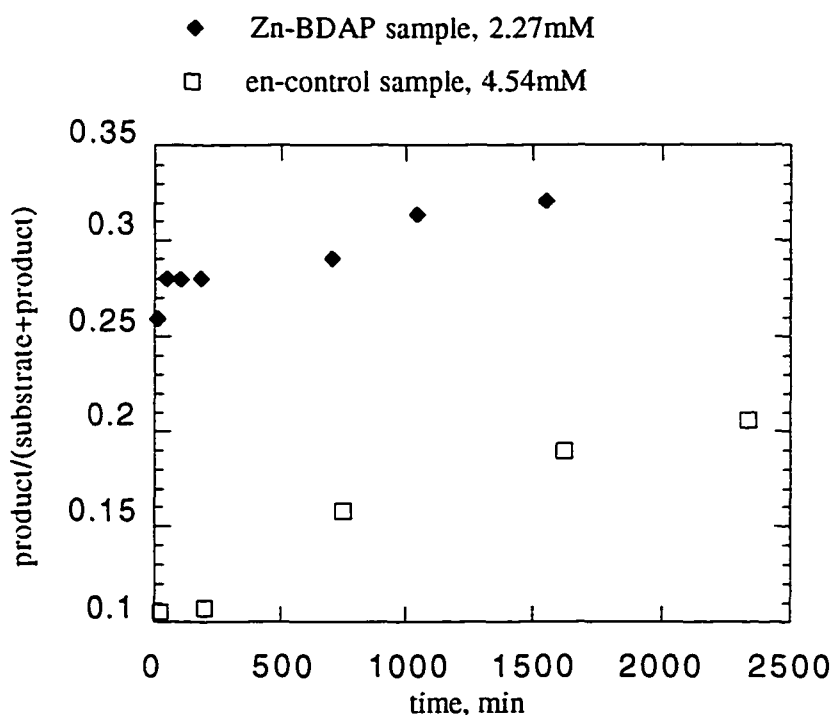
Figure 22   Plot of the ^{1}H-NMR signal integral ratio $C\underline{H}_3$-(alcohol) / {$C\underline{H}_3$-(ester) + $C\underline{H}_3$-(alcohol)} for the hydrolysis of **76** in presence of Zn_2BDAP_2 and $Znen_2$ in 0.025M borate

V. CONCLUSIONS

V.1 General

A new, self-assembled water soluble and stable macrocyclic series of hosts was synthesized and studied. The hosts are based on the BDAP ligand, which contains structural elements that mimic the recognition motifs found in known biological receptors. The preliminary study of the hosts revealed important features found in the biological systems: cooperativity and selectivity in the binding of negatively charged guests.

V.2 Specific

V.2.1 Conclusions Regarding the Synthetic Part (IV.1 and IV.2.3)

1) A cleaner method for the preparation of methyl phosphinate was found,[119] by performing the reactions in the presence of a low dielectric constant solvent. The content of the main impurity in these transesterification mixtures was reduced from 12% to 1% or under. The direct use of these methyl phosphinate solutions in Pd catalyzed couplings with aryl iodides results in less impurities in the crude coupling mixtures.

2) The preparation of pure solutions of *tert*-butyl phosphinate[119] provides access to isolable and pure mono- and di-arylphosphinates whereas the known methyl phosphinate method fails to yield pure compounds, in the cases studied in this research.

3) There is consistent direct (MS, IR, UV) and strong indirect (binding, ion exchange behavior etc.) evidence that the selective synthesis of the $Co_2BDAP_2(CO_3)_2$ was successful. Moreover, the UV evidence shows that the same method may be used in the preparation of PBP and PBP-BDAP mixed complexes. Being kinetically inert, the mixtures

of stereoisomers generated through the macrocyclization-complexation can be resolved. Future facile derivatization of these hosts is also possible, due to the presence of two "handles": the coordination sites of the acid labile carbonate groups.

IV.2.2 Conclusions Regarding the Binding Part (IV.3)

The objective of prepare self-assembling hosts with low dissociation limits has been achieved. The dissociation limit for the Zn_2BDAP_2 host is at least 20 times smaller than that of the Co_2PBP_2 host. The $Co_2BDAP_2(CO_3)_2$ should have an even lower dissociation limit being substitutionally inert.

The binding constants found for the BDAP based hosts have the same range as those of the PBP analogs. At this stage of the study, only the lower limits of the effective molarities (EM) for naphthyl carboxylic acids and phosphates were estimated, due to the lack of an appropriate reference. This "ideal" reference should not be charged and should not ligate the metal. These characteristics are difficult to meet in aqueous solutions, since all the solubility conferring groups are potential metal ligands. Although the estimated lower limits of the EM are not outstanding, they prove that the Zn_2BDAP_2 host is able to bind cooperatively.

The receptors incorporating BDAP ligands show several complementary properties to those shown by the PBP based receptors. The affinities for naphthyl phosphates of the BDAP hosts are more than one order of magnitude higher than those found in the corresponding PBP hosts. The affinity of the BDAP hosts appears to be less sensitive towards the position and lengths of the side-chains in the naphthalenic guests and more sensitive to the number and location of the charges in the guest.

Some of the binding studies were made by using CD measurements. This is the first time when this technique has been used by the Schwabacher group in binding studies. This

method complements the NMR-based determination of the binding constants and, from certain standpoints was found to be more convenient to use, less expensive and more reliable.

As shown in earlier studies[41, 71] the α– or β–substituents of the naphthalenic guests were found to orient the binding in pseudoequatorial or pseudoaxial conformations respectively.

Opposite to the behavior of the PBP analog, the Zn_2BDAP_2 host appears to be less selective with regard to the length of the side-chain. Moreover, the 1,5-naphthalenediol is able to show an outstanding cooperativity effect when binding to the Zn_2BDAP_2 host.

The stereoselective binding to the hosts incorporating BDAP chiral ligands has not been proved yet. However, by knowing the binding patterns of the Zn_2BDAP_2 host, the selection of the appropriate chiral guests, which have more chances to be enantioselectively recognized was made easier. Preliminary hydrolysis studies are less conclusive, but indicate a significant initial rate acceleration when the 1-(5- hydroxy-naphthalene)-oxyacetate substrate is hydrolyzed in presence of excess of Zn_2BDAP_2 host.

In this work, some of the binding characteristics of the hosts incorporating the BDAP ligand were described. Some of these characteristics are well established and also outstanding. Other characteristics such as the hydrolytic capabilities and the selective, guest-templated formation of a strong binding Pd-BDAP host were only preliminarely screened. The most important contribution of this study is that it constitutes a basis for future structural and investigational developments for the host series incorporating BDAP ligands.

VI. EXPERIMENTAL SECTION

VI.1 General Procedures

^{1}H-NMR spectra were acquired at 300 or 400MHz on a Nicolet NT-300, Varian VXR-300 or a Bruker DRX-400 instrument. ^{13}C-NMR spectra were acquired on Varian VXR-300 or a Bruker DRX-400 instrument. All chemical shifts of ^{1}H-NMR and ^{13}C-NMR spectra are reported relative to TMS in organic solvents and DSS in aqueous solutions unless otherwise specified. ^{13}C-NMR spectra are ^{1}H decoupled; ^{31}P-NMR spectra were obtained on a Varian VXR-300, Bruker DRX-400 or AC200 instruments and the chemical shifts are reported relative to an external standard of 85% H_3PO_4. Circular dichroism spectra were acquired with a JASCO spectropolarimeter J210. UV-VIS spectra were obtained with Hewlett Packard 8452A Diode Array Spectrophotometer. FTIR spectra were acquired on a Bio-Rad FTS-7 infrared spectrometer at a 2 cm^{-1} resolution and 8-16 scans. Elemental and mass spectrometry analyses were performed by Galbraith Laboratory or ISU Chemistry Department Instrumentation Facilities. Melting points were determined on a Fisher-Johns melting point apparatus and were not corrected.

Thin-layer chromatography (TLC) was performed on commercially available Merck silica gel 60-F (0.25 mm) coated glass plates and flash chromatography was carried out as described by Still[156] with the use of E. Merck silica gel Kieselgel 60 (230-400 mesh).

All the chemicals were used as obtained from commercial suppliers unless otherwise specified. Anhydrous phosphinic acid was prepared by overnight evaporation under vacuum (~5 torr) at room temperature of a stirred aqueous solution of phosphinic acid (Fisher, 50% w/w) followed by a crystallization step of the neat acid at ~5°C. Pyrene, indole, 1,5-dihydroxynaphthalene, 1,8-dihydroxynaphthalene, 1-naphthol, 1- and 2-naphthyl acetic acids and 1- and 2-naphthyloxyacetic acids were used as obtained after purity check by TLC

and ^{1}H-NMR. Acetonitrile used for reactions was freshly distilled from P_4O_{10}. THF,

CH_2Cl_2, toluene, and triethylamine used for reactions were freshly distilled from CaH_2.

DMF and *tert*-butyl alcohol were dried over activated 4A molecular sieves. Glassware was

pre-dried at >80 °C.

VI.2 (S)-N, N'-1,2-Di-(*tert*-butoxycarbonyl amino)-3-(4-iodophenyl) propane, 45

VI.2.1 Amidation

Into a solution of (S)-4-Iodophenylalanine methyl ester hydrochloride 42 (3.18 g,

9.31 x 10^{-3} mol) in 40 ml of anhydrous methanol, a stream of gaseous ammonia was

bubbled at 0 °C. After 90 minutes the volume of the solution had roughly doubled and

saturation was achieved. The solution was allowed to stay overnight at room temperature in

a sealed tube. Careful depressurisation and rotary evaporation of the methanol and excess

ammonia followed by vacuum drying, gave crude (S)-4-Iodophenylalanine-amide

hydrochloride 43 as white crystals (mp = 254-260 °C (dec.)). This crude product may be

used directly in the following reduction step.

The free amine (1.34 g, yield 50%, mp = 161-4°C) may be isolated by

recrystallization of the crude product from methanol. Addition of Et_2O precipitated a second

crop of product, in the hydrochloride form 43 (0.97g, yield 32%, mp = 266-268°C (dec.)).

The isolated intermediates were partially characterized.

VI.2.2 Reduction

The crude anhydrous (S)-2-amino-3-(4-iodophenyl)-propionamide hydrochloride 43,

2.1g (6.4 x 10^{-3} mol) was treated under N_2 in darkness, at 0 °C with a solution of borane-

THF (75 ml of 0.7M solution, 52.5 x 10^{-3} mol). The resulting suspension was stirred for 2

days at room temperature and for 12 hr at 50 °C. The decomposition of the borane

complexes was made at 0°C by dropwise addition of 20 ml of methanol followed by 1.7 ml

concentrated HCl. After solvent evaporation, the residue was mixed with a minimum

amount of water and solid NaOH (~4g) obtaining a saturated solution in NaOH. The free

diamine **44** is separated by multiple extractions with ether. After the ether was removed by

rotary evaporation, the resulting oil was used directly in the next protection step.

The product may be isolated as a dihydrochloride by dissolving the crude oil in 1-2

ml of methanol and 20 ml of ether and bubbling a stream of dry HCl through the solution.

Solid dihydrochloride salt **44** (mp = 251-6 °C(dec.)) precipitated and was collected by

filtration and partially characterized. (crop I: 32%); an additional crop of salt is separated

after evaporating the mother liquors and crystallizing the residue from MeOH-Et$_2$O mixture

(crop II: 27%, overall 59%).

VI.2.3 Protection

a) (Starting from (S)-1,2-diamino-3-(4-iodophenyl)-propane dihydrochloride).

Dihydrochloride **44**, (1.00 g, 2.86 x 10^{-3} mol), di-*tert*-butyldicarbonate (1.63 g, 7.45 x 10^{-3}

mol) and KHCO$_3$ (1.72 g, 17.2 x 10^{-3} mol) were stirred for 4 hr in 30 ml of anhydrous

methanol, at room temp. After 30 minutes, the product started to precipitate. At the end, the

precipitated product **45** was collected by vacuum filtration, washed on the filter with water,

ether and hexane and vacuum dried (0.956 g, yield 70%, mp = 177.5-179 °C). After the

evaporation of the solvent, from the methanolic mother liquors, an additional crop (0.121 g,

8.9%, mp = 175-178 °C) could be isolated by partition of the product between water-

methylenechloride, evaporation of the solvent and recrystallization from EtOAc of the solid

residue. A third crop of **45** can be obtained from the resulting EtOAc mother liquors, after a flash chromatography step (see next procedure).

b) (Starting from crude, free 1,2-diamino-3-(4-iodophenyl)-propane base). Crude diamine **44** (2.65 g, contains ~37% n-BuOH, ~8.0 x 10^{-3} mol), di-*tert*-butyldicarbonate (4.00 g, 18.3 x 10^{-3} mol) and $KHCO_3$ (2.8 g, 2.8 x 10^{-3} mol) were stirred for 4 hr in 90 ml of anhydrous methanol, at room temp. After 30 minutes the product started to precipitate. At the end, the precipitated product was collected by vacuum filtration, and washed with water on the filter. The resulting mother liquors were concentrated to 1/3 and allowed to crystallize. The two wet, solid crops of product were recrystallized twice from methanol and vacuum dried (crop I: 1.74 g, overall yield for reduction / protection = 52%, mp = 177.5-179 °C). From the methanolic mother liquors, an additional crop of pure product was isolated after a flash-chromatography step, on silica column, with a hexane-EtOAc = 2 : 1 eluent system. Crystallization from MeOH, yields a second crop of pure product (overall yield for reduction / protection: crop II: 0.30 g, 9%; overall crop I+II:61%).

TLC ($CHCl_3$-EtOAc = 3 : 1 / silicagel F-254): Rf = 0.4
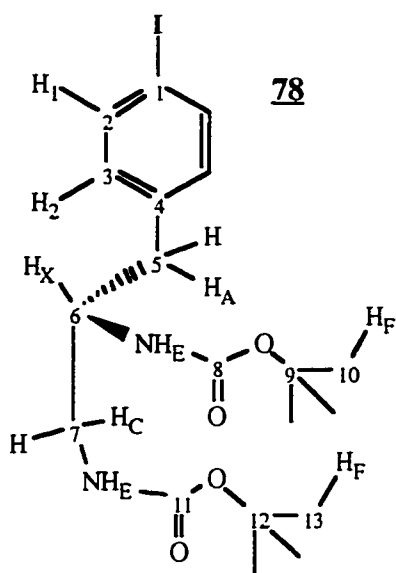
^{1}H-NMR ($CDCl_3$) δ ppm: 7.60 (d, J = 8.2 Hz, $2H_1$), 6.95 (d, J = 8.1 Hz, $2H_2$), 4.85 (broad m, $2H_E$), 3.82 (broad m, $1H_X$), 3.16 (broad m, $2H_A$), 2.74 (broad m, $1H_C$), 2.68 (dd, J = 6.8 13.4 Hz, $1H_C$), 1.42 (s, $9H_F$), 1.37 (s, $9H_F$)

^{13}C-NMR ($CDCl_3$) δ ppm: (156.7, 155.8 for $C_{8,11}$), (137.5, 137.3, 131.3 for C_{2-4}) 91.8 C_1, (79.6, 79.5, for $C_{9,12}$), 52.6 C_6, (43.7, 38.6 for $C_{5,7}$), 28.4 common for $C_{10,13}$

IR (KBr pellet) v cm^{-1}: 3357 (Br), 3009, 2538, 2965, 2931, 2875, 1716,1687, 1576,

1529, 1251, 1227, 797

Elemental Analysis Calc'd for $C_{19}H_{29}N_2O_4I$: C,47.91; H, 6.14; N, 5.88; Found:

VI.2.4 Intermediates

(S)-2-amino-3-(4-iodophenyl) propionamide hydrochloride **43**

TLC (Hexanes-EtOAc-MeOH-NEt$_3$ = 1:3:1:0.2/silicagel F-254): Rf = 0.3.

79

^{1}H-NMR (CD$_3$OD, hydrochloride, see **79**, X = O)

δ ppm: 7.71 (d, J = 7.3Hz, 2H$_1$), 7.13 (d, J = 7.3Hz, 2H$_2$), 4.13

(broad t, J = 6.7Hz, 1H$_X$), 3.21 (dd J = 6.2, 13.5 Hz, 1H$_A$),

3.06 (dd J = 8.8, 13.7 Hz, 1H$_A$)

^{1}H-NMR (MeOH-d6, free amine, see **79**, X = O) δ

ppm: 7.35 (d, J = 7.5Hz, 2H$_1$), 7.03 (d, J = 7.5Hz, 2H$_2$), 3.59

(broad t, J = 6.8Hz, 1H$_X$), 2.97 (dd J = 6.4, 13.2 Hz, 1H$_A$),

2.79 (dd J = 7.5, 13.4 Hz, 1H$_A$)
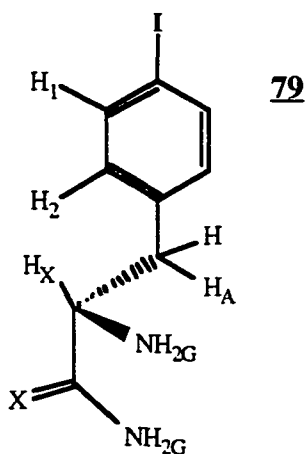
IR (KBr pellet, free amine): v cm^{-1}: 3358, 3269 (Br), 3150, 3043 (Br), 1696, 1604,

833, 818, 751.

(S)-1,2-Diamino-3-(4-iodophenyl) propane dihydrochloride **44**

TLC (EtOAc-MeOH-NEt$_3$ = 2 : 3 : 0.2 / silicagel F-254): Rf = 0.4

^{1}H-NMR (D$_2$O, dihydrochloride, see **79**, X = 2H$_C$) δ ppm: 7.80(d, J = 8.0 Hz, 2H$_1$),

7.12 (d, J = 7.9 Hz, 2H$_2$), 3.89 (q, J = 6.8Hz, 1H$_X$), 3.36 (broad m, 2H$_C$), 3.13 (dd, J = 5.8,

14.6 Hz, 1H$_A$), 2.95 (dd, J = 8.3, 14.5 Hz, 1H$_A$)

^{1}H-NMR (1:1 CD$_3$OD + D$_2$O, crude, free base, see **79**, X = 2H$_C$) δ ppm: 7.63(d, J = 8.2 Hz, 2H$_1$), 7.03 (d, J = 8.2 Hz, 2H$_2$), 2.94(unresolved m 1H$_X$), 2.69 (unresolved m, 2H$_{A,C}$), 2.50 (unresolved m 2H$_{A,C}$). Contains also n-BuOH signals

IR (of the dihydrochloride salt,, KBr pellet) v cm^{-1}: 3000(Br), 3445(Br), 2000(Br), 1590, 1442, 833, 818

VI.3 Methyl phosphinate **47** (improved preparation, modification of Gallagher's method[116])

Trimethyl orthoformate (0.970 ml, 8.69 x 10^{-3} mol) was added at 5°C, under N$_2$, to a stirred solution of anhydrous phosphinic acid **46**, (0.143 g, 2.17 x 10^{-3} mol) in 1 ml of 1:1(v/v) dry THF-toluene mixture. After 1 hr at 5°C, the mixture was allowed to warm to room temperature, and stirred for another 2 hr. The resulting solution was used directly in Pd catalyzed couplings with aryl iodides. For a separate sample dissolved in CDCl$_3$, the product concentration was determined by ^{1}H-NMR integration using added CH$_2$Cl$_2$ as an internal, integration standard. (Yield 93%).

Other solvent mixtures were tested in the above conditions, resulting in solutions of product with compositions listed in Table 2, section IV.1.

^{31}P-NMR (of THF-toluene solution) δ ppm: 17.9 (tq, J = 567, 12.9Hz) 96.3% (product **47**); impurities at δ 29.8, 0.9% (phosphinic acid-orthoformate adduct **49**), 8.2, 2.8% (unreacted phosphinic acid **46**).

^{1}H-NMR (CDCl$_3$) δ ppm:7.19 (d, J = 562.1 Hz, 2H); δ 3.89 (d, J = 12.7 Hz, 3H) and characteristic peaks of THF, toluene, methanol, orthoformate and methyl formate.

VI.4 *tert*-Butyl Phosphinate, 51

Anhydrous phosphinic acid 46,(0.415 g, 6.3 x 10^{-3} mol) in dry *tert*-BuOH (3.000 ml, 31.8 x 10^{-3} mol) was treated under N_2 at room temperature with trimethyl orthoformate (2.700 ml, 24 .0 x 10^{-3} mol). After 3 hr, the ^{31}P-NMR of reaction mixture diluted into $CDCl_3$ shows a 1.1:1 mixture of $H_2PO_2CH_3$: $H_2PO_2C(CH_3)_3$, with no significant side products. Triethylamine (0.4 ml) was added to prevent further reaction of trimethyl orthoformate, and volatiles were removed in vacuo. Two cycles of addition of *tert*-BuOH (3.400 ml), 90 minutes reaction and in vacuo removal of volatiles for 10 minutes followed. The residue was then dissolved in 2 ml of toluene and 0.2 ml triethylamine and filtered through a 5 x 0.4 cm column of basic alumina. The column was rinsed with 1ml of toluene and the concentration of the product 51 in the toluenic solution was determined by ^{1}H-NMR integration in presence of 1,3,5-trimethoxybenzene added as an integration standard. Yield 3.0 ml of 0.82 M solution (37%).The solution was used directly in a Pd catalyzed coupling reactions with aryl iodides.

^{31}P-NMR ($CDCl_3$-toluene 6:1) δ ppm: 4.03

^{1}H-NMR ($CDCl_3$)-toluene 6:1) δppm: 7.10 (d, J = 559.7 Hz, 2H), δ 1.47 (s, 9H) Characteristic peaks of toluene, and *tert*-BuOH are present.

VI.5 *tert* - butyl {4-[2(S) 3-di(*tert*-butoxycarbonylamino)-propyl] phenyl} phosphinate, 52, diastereomeric mixture

A suspension of N, N'-1,2(S)--di-(*tert*-butoxycarbonyl-amino)-3-(4-iodophenyl) propane 45 (0.190 g, 4.00 x 10^{-4} mol), $(Ph_3P)_2PdCl_2$ (0.014 g, 2.0x10^{-5} mol) in CH_3CN (1.0 ml) and triethylamine (0.031 ml, 2.2 x 10^{-4} mol) was treated with a solution of *tert*-butyl phosphinate 51 (8.2 x 10^{-4} mol, added as 1.00 ml of a 0.82 M toluene solution also

0.58 M in Et_3N). The reaction mixture was sealed under N_2, and heated in a 90° oil bath for 100 min. After solvent removal by rotary evaporation, product was isolated by flash chromatography (silica column, eluent 19:1 EtOAc / Et_3N) as a white solid (0.142 g, 75%, mp = 56-60 °C). The product (mixture of diastereoisomers) is difficult to recrystallize: low yields in crystallized product (mp = 76-82 °C) were obtained from concentrated ether solutions which were chilled in dry ice and then allowed to crystallize in freezer for several days.

TLC (EtOAc-NEt$_3$ = 95 : 5 / silicagel F-254): Rf = 0.3
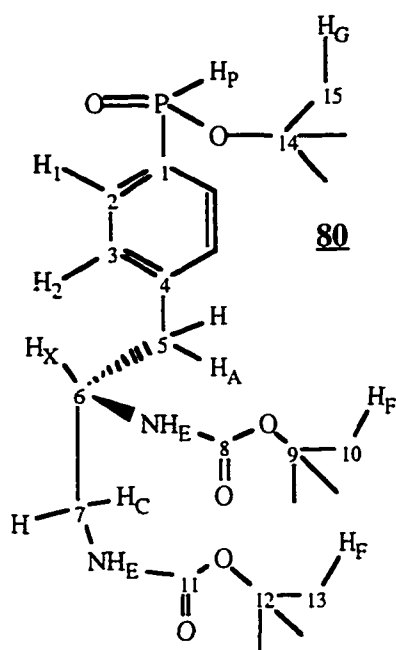
^{1}H-NMR(CDCl$_3$) δ ppm: 7.72 (d, J = 551 Hz, 1Hp),

7.69 (dd, J = 13.8, 7.8 Hz 2H$_1$), 7.33 (dd, J = 8.0, 3.1 Hz,

2H$_2$), 4.95 (broad, 1H$_E$) 4.87 (broad, 1H$_E$), 3.88 (broad m,

1H$_X$), 3.18 (broad m, 2H$_A$), 2.88 (broad m, 1H$_C$), 2.81 (dd,

J = 13.2, 6.8Hz, 1H$_C$), 1.57 (s, 9H$_G$), 1.44 (s, 9H$_F$), 1.39 (s,

9H$_F$)

^{13}C (CDCl$_3$) δ ppm: (156.7, 155.9 for C$_{8,11}$), 142.8.

C$_4$ 131.7(d, J = 11.9 Hz, C$_3$), 129.6 (d, J = 139.3 Hz, C$_1$),

129.6 (d, J = 14.3 Hz, C$_2$), 83.1 (d, J = 11.0Hz, C$_{14}$), (79.7,

79.5 for C$_{9,12}$), 52.6 C$_6$, (43.7, 39.2 for C$_{5,7}$), 30.4 (d, J =

4.5 Hz, C$_{15}$), 28.3 common for C$_{10,13}$

HETCOR-NMR was used for the assignments of C$_{6, 10, 13}$

^{31}P-NMR (CDCl$_3$): Diastereomers δ ppm: 15.66 and 15.70 (^{1}H-coupled: dt, J = 552, 12.3 Hz)

IR(film on NaCl plate) v cm^{-1}: 3328 (Br), 3050, 2978, 2931, 2871, 1710, 1521, 1252,1228, 1041, 735

Electrospray MS(MeOH), positive ions : M = $C_{23}H_{39}N_2O_6P$: Calc'd for $(M+Na^+)$

493.2; Found: 493.1 (62%); Calc'd for $(M + K^+)$: 509.2, Found: 509.1 (62%)

Elemental Analysis: Calc'd for $C_{23}H_{39}N_2O_6P$: C, 58.71; H, 8.35; N, 5.95. Found: C,

57.93; H, 8.73; N, 6.06

VI.6 *tert* - butyl bis-{4-[2(S) 3-di(*tert*-butoxycarbonylamino)-propyl] phenyl} phosphinate 53

In a Pyrex tube with thick walls, a mixture of *tert*- butyl monoarylphosphinate, 52

$(0.515 \text{ g}, 1.09 \times 10^{-3} \text{ mol})$, aryl iodide 45 (1.040 g, 2.18 x 10^{-3} mol), tris(4-N,N'-

dimethylaminophenyl) phosphine (0.108 g, 2.76 x 10^{-4} mol) and $Pd_2(dba)_3$ (0.052 g, 5.6 x

10^{-5} mol) was suspended in 9 ml of freshly distilled anhydrous acetonitrile, propylene oxide

(0.130 ml, 1.84 x 10^{-3} mol) and triethylamine (1.545 ml 1.11 x 10^{-2} mol). The reaction

mixture was sealed under N_2, and heated in a 90 °C oil bath for 8 hr. After removing the

solvent by rotary evaporation, the residue was loaded on a chromatography silica column.

and the nonpolar impurities rinsed with hexanes-EtOAc-AcOH = 126:70:3. Flash-

chromatography with EtOAc-AcOH = 26:70:3 on the same column, yielded a product

which was still impurified with traces of unreacted 52. The impurity was removed by

stirring 16 hr. at 40 °C the solution of the crude product in 5 ml dioxane, with a 0.5 M aq.

$NaIO_4$ solution (0.5 ml, 2.5 x 10^{-3} mol). The mixture was then dissolved in CH_2Cl_2 and

filtered through a short column filled with basic alumina. After rinsing with EtOH-CH_2Cl_2

1:2(v/v) the recombined eluates were evaporated. The solid residue was crystallized from

MeOH-Et_2O yielding a first crop of pure product (0.520 g, 40%, mp = 179-181 °C). After

the concentration of mother liquors and crystallization, a second crop of less pure material

was isolated (0.06 g, 5%, 176-180 °C).

At 100 mg scale preparations, the isolated yields were >50% and the product is free

of any detectable impurity. Larger scale preparations, yield products slightly impurified and

need a second flash-chromatographic separation with Hexanes-CH$_2$Cl$_2$-MeCN-AcOH = 40

: 20 : 10 : 4.

TLC (Hex-EtOAc-AcOH = 2.7:7:0.3 /silicagel F-254): Rf = 0.4
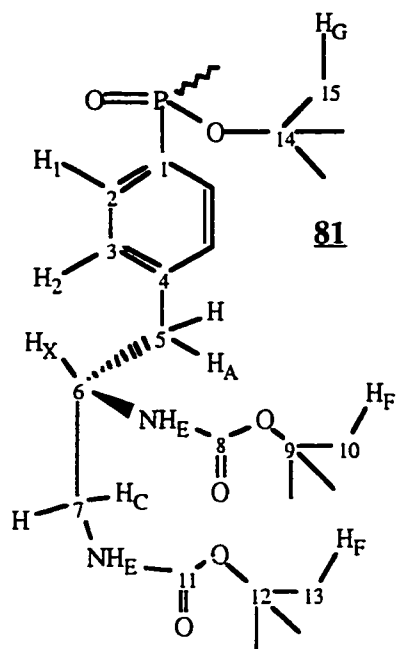
^{1}H-NMR (CDCl3) δ ppm: 7.69 (dd, J = 12.0, 7.8

Hz, 4 H$_1$), 7.24 (dd, J = 7.8, 2.7Hz, 4 H$_2$), 4.93 (broad m, 2

H$_E$), d 4.86 (broad m, 2 H$_E$), 3.86 (broad m, 2 H$_X$), d 3.15

(broad m, 4 H$_A$), 2.84 (broad m, 2 H$_C$), 2.75(dd, J = 13.5,

6.9Hz, 2H$_C$), 1.48 (s, 9 H$_G$), 1.42 (s, 18 H$_F$), 1.37 (s, 18 H$_F$)

^{13}C (CDCl3) δ ppm: (156.7, 155.8 for C$_{8,11}$), 141.6,

C$_4$, 132.8 (d, J = 186.1Hz, C$_1$), [131.8 (d, J = 13.8 Hz),

129.3 (d, J = 17.8 Hz) for C$_{2,3}$], 83.6, (d, J = 10.9 Hz, C$_{14}$),

[79.5, 79.4 for C$_{9,12}$] 52.6 C$_X$, [43.7, 39.0 for C$_{5,7}$], 30.9 (d,

J = 5.2 Hz, C$_{15}$), 28.4 common for C$_{10,13}$

^{31}P-NMR(CDCl3): δ ppm: 26.51(^{1}H-coupled: quintet, J = 11.7Hz) (see also the

Appendix, Figure A7-8)

IR(film on NaCl plate) v cm^{-1}: 3335 (Br), 3054, 2977, 2932, 2872, 1716, 1539,

1271, 1251,1228, 1040, 737

Electrospray MS(MeOH) positive ions : Calc'd for M+Na = C$_{42}$H$_{67}$N$_4$O$_{10}$P$_1$Na$_1$:

841.4; Found: 840.7 (100%)

Elemental Analysis; Calc'd for C$_{42}$H$_{67}$N$_4$O$_{10}$P: C, 61.60; H, 8.25; N, 6.48. Found:

C, 61.22; H, 8.27; N, 6.68

VI.7 Bis-[4-(2(S) 3-diaminopropyl) phenyl] phosphinate trihydrochloride tetrahydrate -"BDAP", 35

Concentrated hydrochloric acid (1.5 ml) and distilled water (0.5 ml) were added to solid *tert*- butyl diarylphosphinate 53 (0.117 g, 1.43 x 10^{-4} mol) and the suspension was stirred for 30 minutes at 80 °C. The resulting solution was rotary evaporated and the solid residue was redissolved in 1 ml of water. The solution was treated with charcoal, filtered and reevaporated to dryness. The residue was redissolved in 0.5 ml of water and the product precipitated as a white solid on addition of 5 ml of anhydrous ethanol. The white precipitate was separated by centrifuge and dried under vacuum. Two cycles of redissolution in 1 ml of distilled water and lyophilization were necessary in order to obtain the pure BDAP (0.050 g, 64%) free of any traces of ethanol.

HPLC (MeCN - 0.05% 0.005 M sodium HSA in aq. TFA = 15:85 / Column 86-200-E3 Microsorb MV C-18, at 0.5ml / min, detection at 230 nm): R_T = 4.7 min(100%)
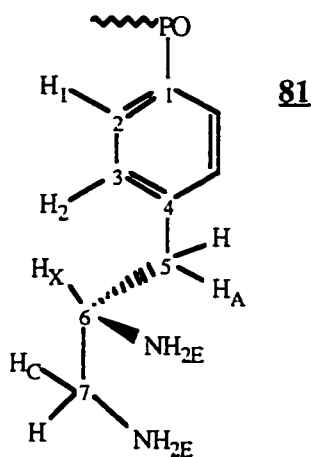
^{1}H-NMR (D$_2$O, trihydrochloride) δ ppm: 7.72 (dd, J = 11.7, 8.1 Hz, 4 H$_1$), 7.42 (dd, J = 8.1, 2.4 Hz, 4 H$_2$), 3.78 (dq, J = 8.7, 6.3 Hz, 2 H$_X$), 3.40 (dd, J = 16.7, 6.3, 1 H$_C$), 3.35 (dd, J = 16.7, 6.8, 1 H$_C$), 3.23 (dd, J = 14.4, 6.3, 1 H$_A$), 3.04 (dd, J = 14.4, 8.7, H$_A$) (see also Appendix, Figure A9)

^{13}C (CDCl$_3$) δ ppm: 139.9 C$_4$, 138.6 (d, J = 177.2 Hz, C$_1$), [134.4 (d, J = 13.5 Hz), 132.2 (d, J = 16.7 Hz)C$_{2,3}$], 55.2, C$_6$ [43.4, 38.8, C$_{5,7}$]

^{31}P-NMR(CDCl$_3$): δ: 23.55 (^{1}H-coupl.: qv, J = 11.6Hz) (see Appendix, Figure A10)

IR(KBr pellet) ν cm^{-1}: 3430, 2972,(Br), 1606,1508, 1403, 1205, 1044, 741

UV (0.1M aq. HCl) ε^{230} = (2.51±0.02x10^4) M^{-1} cm^{-1}

Electrospray MS(H_2O-MeOH), positive ions : M = $C_{18}H_{27}N_4O_2P$: Calc'd for

[M+H$^+$, (M+2H$^+$)/2, (M+H$^+$+Na$^+$)/2] 363.2, 182.6, 193.6; Found: 362.8, (30%) 181.8,

(100%) 192.5 (43%); negative ions: Calc'd for [M-H$^+$, 2M-H$^+$] 361.2, 723.4; Found: 361.0

(16%), 723.6 (8%). For MS(H_2O-MeOH+ NaOH, pH9): positive ions : Calc'd for [M+H$^+$,

(M+Na$^+$) (M-H$^+$+2Na$^+$)] 363.2, 385.4 407.2 Found: 363.4, (20%) 385.3 (25%)

406.8(100%); negative ions: Calc'd for [M-H$^+$] 361.2; Found: 361.8 (100%)

Elemental Analysis: Calc'd for $C_{18}H_{27}N_4O_2P_1$(HCl)$_3$(H_2O)$_4$: C, 39.75 H, 7.04; N,

10.30. Found: C, 39.52; H, 7.08; N, 10.07

VI.8 Tripotasium tris-carbonato-cobalt (III) complex 64 (modification of Shibata's[141] method)

Cobaltous dichloride hexahydrate, (2.5 g, 1.0 x 10^{-2} mol) was dissolved in hydrogen

peroxide 30% (3.0 ml, 3.0 x 10^{-2} mol) and 2.5 ml distilled water and added at 0 °C during

30 minutes, using a syringe pump, to a stirred suspension of potassium bicarbonate (7.0 g,

7.0 x 10^{-2} mol) in 4 ml of water. During the addition, the foaming mixture became dark-

green and care was given to avoid early catalytic decomposition of H_2O_2 before the

addition, by contamination with the forming tris-carbonato-cobaltic complex. After 30

minutes, the complex formation is complete, and the suspension was diluted in a 100 ml

volumetric flask after adding solid potassium bicarbonate (16.0 g, 1.60 x 10^{-1} mol final

concentration of solution: 2 M $KHCO_3$) and water. The UV-VIS spectrum of a 0.020 ml

aliquot of this solution diluted to 1.000 ml in 2 M $KHCO_3$ is consistent with the literature

data[141] showing maxima at 638 and 436 nm (lit : 645, 440[157] or 635, 440.[140] The reaction

yield estimated from extinction coefficients is 94%.

After 1 month of refrigeration, the solution shows 94% of the initial absorption at

the same λ_{max} values and some traces of precipitate were formed.

VI.9 Di-carbonato-bis-{μ-di-[4-(2(S)3-diaminopropyl) phenyl] phosphinate}-dicobalt (III)} complex: "Co$_2$BDAP$_2$(CO$_3$)$_2$", 62

The following aqueous solutions were diluted in 7 ml of water, in a sealed tube:

A:	6.3x10^{-3} M BDAP x 3HCl 35	(3.500 ml, 2.21 x 10^{-5} mol)
B:	6.79 x 10^{-2} M 64, also 2.0M in KHCO$_3$	(.583 ml, 3.95 x 10^{-5} mol 64)
C:	2.0 M KHCO$_3$	(1.750 ml, 3.5 x 10^{-3} M)

(total KHCO$_3$ added: 4.67 x 10^{-3} mol)

The reaction tube was heated to 90-95 °C for 90 minutes, when the characteristic color and UV-VIS absorption maxima of 568 and 398 nm (lit[143] 567 and 388 nm) of the derivatives of ethylenediamino-dicarbonato cobalt complexes indicates that the first "CO$_3$" substitution step proceeded with a 93% yield. A new amount of BDAP x 3 HCl (3.175 ml, 2.00 x 10^{-5} mol) was added to the solution and the heating in sealed tube at 90-95 °C was continued while monitoring the change in λ_{max}. After 22 hr of heating, the λ_{max} is decreased at 528 nm and the conversion calculated with the equations 1-4 is 64% for this second step "CO$_3$" substitution. In order to increase conversion, the HCO$_3$ $^-$ concentration of the solution was reduced by precipitation at RT with a 1.00 M solution of Ca(ClO$_4$)$_2$ (1.000 ml, 1.00 x 10^{-3} mol). The suspension was heated for 30 minutes at 90°C and then cooled and filtered. Another amount of BDAP x 3 HCl (0.263 ml, 1.66 x 10^{-6} mol) was added to the solution and the heating continued for another 22 hr. The final λ_{max} = 518 nm indicated a 78% conversion (second step "CO$_3$" substitution) by BDAP. A cation exchange column loaded with 1g of Sephadex CM-25 equilibrated with 0.1M KHCO$_3$ solution and washed with nanopure water was used for the retention of BDAP and other cationic species, the product being eluted with water. The separated yield in products with an equimolar

$BDAP^-$: $Co(CO_3)^+$ stoechiometry was estimated by UV-VIS methods to 74%. An anion

exchange column loaded with 1 g of DEAE-Sephadex equilibrated with 0.1M $KHCO_3$

solution and washed with nanopure water was used for the retention of anionic impurities.

Several pink fractions, with λ_{max} = 518-512 nm were eluted with water, indicating a

mixture of complexes which probably coeluted with the desired product due to the high

concentration of the HCO_3^- ion in the sample. Therefore, the sample was "desalted" by

dropwise addition of 1 M solution of $Ca(ClO_4)_2$, until no precipitate was forming anymore,

and the cation and anion exchange purification steps were repeated. The UV-VIS absorption

maxima of pink solution at 512 and 360 nm is characteristic for the derivatives of bis-

ehtylenediamin-carbonato cobalt complexes (lit:[158] 512 and 360 nm). After concentration

and lyophilization of the solution, a solid, pink product was obtained which contains 7.8%

of the equimolar $BDAP^-$: $Co(CO_3)^+$ complex in a mixture of mineral matrix (overall yield

by UV: 29%).

^{1}H-NMR (D_2O) δ ppm: 7.66(broad m 8H), 7.31 (broad m, 8H), 2.95, 2.65, 2.48

(unresolved signals, 20H)

^{31}P-NMR($CDCl_3$) δ ppm: 20.64-23.24 several signals

IR(nujol) ν cm^{-1}: 1693, 1666, 1633, 1405,1307, 1008, 831

Electrospray (data listed also in Table 3, section IV.2.3) MS: $Co_2BDAP_2(CO)_2$ =

M= $C_{38}H_{52}N_8O_{10}P_2Co_2$ = 960.20

Sample 1&2, (H_2O), positive ions: Calc'd for $(M+H^+-CO_3^{2-})/3$, $(M+2H^+)/2$ = 300.4,

481.1; Found: 301.1(24%), 481.2(9%)

Sample 3 (H_2O-MeOH) positive ions: Calc'd for $(M+K^++H^+-CO_3^{2-})/4$,

$(M+4H^++2KHCO_3)/4$, $(M+2H^++2K_2CO_3+H_3O^+)/3$, $(M+2H^++K_2CO_3)/2$: 235.0, 291.0,

373.1, 550.1; Found: 235.1(100%), 291.1(53%), 373.2(48%), 551.2(12%)

Sample 3 (H$_2$O-MeOH) negative ions: Calc'd for (M+KCO$_3^-$-2H$^+$)/3, (M-Co^{3+}+H$^+$)/2, (M+K$_2$CO$_3$-2H$^+$)/2]: 352.4, 451.1, 548.1; Found: 353.6(100%), 451.5(32%), 549.5(17%)

VI.10 Labile bis-{µ–di-[4-(2(S) 3-diaminopropyl) phenyl] phosphinate } -transition metal complexes (M$_2$BDAP$_2$), M = Cu, Ni, Pd, Zn

Concentrations in the range of 1.4 x 10^{-5} to 5.0 x 10^{-3} M of M$_2$BDAP$_2$ complexes were prepared using nanopure water or D$_2$O 99.96% for transport and CD or NMR experiments respectively. V$_1$ ml of BDAP x 3 HCl x 4 H$_2$O, 35, solution were mixed with V$_2$ ml of 0.2 M borate and then diluted with V$_4$ = V$_2$-V$_1$-V$_3$ ml of water. A final concentration of 0.1M borate is obtained after adding the final V$_3$ ml of 0.8-1.1 equival. of metal salt solution (CuCl$_2$ x 2 H$_2$O, Ni(OAc)$_2$ x 4 H$_2$O, Na$_2$PdCl$_4$ anh., Zn$_2$SO$_4$ x 7H$_2$O). The transition metal salt solutions for NMR use were prepared from dehydrated salts (at 150 °C, vacuum, 2 hr) after being lyophilized once from D$_2$O. In the case of Pd$_2$BDAP$_2$ the solutions were heated 30 min at 80 °C for the thermodynamic equilibration of the complex mixture.

VI.10.1 Pd$_2$BDAP$_2$

^{1}H-NMR (0.1M borate in D$_2$O) δ ppm:7.66 (dd, J$_{total}$ = 19.2Hz), 7.63 (dd, J$_{total}$ = 19.2Hz), 7.55 (dd, J = 11.6, 7.6 Hz), 7.34 (broad, unresolved), 7.27 (broad, unresolved), 3.21 (unresolved), 2.93 (unresolved), 2.77 (unresolved), 2.67 (dd, J = 13.2, 8.4Hz), 2.59 (t, J= 10.8Hz), 2.49 (t, J = 14.0Hz). mixture of three components, in slow equilibrium.

Electrospray MS (H_2O-MeOH), positive ions : ligand = M = $C_{18}H_{27}N_4O_2P$,

complex = {2M-2H$^+$+2Pd^{2+}}$^{2+}$ = 934.2; Calc'd for [(2M-2H$^+$+Pd^{2+}+Na$^+$)/2, or (2M-

4H$^+$+2Pd^{2+}+2Na$^+$) /2] 489.1; Found: 489.7(20%)

Other intense peaks: 269(48%), 351.3(14%); 719.6(100%) 735.8(96%); no M+H$^+$ found.

VI.10.2 Cu$_2$BDAP$_2$

Electrospray MS (H_2O-MeOH) positive ions : ligand = M = $C_{18}H_{27}N_4O_2P$,

complex = {2M-2H$^+$+2Cu^{2+}}$^{2+}$ = 848.2; Calc'd for (M+H$^+$), 363.2

Found: sample 1: 362.2 (not picked); Other intense peaks: 720.0 (100%), ~735 (10%)

Found: sample 2: 363.1 (14%), Other intense peaks: 719.4 (100%), ~735.3 (10%)

VI.10.3 Zn$_2$BDAP$_2$

^{1}H-NMR (0.1M borate in D_2O) δ ppm: 7.662 (dd, J = 11.0, 8.2 Hz, 8H), 7.28 (d, J =

7.2 Hz, 8H), 3.02 (d, J = 10.4 Hz, 4H), 2.86 (d, J = 12.8 Hz, 8H), 2.60 (dd, J = 12.8, 8.4 Hz,

4H) 2.31 (broad, 4H), see also Table 4, section IV.2.1.

Electrospray MS (H_2O-MeOH) positive ions : ligand = M = $C_{18}H_{27}N_4O_2P$, complex =

{2M-2H$^+$+2 Zn^{2+}}$^{2+}$ = 950.2); Calc'd for [(M+H$^+$), (2M-3H$^+$+2 Zn), 363.2, 849.2;

Found: sample 1: 362.2 (18%), 850.8(2%); Other intense peaks: 224.1(24%) 717.3 (87%),

732.4 (5%);

sample 2: 363.5 (14%), no 850.8 (0%); Other intense peaks: 719.9 (100%), ~734.? (4%);

MALDI-MS: (sDHB matrix): Calc'd for (M+H$^+$) 363.2; Found: 362.5

VI.11 1,5-Naphthalene-bis-(oxyacetic Acid) 65

Sodium hydride (2.4×10^{-2} g of 80% suspension in mineral oil, ~8×10^{-4} mol) was washed with 2 ml of anhydrous THF in a septum stoppered flask, under a slow flow of N_2. The THF was removed using a canula and a solution of 1,8-dihydroxynaphthalene (5.0×10^{-2} g, 3.1×10^{-4} mol) in 1ml of dry DMF were injected. While stirring the resulting suspension on an ice bath, ethyl bromoacetate (3.0 ml, 2.6×10^{-3} mol) was added. (Reaction is exothermic.)

After stirring 20 hr. at room temperature, the reaction mixture was cooled on ice bath, diluted with 5ml of ether, and quenched with 3.5 ml of a cold, 0.5M aq. citric acid. After repeating 3 extractions, and rotary-evaporation of the solvent, the residue was flash-chromatographed on a silica column using Hexanes-EtOAc 7:3 as eluent. Two fractions were isolated: crop I (pure: 4.7×10^{-2} g, 45%) and crop II (impure: 45 mg). The product can be further purified by recrystallizationation from EtOH.

The first crop of diester was dissolved in 2 ml of EtOH and titrated /saponified with a ~ 0.3ml of 1M solution of NaOH, until the pH remained higher than 11 for 10 minutes. At cooling, most of the product precipitates and is collected by centrifugation, after washing the crystals with 1 ml of fresh EtOH. The crystals were vacuum dried. Further purification of the disodium salt from impurities containing aliphatic residues was made by dissolving it in water and precipitating the free acid with small portions of 1 M HCl solution, until the pH < 1. After recrystallizationation from water, white crystals of diacid were obtained (2.4×10^{-2} g 28%, mp = 204-6°C). The yield was increased to 51% by reflashing the second crop of diester and following the same procedure for the separation of the diacid.

^{1}H-NMR (MeOH-d$_6$) δ 7.51 ppm: (d, J = 8.3 Hz, 2H), 7.36 (t, J = 8.0, 7.7 Hz, 2H), 6.97 (d, J = 7.6 Hz, 2H), 4.76 (s, 1H)

^{1}H-NMR (0.1 M borate in D_2O) δ ppm: 7.53 (d, J = 8.2 Hz, 2H), 7.43 (t, J = 8.2, 7.8

Hz, 2H), 6.83 (d, J = 7.7 Hz, 2H), 4.64 (s, 1H)

IR (film from MeCN on NaCl plate) ν cm^{-1}: ~3280 (Br), 3050 (Br), 3015, 2920,

1761, 1714, 1575, 1358, 1375, 1274. 1211, 1108, 915, 844, 810, 759, 735

High Resolution EI-MS: Calc'd for $C_{14}H_{12}O_6$: 276.06339; Found: 276.06385

(100%)

VI.12 ^{1}H-NMR titrations

VI.12.1 General procedure

The ^{1}H-NMR titrations were performed on the VXR 300 and DRX 400 MHz

spectrometers at 20.0 ± 0.5 °C. The 0.2 M borate buffer in D_2O was prepared using

anhydrous $Na_2B_4O_7$. All volumes were measured by microsyringes. All the solutions of

host and guest+host were prepared from volumes of D_2O, concentrated solutions of ligand,

metal salt, guest, NaOD or tert-BuOH, totaling a volume equal with that of the 0.2 M borate

used. Some of the guests were dissolved directly in the host solution. The first points of

titrations are obtained by adding to the host solution amounts from the guest+host mixture.

The final titration points are acquired by reversing the addition, from the resulting diluted

guest+host solution aliquots are added to the concentrated guest+host solution. Other

titration schemes are also possible. After each addition of an appropriate amount of host or

host+guest, the solutions were mixed thoroughly by inverting 10 times followed by mixing

with Vortex-Genie for more than 1 minute. Two sets of acquisition parameters were used

for the DRX400 NMR spectrometer, one for PBP complexes (~600 scans PCL program

"ZG", spectral width = 160; acquisition time = 0.43; O_1 = 28009 Hz; O_1P = 70 ppm) and

one for BDAP complexes (~200 scans PCL program "ZG", spectral width = 15 acquisition

time = 0.50; O_1 = 2800Hz; O_1P = 7 ppm). A 5-20Hz line broadening was used for the processing of the spectra. The dissociation constants were determined using the Macintosh non-linear least-squares curve-fitting procedure described in the "Results" section. The $\alpha \pm$ J•Q statistical method for small number of samples[159] was used for the calculation of error ranges corresponding to 95% confidence limits.

VI.12.2 Example: The ^{1}H-NMR titration of the Zn$_2$BDAP$_2$ host with AMP

The following aqueous stock solutions were prepared using 99.96 % D_2O:

Stock Zn$_2$BDAP$_2$:

0.0435 M aqueous BDAP x 3HCl	0.015 ml	6.53×10^{-7} mol
0.100 M aqueous ZnSO$_4$	0.0052 ml	5.20×10^{-7} mol
0.200 M aqueous borate buffer	1.250 ml	2.50×10^{-4} mol
0.050 M aqueous *tert*-BuOH	0.010 ml	5.00×10^{-7} mol
D_2O	1.220 ml	-

The resulting solution is 1.04×10^{-4} M in Zn$_2$BDAP$_2$ and 0.1 M in sodium borate

The "host + guest" titration solution:

crystallized AMP-Na$_2$ x 4H$_2$O 99%	0.0117 g	2.50×10^{-5} mol
1.04×10^{-4} M Stock Zn$_2$BDAP$_2$	0.600 ml	6.24×10^{-8} mol
D_2O	0.050 ml	-
0.200 M aqueous borate buffer	0.050 ml	-

The solution was prepared directly in an NMR tube and has 8.9×10^{-5} M in Zn$_2$BDAP$_2$, 3.57×10^{-2} M in AMP and 0.1 M in sodium borate.

The "host" titration solution:

1.04 x 10^{-4} M Stock Zn$_2$BDAP$_2$	0.600 ml	6.24 x 10^{-8} mol
0.200 M aqueous borate buffer	0.050 ml	-
D$_2$O	0.050ml	-

This solution was prepared directly in a NMR tube and has 8.9 x 10^{-5} M in Zn$_2$BDAP$_2$ and 0.1 M in sodium borate

The ^{1}H-NMR spectra of the "host" and "host+guest" stock solutions were recorded in the conditions shown in section VI.12.1 and then, aliquots of 5, 5, 10, 20, 40, 50, 100, 200 μl the "host+guest" solution were transferred by syringe into the NMR tube containing the "host" titration solution. An additional titration point was obtained by transferring back, 400 μl of the "host" (which in fact at this point contains also guest) into the "host+guest" titration solution. The shifts of the aryl protons H$_1$ and H$_2$ (see **81**) and the aliphatic protons H$_X$, H$_A$ and H$_C$ were monitored and fitted with the equation 13. The last 4 titration points were ignored, since the saturation of the host was more than 80% and also some deviations from the 1:1 binding isotherm were seen in the fitted plot.

VI.13 CD Titrations

VI.13.1 General procedure

Same procedures as those described in the NMR titration section were followed for the preparation of the ~5-10 times more diluted titration solutions needed for the CD measurements. To achieve a good sensitivity of each measurement, concentrations of the host were chosen to present ellipticities of 1-5 degrees. Quartz cells with the light-path of 0.1 cm were used for the determination of the stronger binding constants and when the induced CD is more sensible on binding. For weaker binding constants, 1cm cells were

used. Microliter pipettes were used to manipulate the titration solutions. Withdrawing and

adding equal amounts of solutions in the CD cell was found to be a convenient titration

method. The following acquisition parameters were found to represent a fair compromise

between signal/noise ratio and acquisition time: Resolution step = 0.5 nm; speed = 20

nm/min; Response = 1 second; Bandwidth = 2 nm; Sensitivity = 5 mdeg. Accumulation = 4-

10). During the processing of the spectra, it becomes obvious that under 230 nm the signal

noise ratios are smaller. The same degree of noise reduction processing was used for each

scan of the experiment. The dissociation constants were determined using the Macintosh

non-linear least-squares curve-fitting procedure described in the "Results" section.

VI.13.2 Example: The CD titration of the Zn_2BDAP_2 host with Cis-1,5-Cyclooctanol (COD)

The following aqueous stock solutions were prepared using nanopure water:

The "host" titration solution:

0.00871 M aqueous BDAP x 3HCl	0.041 ml	3.57×10^{-7} mol
0.050 M aqueous $ZnSO_4$	0.060 ml	3.00×10^{-7} mol
0.200 M aqueous borate buffer	1.265 ml	2.50×10^{-4} mol
H_2O	1.165 ml	-

The resulting solution (2.530 ml) has 5.92×10^{-5} M in Zn_2BDAP_2 and 0.1 M

in sodium borate

The "host + guest" titration solution:

0.00871 M aqueous BDAP x 3HCl	0.041 ml	3.57×10^{-7} mol
0.050 M aqueous $ZnSO_4$	0.060 ml	3.00×10^{-7} mol
COD	0.285 g	1.98×10^{-3} mol

D$_2$O	0.810 ml	-
0.200 M aqueous borate buffer	1.265 ml	-

The resulting solution (2.530 ml) has 5.92 x 10^{-5} M in Zn$_2$BDAP$_2$, 7.82 x 10^{-1} M in COD and 0.1 M in sodium borate.

The "host" and "host+guest" solutions were placed in separate quartz cells (light-path 1 cm, volume 3 ml) and the CD spectra were recorded for the 250-230 nm wavelengths region in the conditions shown in section VI.13.1. Then, the following volumes of aliquots were withdrawn from the cell containing the "host" and replaced with the same volumes of "host+guest" solution: 100, 200, 400, 500 and 1000 µl. After each transfer, the cell was stoppered and reversed 20 times for homogenization of the resulting new "host+guest" solutions. The changes in the CD spectra between 250 and 245 nm were monitored and fitted-see section IV.3.2 Figure 19 and Figure A6.
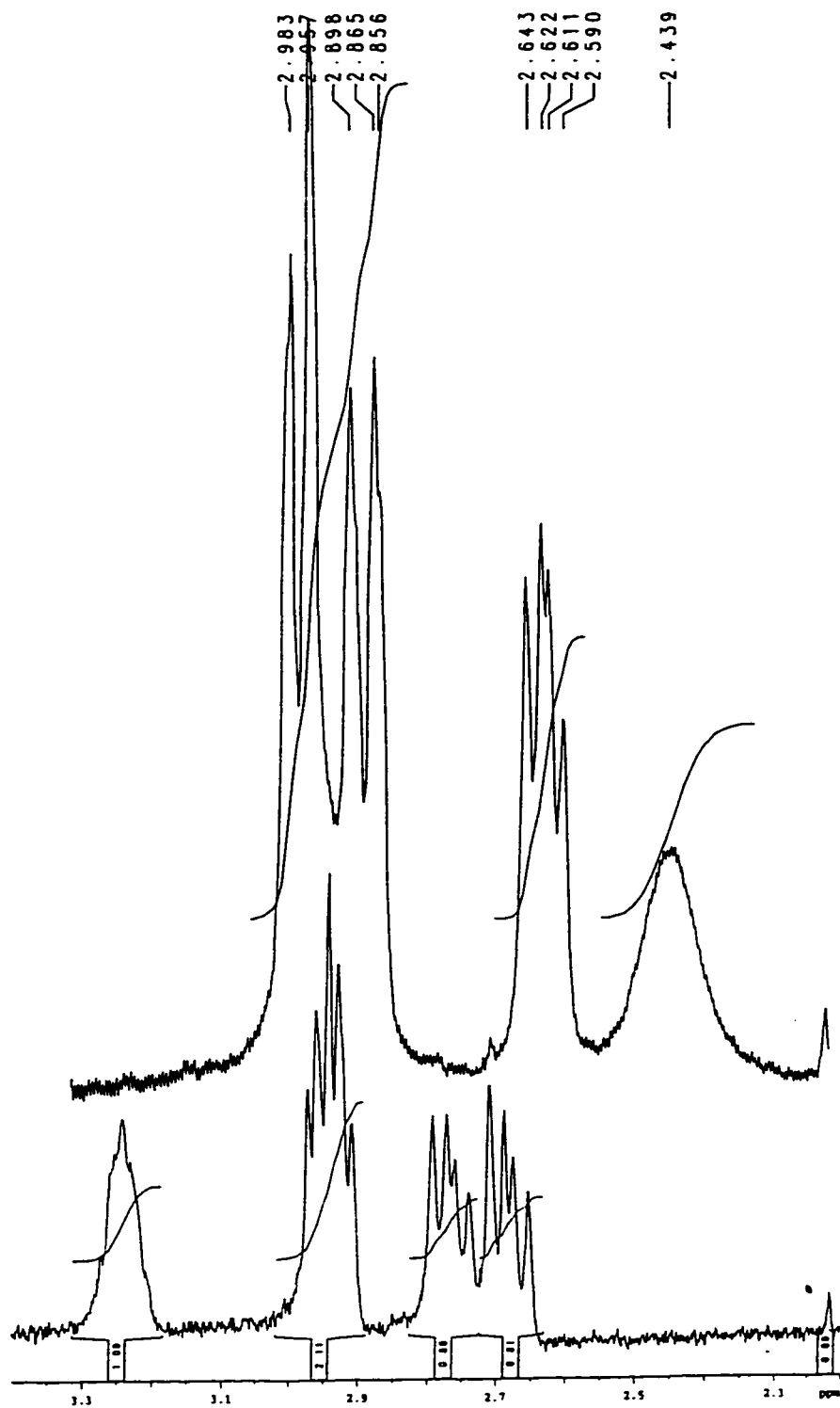
APPENDIX

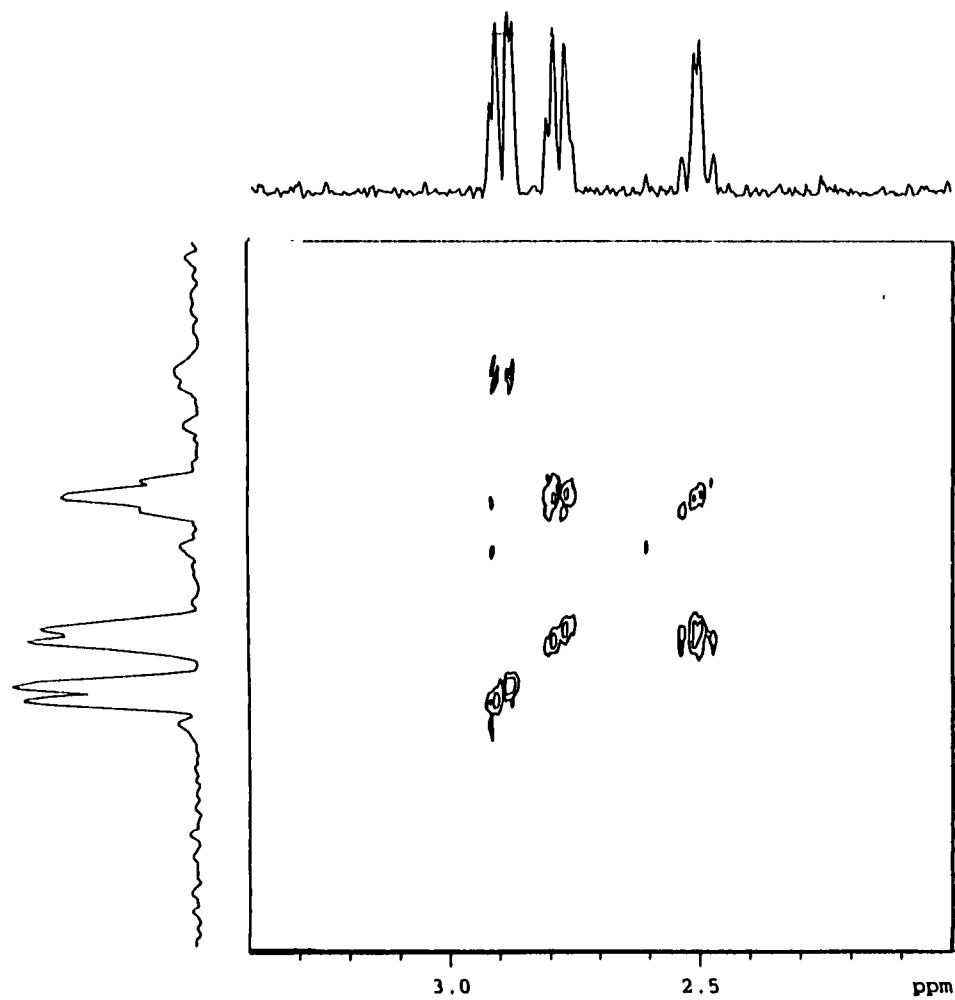Figure A1: a- ¹H-NMR of BDAP in 0.1M borate solution; b-¹H-NMR of BDAP₂Zn₂ in 0.1M borate solution

Figure A2: COSY- NMR of BDAP in 0.1M borate solution

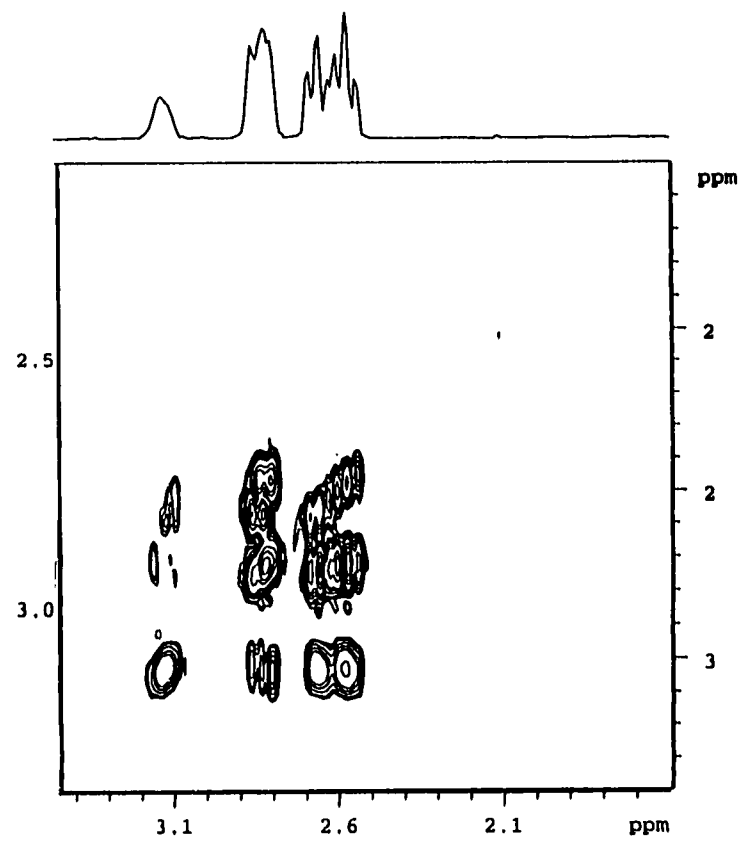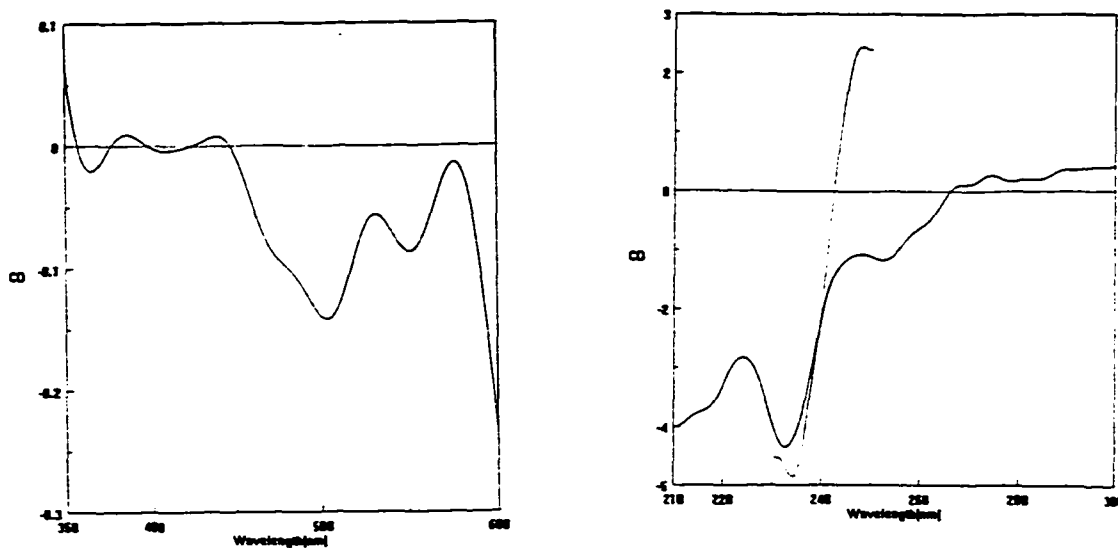Figure A3: COSY- NMR of BDAP$_2$Zn$_2$ in 0.1M borate

Figure A5: (A) CD of Zn and Co(III) complexes of BDAP, at ~2.0x10⁻⁶M concentrations in the 210-300 nm range; (B) CD of aq.~2.0x10⁻⁶M BDAP-Co complex in the 350-600 nm range
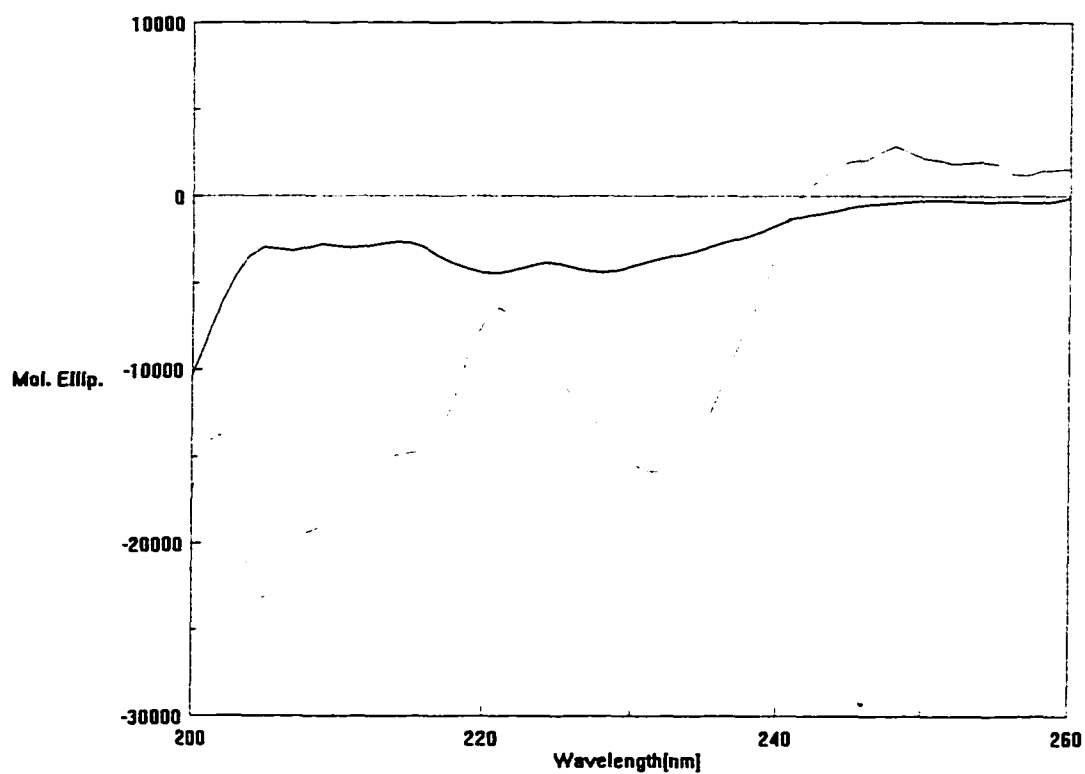

Figure A4: Changes in the CD of an aq. soln of 0.32mM BDAP when 0.8eq. of ZnSO₄ are added.

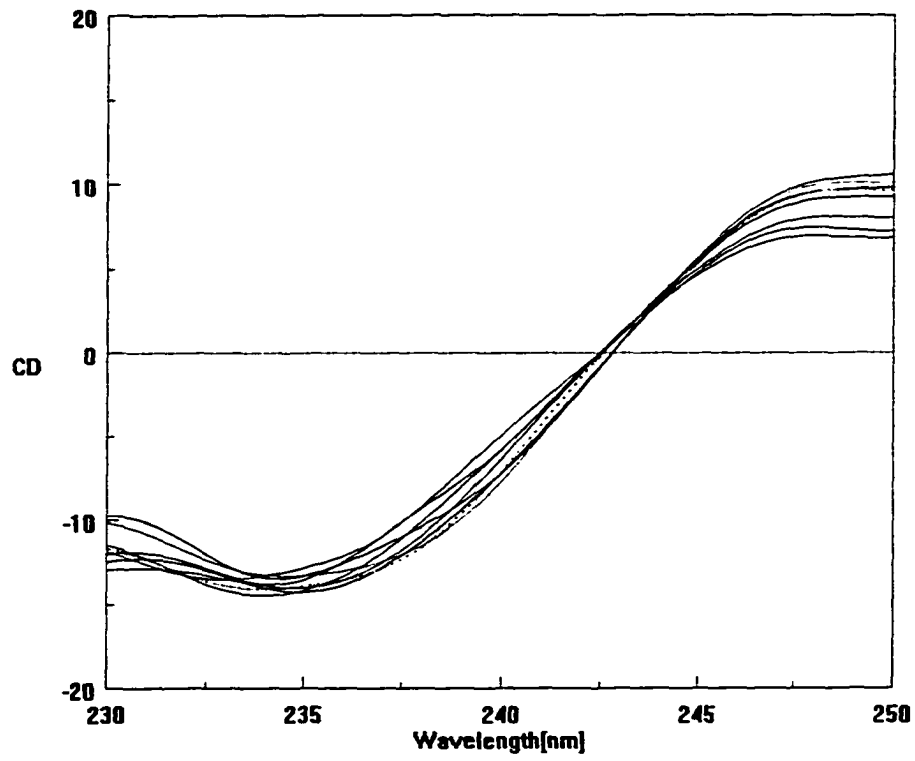Figure A6: Titration of aq. 6.0×10^{-5}M Zn_2BDAP_2 with $\sim 10^5$ molar excess of 1.5-cis-cyclooctanediol

Figure A8   300 MHz ^{1}H-NMR of protected ligand **40** in CDCl$_3$ solution

bis-BOC tBu protected BDAP / CDCl3

26.510

55   50   45   40   35   30   25   20   15   10   5   0   -5   ppm
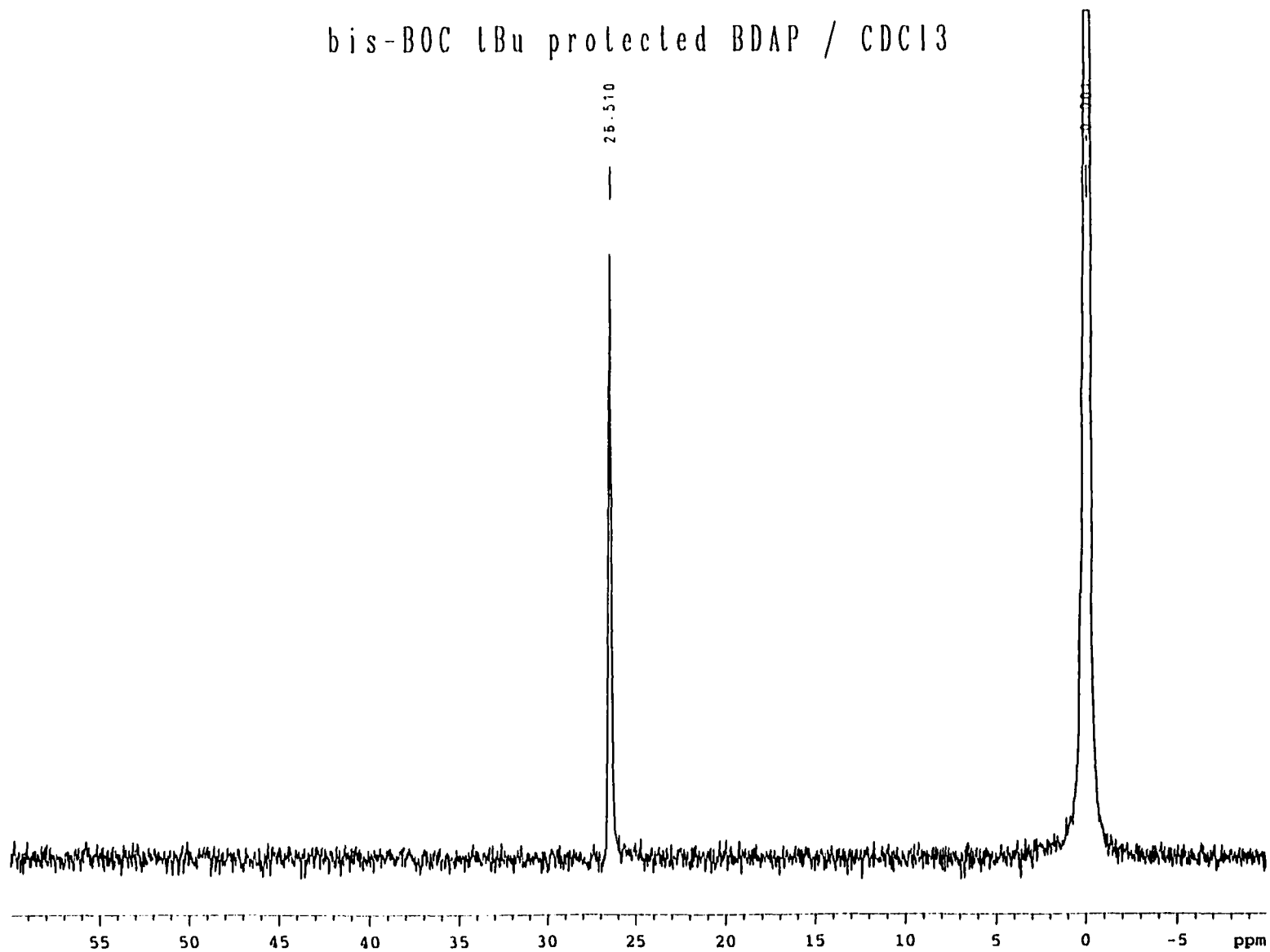
Figure A9   200 MHz ^{31}P-NMR of protected ligand **40** in CDCl3 solution

BDAP hydrochloride / D2O

7.589
7.562
7.550
7.523
7.278
7.270
7.251
7.243

3.825
3.804
3.796
3.783
3.776
3.762
3.755
3.734

3.277
3.255
3.230
3.222
3.207
3.202
3.174
3.105
3.084
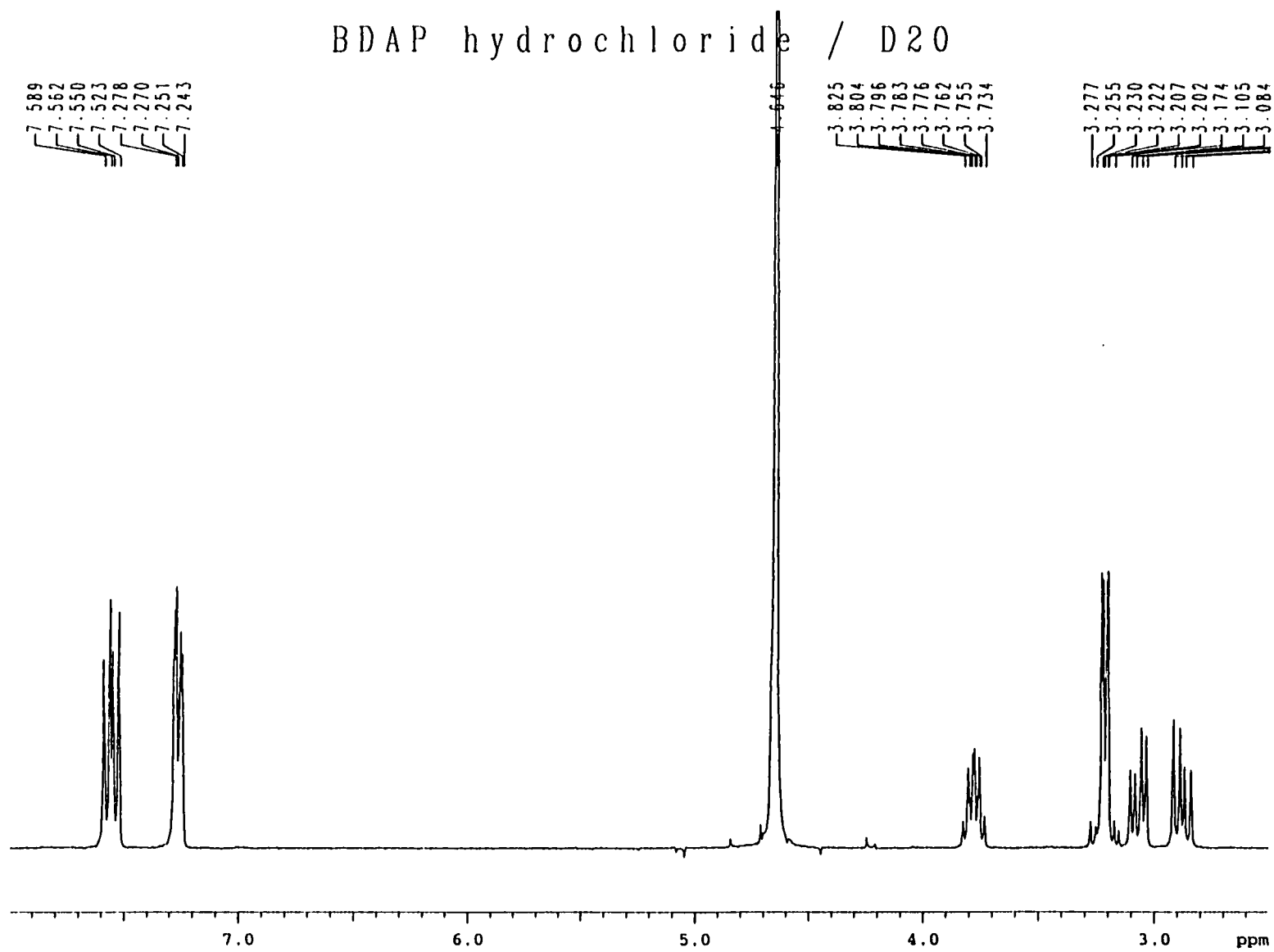
Figure A10   300 MHz ¹H-NMR of the BDAP x 3 HCl ligand **35** in D₂O solution (not calibrated)

BDAP FROM tBu ester decomposed in H2O-HCl
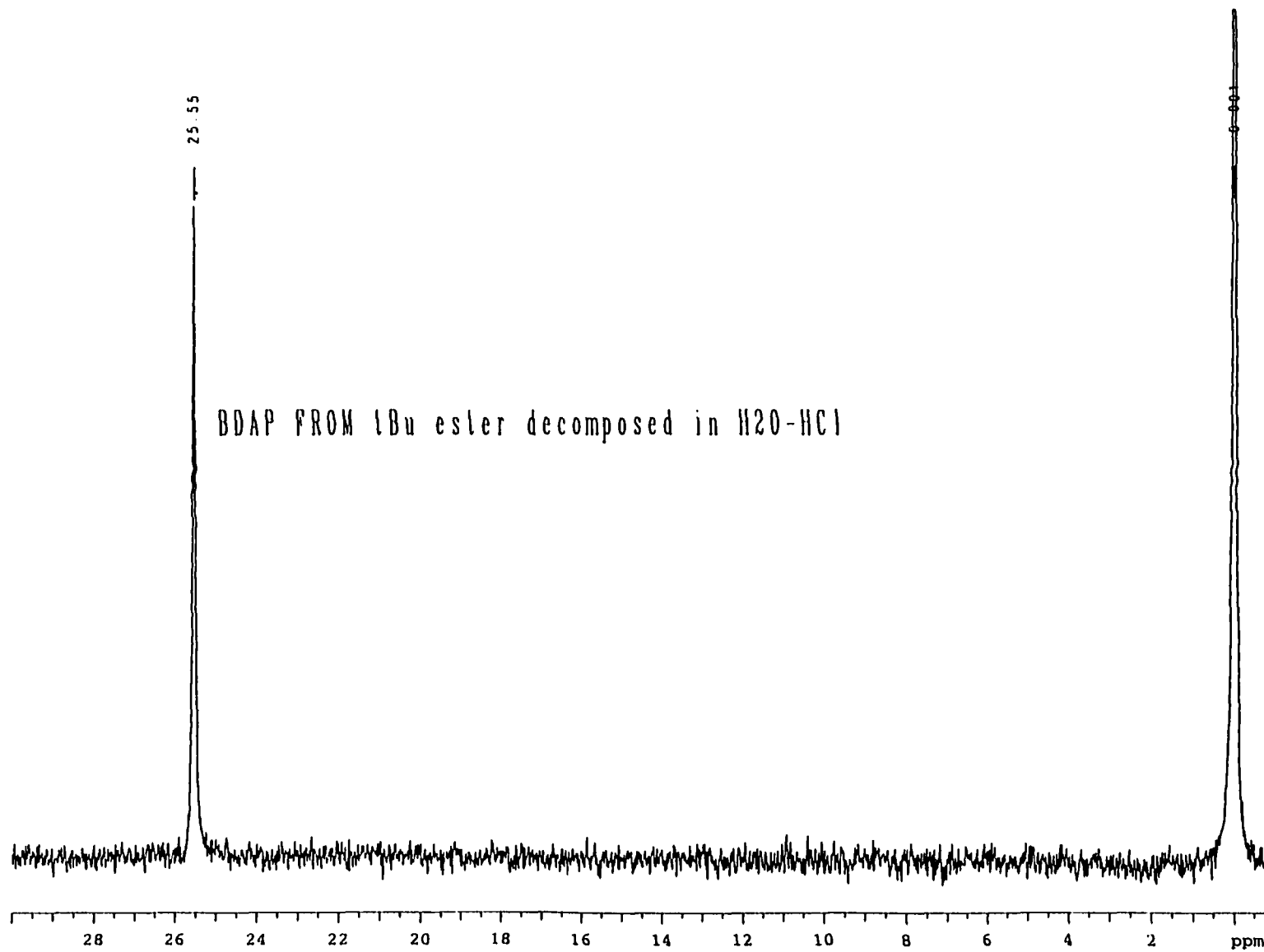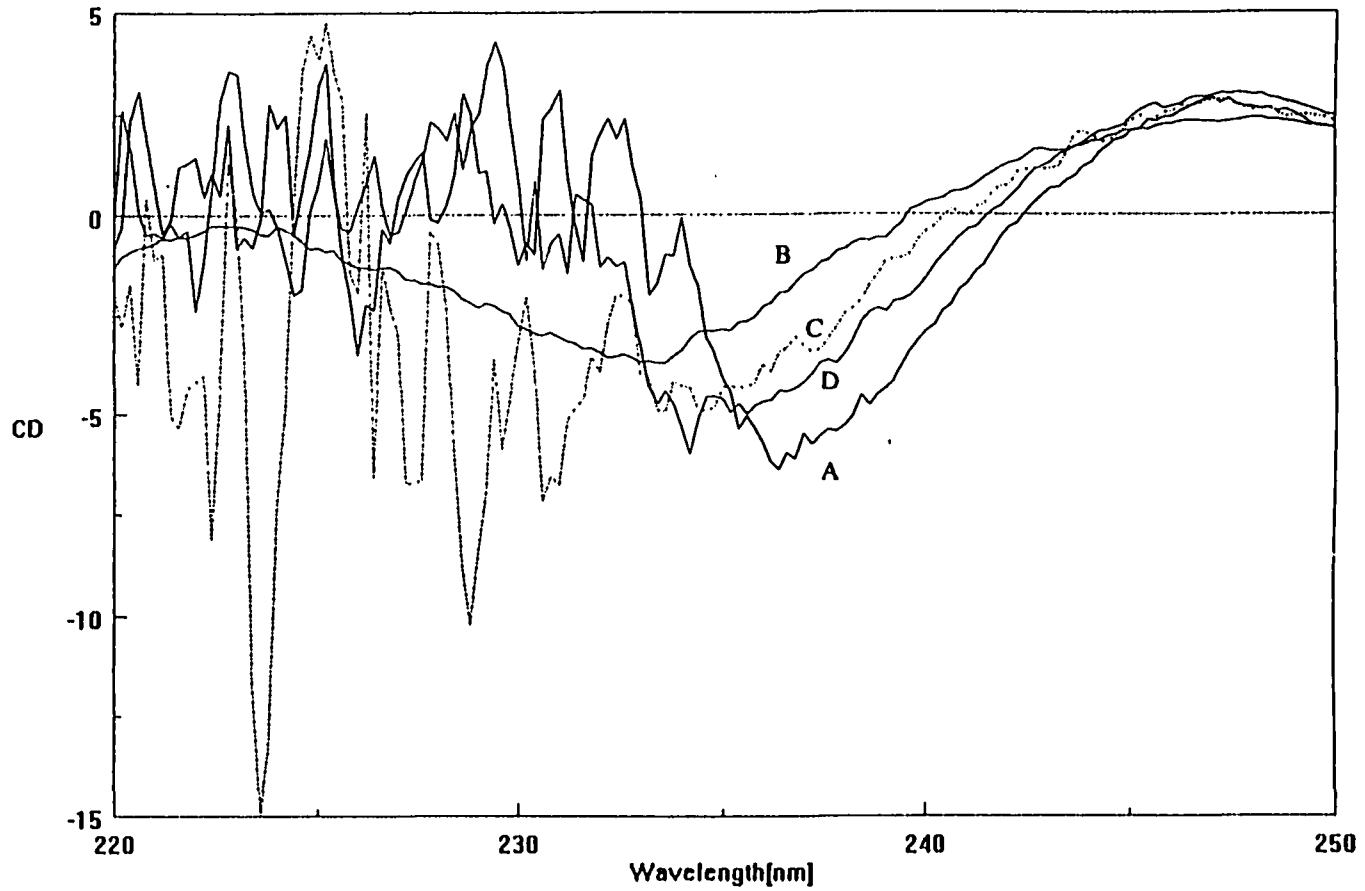
25.55

Figure A11   200 MHz 31P-NMR of ~40 mM BDAP x 3 HCl ligand 35 in D2O solution

16:35:59 1995

144

A ———————— [2-Np]=0.000296M
B ———————— [BDAP2Zn2, only]=0.0000267M
C ················· [2-Np]=0.000075M
D ———————— [2-Np]=0.000149M

Figure A7   Titration of 2.67 x 10⁻⁵ M aq. Zn₂BDAP₂ with 75 molar excess of 2- naphthyl phosphate

REFERENCES

(1) Williams, D. H.; Searle, M. S. in *Molecular Recognition: Chemical and Biochemical Problems II*; Roberts, S. M. (ed.); Royal Society in Chemistry, Cambridge, 1992; pp 19.

(2) Williams, D. H.; Cox, J. P. L.; Doig, A. J.; Gardner, M.; Gerhard, U.; Kaye, P. T.; Lal, A. R.; Nicholls, I. A.; Salter, C. J.; Mitchell, R. C. *J. Am. Chem. Soc.* **1991**, *113*, 7020

(3) Searle, M. S.; Williams, D. H. *J. Am. Chem. Soc.* **1992**, *114*, 10690.

(4) Hou, Z.; Raymond, K. N. *J. Am. Chem. Soc.* **1996**, *118*, 5148.

(5) Janout, V.; Lanier, M.; Regen, S. L. *J. Am. Chem. Soc.* **1996**, *118*, 1573.

(6) Gokel, G. W. in *Host-Guest Interactions; from Chemistry to Biology*, Chadwick, D. J. (ed.) Chichester, John Wiley & Sons, London, 1991; pp 23-41.

(7) Armstrong, A.; Still, W. C. *J. Org. Chem.* **1992**, 4580.

(8) Kubo, Y.; Maeda, S.; Tokita, S.; Kubo, M. *Nature* **1996**, *382*, 522.

(9) Whitesides, G. M.; Mathias, J. P.; Seto, C. T. *Science* **1991**, *254*, 1312.

(10) Cramer, F. in *Einschlussverbindungen*; Springer Vlg., Berlin, 1954;

(11) Anslyn, E.; Breslow, R. *J. Am. Chem. Soc.* **1989**, *111*, 8931.

(12) Eliseev, A. V.; Schneider, H. J. *J. Am. Chem. Soc.* **1994**, *116*, 6081.

(13) Breslow, R.; Hammond, M.; Lauer, M. *J. Am. Che. Soc.* **1980**, *102*, 421.

(14) Ikeda, T.; Yoshida, K.; Schneider, H. J. *J. Am. Chem. Soc.* **1995**, *117*, 1453.

(15) Harada, A.; Li, J.; Kamachi, M. *J. Am. Chem. Soc.* **1994**, *116*, 3192.

(16) Harada, A.; Li, J.; Kamachi, M. *Nature* **1994**, *380*, 126

(17) Harada, A.; Li, J.; Kamachi, M. *Nature* **1993**, *364*, 516.

(18) Pedersen, C. J. *J. Am. Chem. Soc.* **1967**, *89*, 2495, 7017.

(19) Cram, D. J. *J. Am. Chem. Soc* **1986**, *108*, 839.

(20)   Cram, D. J. *Angew. Chem. Int. Ed. Engl.* **1986**, *25*, 1039.

(21)   Bazzicalupi, C.; Bencini, A.; Bianghi, A.; Fusi, V.; Paoletti, P.; Piccaedi, G.; Valtancoli, V. *Inorg. Chem.* **1995**, *34*, 5622.

(22)   Tsukube, H.; Uenishi, J.; Higaki, H.; Kikkawa, K.; Tanaka, T. *J. Org. Chem.* **1993**, *58*, 4389.

(23)   Schneider, H. J.; Blatter, T.; Cuber, U.; Juneja, R.; Schiestel, U.; Theis, I.; Zimmerman, P. in *Frontiers in Supramolecular Organic Chemistry and Photochemistry*; Schneider H.J.; Durr, H. (eds.) VCH Publishers, Weinheim. 1991.

(24)   Burke, S. D.; O'Donnell, C. J.; Porter, W. J.; Song, Y. *J. Am. Chem. Soc.* **1995**, *117*, 12649.

(25)   Chand, D. K.; Ragunathan, K. G.; Mak, T. C. W.; Bharadwaj, P. K. *J. Org. Chem.* **1996**, *61*, 1169.

(26)   Gutsche, C. D. *Acc. Chem. Res.* **1983**, *16*, 162-170.

(27)   Zhang, L.; Lu, T.; Gordon, J.I.; Gokel, G.W.; Kaifer, A.E. *Chem. Commun.* **1993**, 1017.

(28)   Dave, P. R.; Doyle, G. *J. Org. Chem.* **1995**, *60*, 6946.

(29)   Atwood, J. L.; Orr, G. W.; Bott, S. G.; Robinson, K. D. *Angew. Chem. Int. Ed. Engl.* **1993**, *32*, 1093.

(30)   Mallik, S.; Johnson, R. D.; Arnold, F. H. *J. Am. Chem. Soc* **1994**, *116*, 8902.

(31)   Mallik, S.; Johnson, R. D.; Arnold, F. H. *J. Am. Chem. Soc.* **1993**, *115*, 2518.

(32)   Newcomb, L. F.; Gellman, S. H. *J. Am. Chem. Soc.* **1994**, *116*, 4993.

(33)   Newcomb, L. F.; Haque, T. S.; Gellman, S. H. *J. Am. Chem. Soc.* **1995**, *117*, 6509.

(34)   Hunter, C. A.; Sanders, J. K. M. *J. Am. Chem. Soc.* **1990**, *112*, 5525.

(35)   Kato, Y.; Morgan Conn, M.; Rebek Jr., J. *J. Am. Chem. Soc.* **1994**, *116*, 3279.

(36)   Paliwal, S.; Geib, S.; Wilcox, C. S. *J. Am. Chem. Soc.* **1994**, *116*, 4497.

(37)   Schladetzky, K. D.; Haque, T. S.; Gellman, S. H. *J. Org. Chem.* **1995**, *60*, 4108.

(38)   Stetter, H. *Chem. Ber.* **1955**, *88*, 1390.

(39)   Odashima, K.; Itai, A.; Itaka, K.; Koga, K. J. *J. Am. Chem. Soc.* **1980**, *102*, 2504.

(40)   Lorente, A.; Fernandez-Saiz, M.; Lehn, J. M.; Vigneron, J. P. *Tetrahedron Lett.* **1995**, *36*, 8279.

(41)   Odashima, K.; Soga, T.; Koga, K. *Tetrahedron Lett* **1981**, *22*, 5311.

(42)   Diederich, F.; Griebel, D. *J. Am. Chem. Soc.* **1984**, *106*, 8037.

(43)   Diederich, F.; Dick, K. *J. Am. Chem. Soc.* **1984**, *106*, 8024.

(44)   Diederich, F.; Carcanague, D. R. *Helv. Chim. Acta* **1994**, *77*, 800.

(45)   Zhang, B.; Breslow, R. *J. Am. Chem. Soc.* **1996**, *118*, 8495.

(46)   Niedlein, U.; Diederich, F. *Chem. Commun.* **1996**, 1493.

(47)   Jorgensen, W. L.; Nguyen, T. B.; Sanford, E. M.; Chao, I.; Houk, K. N.; Diederich. F. *J. Am. Chem. Soc.* **1992**, *114*, 4003.

(48)   Vyas, N. K.; Wilson, D.K.; Quiocho, F.A. *Nature* **1989**, *340*, 404.

(49)   Lemieux, R. U. *Acc. Chem. Res.* **1996**, *29*, 373.

(50)   Thorson, J. S.; Chapman, E.; Schultz, P. G. *J. Am. Chem. Soc.* **1995**, *117*, 9361.

(51)   Schneider, H. J.; Blatter, T.; Zimmerman, P. *Angew. Chem. Int. Ed. Eng.* **1990**, *29*, 1161.

(52)   Jencks, W. P. *Proc. Natl. Acad. Sci. USA* **1981**, *78*, 4046-4050.

(53)   Meric, R.; V., J.P.; Lehn, J.M. *Chem. Commun.* **1993**, 129.

(54)   Petti, M. A.; Shepodd, T. J.; Barrans, R. E.; Dougherty, D. A. *J. Am. Chem. Soc.* **1988**, *110*, 6825.

(55)   Dougherty, D. A.; Stauffer, D. A. *Science* **1990**, *250*, 1558.

(56)   Kearney, P. C.; Mizoue, L. S.; Kumpf, R. A.; Forman, J. E.; McCurdy, A.; Dougherty, D. A. *J .Am. Chem. Soc.* **1993**, *115*, 9907.

(57)   Forman, J. E.; Barrans, R. E.; Dougherty, D. A. *J. Am. Chem. Soc.* **1995**, *117*, 9213.

(58)   Buchner, M.; Geuder, W.; Gries, W. C.; Hunig, S.; Koch, M.; Poll, T. *Angew. Chem. Int. Ed. Engl.* **1988**, *27*, 1553.

(59)   Bissel, R. A.; Cordova, E.; Kaifer, A. E.; Stoddart, J. F. *Nature* **1994**, *369*, 133.

(60)   Ballardini, R.; Balzani, V.; Gandolfi, M. T.; Prodi, L.; Venturi, M.; Philip, D.; Ricketts, H. G.; Stoddart, J. F. *Anghew. Chem. Int. Ed. Engl.* **1993**, *32*, 1301-1303.

(61)   Anelli, P. L.; Ashton, P. R.; Ballardini, R.; Balzani, V.; Delgado, M.; Goodnow, T. T.; Kaifer, A.; Gandolfi, M. T.; Philip, D.; Pietraszkiewicz, M.; Prodi, L.; Reddington, M. V.; Slawin, A.; Spencer, N.; Stoddart, J. F.; Vincent, C.; Williams, D. J. *J. Am. Chem. Soc.* **1992**, *114*, 193.

(62)   Scheerder, J.; Engbersen, J. F. J.; Reinhoudt, D. N. *Rec. Trav. Chim.* **1996**, *115*, 307.

(63)   Aguillar, J. A.; Espana, E. G.; J.A., G.; Luis, S. V.; Llinares, J. M.; Miravet, J. F.; Ramirez, J. A.; Soriano, C. *Chem. Commun.* **1995**, 2237.

(64)   Fujioka, H.; Kioke, T.; Yamada, N.; Kimura, E. *Heterocycles* **1996**, *42*, 775.

(65)   Martell, A. E.; Smith, R. M. in *Critical Stability Constants*; Plenum Press, New York, 1974

(66)   Delaage, M. in *Physico-Chemical Aspects of Molecular Recognition*; Delaage, M.(ed.) VCH Publishers, New York, 1991; pp 1.

(67)   Webb, T. H.; Wilcox, C. S. *Chem. Soc. Reviews* **1991**, 383.

(68)   Takahashi, I.; Odashima, K.; Koga, K. *Tetrahedron Lett.* **1984**, *25*, 973

(69)   Castro, P. P.; Georgiadis, T. M.; Diedrich, F. *J. Org. Chem.* **1989**, *54*, 5835.

(70)   Webb, T. H.; Suh, H.; Wilcox, C. S. *J. Am. Chem. Soc.* **1991**, *113*, 8554.

(71)   Lee, J. in *Thesis: Cooperative Binding by a Self-Assembled Receptor: Metal in a Structural and Functional Role*; Iowa State University; Ames, 1994

(72)   Lee, J.; Schwabacher, A. W. *J. Am. Chem. Soc.* **1994**, *116*, 8382.

(73) Boyce, R.; Li, G.; Nestler, H. P.; Suenaga, T.; Still, W. C. *J. Am. Chem. Soc.* **1994**, *116*, 7955.

(74) Cheng, Y.; Suenaga, T.; Still, W. C. *J. Am. Chem. Soc.* **1996**, *118*, 1813.

(75) Wennemers, H.; Yoon, S. S.; Still, W. C. *J. Org. Chem* **1995**, *60*, 1108.

(76) Torneiro, M.; Still, W. C. *J. Am. Chem. Soc.* **1995**, *117*, 5887.

(77) Gennari, C.; Nestler, H. P.; Salom, B.; Still, W. C. *Angew. Chem. Int. Ed. Engl.* **1995**, *34*, 1765.

(78) Meissner, R. S.; Rebek, J.; Mendoza, J. *Science* **1995**, *270*, 1485.

(79) Valdes, C.; Spitz, U. P.; Toledo, L. M.; Kubik, S. W.; Rebek, J. *J. Am. Chem. Soc.* **1995**, *117*, 12733.

(80) Grotzfeld, R. M.; Branda, N.; Rebek, J. *Science* **1996**, *271*, 487.

(81) Fujita, M.; Nagao, S.; Iida, M.; Ogata, K.; Ogura, K. *J. Am. Chem. Soc.* **1993**, *115*, 1574.

(82) Fujita, M.; Ibukuro, F.; Hagihara, H.; Ogura, K. *Nature* **1994**, *367*, 721.

(83) Fujita, M.; Nagao, S.; Ogura, K. *J. Am. Chem. Soc.* **1995**, *117*, 1649.

(84) Fujita, M.; Oguro, D.; Miyazawa, M.; Oka, H.; Yamaguchi, K.; Ogura, K. *Nature* **1995**, *378*, 469.

(85) Beer, P. D.; Drew, M. G. B.; Hodacova, J.; Stokes, S. E. *J. Chem. Soc. Dalton Trans.* **1995**, 3447.

(86) Maverick, A. V.; Ivie, M. L.; Waggenspack, J. H.; Fronczeck, F. R. *Inorg. Chem.* **1990**, *29*, 2403.

(87) Schneider, H.-J.; Ruf, D. *Angew. Chem. Int. Ed. Eng.* **1990**, *29*, 1159.

(88) Baldes, R.; Schneider, H. J. *Angew. Chem. Int. Ed. Engl.* **1995**, *34*, 321

(89) Pauling, L. *Nature* **1946**, *161*, 707.

(90) Menger, F. M. *Biochemistry* **1992**, *31*, 5368.

(91) Breslow, R. *Acc. Chem. Res.* **1995**, *28*, 146.

(92)   McCurdy, A.; Jimenez, L.; Stauffer, D. A.; Dougherty, D. A. *J. Am. Chem. Soc.* **1992**, *114*, 10314.

(93)   Winkler, G.; Coutouli-Argyropolou, E.; Leppkes, R.; Breslow, R. *J. Am. Chem. Soc.* **1983**, 7198.

(94)   Fenniri, H.; Lehn, J. M.; Marquis-Rigault, A. *Angew. Chem. Int. Ed. Engl.* **1996**, *35*, 337.

(95)   Goodwin, J. T.; Lynn, D. G. *J. Am. Chem. Soc.* **1992**, *114*, 9197.

(96)   Rotello, V.; Hong, J. I.; Rebek, J. *J. Am. Chem. Soc.* **1991**, *113*, 9423.

(97)   Wintner, E. A.; Morgan Conn, M.; Rebek Jr., J. *J. Am. Chem. Soc.* **1994**, *116*, 8877.

(98)   Pieters, R. J.; Huc, I.; Rebek Jr., J. *Angew. Chem. Int. Ed. Engl.* **1994**, *33*, 1579.

(99)   Morgan Conn, M.; Rebek Jr., J *Angew. Chem. Int. Ed. Engl.* **1994**, *33*, 1577.

(100)   Lee, H. D.; Granja, J. R.; Martinez, J. A.; Ghadiri, M. R. *Nature* **1996**, *382*, 525.

(101)   Breslow, R.; Zhang, B. *J. Am. Chem. Soc.* **1994**, *116*, 7893.

(102)   Schramm, V. L.; Kline, P.C. *J. Biol. Chem.* **1994**, *269*, 18259.

(103)   Smith, J.; Ariga, K.; Anslyn, E. V. *J. Am. Chem. Soc* **1993**, *115*, 362.

(104)   Schultz, P. G. *Acc. Chem. Res.* **1993**, *26*, 391.

(105)   Schultz, P. G.; Lerner, R.A.; Bencovic, S.J. *Chem. Eng. News* **1990**, *May 28*, 26.

(106)   Ohkubo, K.; Urata, Y.; Hirota, S.; Honda, Y.; Sagawa, T. *J. Molecular Catalysis* **1994**, *87*, L21.

(107)   Robinson, D. K.; Mosbach, K. *Chem. Commun.* **1989**, 969.

(108)   Breslow, R. *Acc. Chem. Res.* **1995**, *28*, 146-153.

(109)   Chin, J. *Acc. Chem. Res.* **1991**, *24*, 145.

(110)   Connolly, J. A.; Banaszczyrk, M.; Hynes, R.C.; Chin, J. *Inorg. Chem.* **1994**, *33*, 665.

(111)   Jones, D. R.; Lindoy, L. F.; Sargeson, A. M. *J. Am. Chem. Soc.* **1984**, *106*, 7807.

(112)   Mensi, N.; Isied, S. S. *Inorg. Chem.* **1986**, *25*, 147.

(113)   Lei, H.; Stoakes, M.; Schwabacher, A. W. *Synthesis* **1992**, 1255.

(114)   Bodanszky, M.; Bodanszky, A. *The Practice of Peptide Synthesis*; Springer: New York, 1984; pp 199.

(115)   Fitch, S. J. *J. Am. Chem. Soc.* **1964**, *86*, 61.

(116)   Gallagher, M. J.; Honegger, H. *Tetrahedron Lett.* **1977**, *34*, 2987.

(117)   McKennon, M. J.; Meyers, A. I. *J. Org. Chem.* **1993**, *58*, 3568.

(118)   Brown, H. C.; Heim, P.; Yoon, N. M. *J. Am. Chem. Soc.* **1970**, *92*, 1637.

(119)   Schwabacher, A. W.; Stefanescu, A. D. *Tetrahedron Lett.* **1996**, *37*, 425.

(120)   Gallagher, M. J.; Honegger, H. *Chem. Commun.* **1978**, 55.

(121)   Tzokov, S. B.; Devedjiev, I. T.; Petkov, D. D. *J. Org. Chem.* **1996**, *61*, 12.

(122)   Karanewsky, D. S.; Badia, M. C. *Tetrahedron Lett.* **1986**, *27*, 1751.

(123)   Morita, D. K.; Stille, J. K.; Norton, J. R. *J. Am. Chem. Soc.* **1995**, *1995*, 8576.

(124)   Kong, K. C.; Cheng, C. H. *J. Am. Chem. Soc.* **1991**, *113*, 6313.

(125)   Habeeb, A. F. S. A. *Anal. Biochemistry* **1966**, *14*, 328-336.

(126)   Sarin , A. K.; Kent, S. B. H.; Tam, J. P.; Merrifield, R. B. *Anal. Biochemistry* **1981**, *117*, 147-157.

(127)   Kirby, A. J. *Adv. Phys. Org. Chem.* **1980**, *17*, 183.

(128)   Drummond, J. T.; Ogorzalek Lou, R. R.; Matthews, R. G. *Biochemistry* **1993**, *1993*, 9282-9289.

(129)   Yano, S.; Yoshikawa, S.; Fujita, J. *Bull. Chem. Soc. Japan* **1976**, *49*, 101-105.

(130)   Tobe, M. L.; Martin, D. F. *Inorg. Syntheses* **1966**, *8*, 199.

(131)   Buckingham, D.; Clark, C. R. in *Comprehensive Coordinative Chemistry* Wilkinson, G.(ed.); Pergamon Press, Oxford, 1987; pp 811.

(132)   Williams, J. M. *Inorg. Syntheses* **1972**, *13*, 232.

(133)   Holtzclaw, H. F.; Sheetz, D. P.; McCarty, B. D. *Inorg. Syntheses* **1953**, *4*, 177.

(134)   Vaughn, J. W.; Lindholm, R. D. *Inorg. Syntheses* **1967**, *9*, 163.

(135) Kirshner, S.; Gish, T. J.; Barber, S. *Inorg. Syntheses* **1990**, *29*, 197.

(136) Bailar, J. C. *Inorg. Syntheses* **1946**, *2*, 223.

(137) Harbulak, E. P.; Albinak, M. J. *Inorg. Syntheses* **1966**, *8*, 196.

(138) Illuminati, G.; Mandolini, L. *Acc. Chem. Res.* **1981**, *14*, 95.

(139) Shibata, M. *Top. Curr. Chem.* **1983**, *110*, 26-45.

(140) Bauer, H. F.; Drinkard, W. C. *J. Am. Chem. Soc.* **1960**, *82*, 5031.

(141) Shibata, M. B., H.G. *Inorg Syntheses* **1985**, *23*, 62.

(142) Rowan, N. S.; Storm, C. B.; Hunt, J. B. *Inorg. Chem.* **1978**, *17*, 2853.

(143) Mori, M. S., M.; Kyuno, E.; Hoshiyama, K *Bull. Chem. Soc. Japan* **1958**, *31*, 291.

(144) Sprinborg, J. *Inorg. Syntheses* **1973**, *14*, 63.

(145) Tong, J. Y.; StAndre-Kean, E.; Hall, B. B. *Inorg. Chem.* **1964**, *8*, 1103.

(146) Reid, I. K.; Sargeson, A. M. *Inorg. Syntheses* **1967**, *9*, 167.

(147) Jackson, W. G.; Begbie, C. M. *Inorg. Syntheses* **1983**, *21*, 118.

(148) Nakamoto, K.; McCarthy, P. J. in *Spectroscopy and Structure of Metal Chelate Compounds*; John Wiley & Sons, New York, 1968

(149) Murakami, Y.; Ohno, T.; Hirayama, T.; Hisaeda, Y.; Nishimura, H.; Snyder, J. P.; Steliou, K. *J. Am. Chem. Soc.* **1991**, *113*, 8229.

(150) Wilcox, C. H. in *Frontiers in Supramolecular Organic Chemistry and Photochemistry*; Schneider H.J.; Durr, H.;(eds.) VCH Publishers, Weinheim, 1991

(151) Castro, R.; Nixon, K. R.; Evanseck, J. D.; Kaifer, A. E. *J. Org. Chem.* **1996**, *61*, 7298.

(152) Rosen, A. *Biochem. Pharmacol.* **1970**, *19*, 2075-2081.

(153) Breslow, R.; Berger, D.; Huang, D. L. *J. Am. Chem. Soc.* **1990**, *112*, 3686.

(154) Kioke, T.; Kimura, E.; Nakamura, I.; Hashimoto, Y.; Shiro, M. *J. Am. Chem. Soc.* **1992**, *114*, 7338.

(155) Chin, J.; Banaszczyc, M.; Jubian, V. *Chem. Commun.* **1988**, 735.

(156) Still, W. C.; Khan, M.; Mitra, A. *J. Org. Chem.* **1978**, *43*, 1613-1615.

(157) Mori, M. S., M.; Kyuno, E.; Adachi, E. *Bull. Chem. Soc. Japan* **1956**, *29*, 883.

(158) Springborg, J; Shaffer, C.E. *Inorg. Syntheses* **1973**, *14*, 67.

(159) Department of Chemistry, Massachusetts Institute of Technology, *MIT Laboratory Techniques Manual*, volume 1, **1974**.